

INVESTIGATING OIL DEGRADATION AND MIXING
IN COASTAL ENVIRONMENTS USING RAMPED PYROLYSIS

AN ABSTRACT

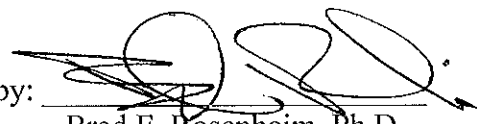
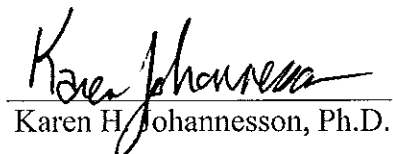
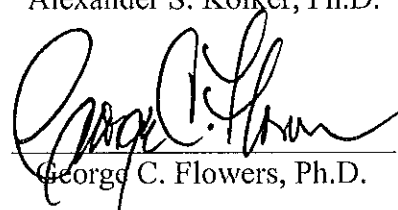
SUBMITTED ON THE TWENTY-FIFTH DAY OF JULY 2013 TO THE
DEPARTMENT OF EARTH AND ENVIRONMENTAL SCIENCES
IN PARTIAL FULFILLMENT OF THE REQUIREMENTS OF THE
SCHOOL OF SCIENCE AND ENGINEERING OF
TULANE UNIVERSITY
FOR THE DEGREE OF
MASTER OF SCIENCE

BY



Matthew Allen Pendergraft

Approved by:


Brad E. Rosenheim, Ph.D.
Advisor
Karen H. Johannesson, Ph.D.
Alexander S. Kolker, Ph.D.
George C. Flowers, Ph.D.

Abstract

Degradation processes change the chemical composition of oil and can be affected by the mixing of oil into the environment. Here, a ramped pyrolysis (RP) isotope technique is implemented to investigate thermochemical and isotopic changes in coastal environments impacted by the 2010 BP Deepwater Horizon oil spill (DwH). Marsh sediment determined to contain oil by PAH analysis display relatively low thermochemical stability and depleted stable carbon (^{13}C) and radiocarbon (^{14}C) isotopic signatures. The ability of RP to separate oil from background organic material (OM) is established by high oil composition for pyrolysates evolved at low temperatures, as determined by radiocarbon measurement. Applying the RP isotopic technique to beach sediment, tar, and marsh samples collected over a span of 881 days reveals a predominance of oil in the organic material for up to 881 days and varying rates of degradation. Pyrolysis profiles show that the oil degraded faster where rates of mixing were higher. Observing how oil changes thermochemically over time provides a new perspective on oil degradation and its relationship with mixing.

INVESTIGATING OIL DEGRADATION AND MIXING
IN COASTAL ENVIRONMENTS USING RAMPED PYROLYSIS

A THESIS

SUBMITTED ON THE TWENTY-FIFTH DAY OF JULY 2013 TO THE
DEPARTMENT OF EARTH AND ENVIRONMENTAL SCIENCES
IN PARTIAL FULFILLMENT OF THE REQUIREMENTS OF THE
SCHOOL OF SCIENCE AND ENGINEERING OF

TULANE UNIVERSITY

FOR THE DEGREE OF

MASTER OF SCIENCE

BY



Matthew Allen Pendergraft

Approved by:



Brad E. Rosenheim, Ph.D.
Advisor



Karen H. Johannesson, Ph.D.



Alexander S. Kolker, Ph.D.



George C. Flowers, Ph.D.

© Copyright by Matthew A. Pendergraft, 2013

All Rights Reserved

Acknowledgements

The work detailed here is the result of much effort and support by many people. I would like to thank my advisor Brad E. Rosenheim for the opportunity to pursue this Master of Science degree, for all of the guidance he provided me in the process, and for the financial assistance I was given. I would also like to thank Nicole Gasparini for her role in securing me funding. During a large portion of my research I was funded by a grant from the Louisiana Sea Grant Coastal Sciences Assistantship Program through the Office of Coastal Protection and Restoration and I am thankful for their assistance. I am also grateful for the support I received from the Consortium for Advanced Research on Transport of Hydrocarbon in the Environment (CARTHE), part of the Gulf of Mexico Research Initiative (GoMRI). Additionally, funding for analyses was provided by NSF grants EAR-1058517 and EAR-1045845 to Brad E. Rosenheim.

I am especially grateful to the members of my research group, the Stable Isotope Laboratory at Tulane University (SILTU), for the great amount of assistance they provided me. Elizabeth Williams and Alvaro Fernandez helped me tremendously throughout this process and also provided me with data that was used in this work. I thank Jianwu Tang for all of the analyses that he completed for me and the subsequent data provided. I would also like to thank Joanna Kolasinski for her valuable feedback and for the data she provided me. Acknowledgement is also due for everyone who participated in collecting the samples that I used in my research.

I would like to express my gratitude to my thesis committee: Karen H. Johannesson, Alexander S. Kolker, and George C. Flowers, for their guidance, and the rest of the Department of Earth and Environmental Sciences at Tulane University.

Most of all I would like to thank my family for their unconditional support and for the foundation they have provided me.

Matthew A. Pendergraft
New Orleans, 2013

TABLE OF CONTENTS

Acknowledgements	ii
List of tables	v
List of figures	vi
Chapters	
1. Introduction	1
2. Methods	11
2.1 Geological setting and sample collection	11
2.2 Addressing remediation	15
2.3 Sample processing	16
2.4 Analyses	17
3. Linking ramped pyrolysis isotope data to oil content through PAH analysis	19
3.1 Introduction	20
3.2 Methods	22
3.3 Results and discussion	25
3.4 Conclusions	36
4. Investigating oil degradation and mixing in coastal environments using ramped pyrolysis	37
4.1 Introduction	38
4.2 Methods	41
4.3 Results	44

4.4 Discussion	53
4.5 Conclusions	72
5. Conclusions	73
6. Appendices	
Appendix A: A brief description of investigations into isotopic ($\delta^{13}\text{C}$) and thermochemical signals of evaporation	75
Appendix B: Compiled elemental and isotopic data from EA-IRMS	76
Appendix C: Compiled isotopic data from the National Ocean Sciences Accelerator Mass Spectrometer Facility (NOSAMS) for samples analyzed by ramped pyrolysis	82

List of tables

3.1 Sediment sample PAH concentration, temperature of maximum CO ₂ production, and geometric mean isotopic data	25
3.2 CO ₂ aliquot temperatures, sample sizes, isotopic data, and compositional data	28
3.3 Isotopic values for assumed endmembers	32
4.1 EA-IRMS compositional and isotopic data and NOSAMS isotopic data for samples analyzed by both techniques	50
4.2 Isotopic data for CO ₂ aliquots from 16 samples analyzed by RP	51

List of figures

2.1 Sampling locations of Bay Jimmy and Grand Isle, Louisiana	12
2.2 Grand Isle sediment sample trench photograph	14
2.3 Sampling timeline	15
3.1 Ramped pyrolysis reaction profiles for sediments with known PAH content	26
3.2 PAH concentration versus T_{\max}	27
3.3 Thermochemical and isotopic data for low and high PAH samples	30
3.4 A. $\delta^{13}\text{C}$ vs. $1/f_{\text{oil}}$; B. $\Delta^{14}\text{C}$ vs. $1/\text{PAH}$	35
4.1 %OC and $\delta^{13}\text{C}$ over time	46
4.2 Thermochemical trends of beach sediments, tar, and marsh samples	48
4.3 $\Delta^{14}\text{C}$ vs. $\delta^{13}\text{C}$ for aliquots of CO_2 produced during ramped pyrolysis	52
4.4 Conceptual model of ramped pyrolysis profiles	55
4.5 Ramped pyrolysis isotopic data for high energy beach sediment	58
4.6 Ramped pyrolysis isotopic data for low energy beach sediment	60
4.7 Ramped pyrolysis isotopic data for tar samples	62
4.8 Ramped pyrolysis isotopic data for marsh samples	63
4.9 $\delta^{13}\text{C}$ data for evaporated oil and for oil from a rocky groin	65

4.10 Evaporation's effect on crude oil's ramped pyrolysis profile	66
4.11 Ramped pyrolysis isotopic data for tar deposits from a rocky groin	67
4.12 $f_{oil} - f_{oil-cb}$ over temperature	69
4.13 $\Delta^{14}C$ vs. $\delta^{13}C$ from A. beach sediment and B. tar samples	71

Chapter 1. Introduction

Marine oil contamination is prevalent and, as consumption of oil rises in developing nations, is likely to increase. It is estimated that 9.5 million barrels (1.3×10^6 metric tons) of oil enter the ocean each year worldwide, with 46% coming from natural seeps, 37% from consumption, 12% from transportation, 3% from extraction, and 2% from other sources [NRC, 2003]. Spills occur during consumption, transportation, and extraction, and account for 7% of the total amount of oil released into the ocean [NRC, 2003]. In comparison, the 2010 BP Deepwater Horizon oil spill (DwH) released 4.9 million barrels (6.7×10^5 metric tons) of oil into the Gulf of Mexico from the Macondo well, or 51% of the average amount of oil released into the ocean worldwide each year [Ramseur, 2010; Crone and Tolstoy, 2010; Griffiths, 2012]. DwH is the largest accidental oil spill to date, having released roughly ten times the oil as the Exxon Valdez [Crone and Tolstoy, 2010].

In addition to its large magnitude, DwH occurred in an ecologically and economically important region. Approximately 1,600 km of Gulf of Mexico shoreline and 75 linear km of Louisiana coastal marsh received moderate to heavy oiling from DwH [Barron, 2012; Silliman *et al.*, 2012]. Coastal Louisiana makes up a major portion of the Mississippi River Delta ecosystem, which constitutes about 37% of the coastal wetlands of the 48 conterminous United States [Couvillion *et al.*, 2011; Mendelssohn *et*

al., 2012]. These wetlands support roughly 30% of the total United States fishing industry and protect a network of infrastructure responsible for an equal proportion of the country's oil and gas supply [*Mendelssohn et al.*, 2012]. At the same time, the Mississippi River Delta suffers from significant land loss, estimated at 4877 km² during 1932 to 2010 [*Couvillion et al.*, 2011] and expected to reach 10,000+ km² by the year 2100 if measures are not taken [*Blum and Roberts*, 2009]. Thus, a disaster in such an important area already in jeopardy could have significant effects.

Oil is toxic and can have deleterious effects to biota [*Sanders et al.*, 1980; *Kennish*, 1996; *Lee and Page*, 1997; *NRC*, 2003]. Particularly relevant to DwH is oil's potential to harm marsh vegetation [*Hester and Mendelssohn*, 2000 and references therein; *Mendelssohn et al.*, 2012], which stabilizes sediment within the Mississippi River Delta [*Day et al.*, 2011]. When marsh vegetation dies, as a result of oil contamination or otherwise, the substrate sediments become more susceptible to erosion by tidal action and storm events, potentially exacerbating land loss [*Day et al.*, 2011; *Deegan et al.*, 2012]. The overall impact oil has on a marsh (or other environment) depends on multiple factors, including the intensity of the oil contamination and how long it remains in the environment.

Oil that enters the environment can persist for decades while changing over time due to various natural processes [*Reddy et al.*, 2002; *Short et al.*, 2007]. Persistence is a measure of how long oil compounds remain in a given environment and is a function of the type of oil and the type of environment. The various components in oil persist in the environment on scales from seconds to decades. Volatile oil components begin to evaporate immediately upon release into the environment [*Wolfe et al.*, 1994]. In

contrast, *Short et al.* [2007] detected oil compounds within the sediment of a Gulf of Alaska beach sixteen years after the Exxon Valdez oil spill and deduced that subsurface oil components may persist with little change for decades. After studying the site of the West Falmouth oil spill, *Reddy et al.* [2002] discovered residual oil compounds persisting in sediments for thirty years and predicted that they would likely remain indefinitely in this low energy, low oxygen environment. DWH released light Louisiana crude oil, which has a composition of over 50% (w/w) low-molecular-weight (LMW) hydrocarbons (1-11 carbon atoms) such as n-alkanes, which generally tend to not persist in the environment [*Ryerson et al.*, 2011; *Liu et al.*, 2012]. The remainder of the DWH oil released contained polycyclic aromatic hydrocarbons (PAHs), their alkylated homologues, and asphaltenes and resins (roughly 20% (w/w)), which all persist in the environment [*Bence et al.*, 1996; *Ryerson et al.*, 2011; *Liu et al.*, 2012].

In addition to variations in oil composition, oil persistence is also determined by environmental factors that change oil's physical form and chemical composition while decreasing its concentration over time. Weathering includes all environmental processes that act on oil in the environment, as well as how they change the oil, and can be divided into mixing and degradation. Mixing is the incorporation of oil into the environment through physical transport. Oil mixes into coastal environments by diffusion and the effects of mechanical energy from waves, tides, and wind, as well as through bioturbation [*Rashid*, 1974; *Owens*, 2008]. Mixing does not directly impart chemical changes on the oil, as it is solely a physical process of dispersion, yet it can influence rates of degradation, particularly by breaking up the oil. Both *Rashid* [1974] and *Owens* [2008] related shoreline energy to oil weathering rates, with high shoreline energy corresponding

to high rates of weathering. *Rashid* [1974] speculated that link to be an increase in oxygen availability, while *Owens* [2008] emphasized the significance of secondary dynamic processes that affect mixing, including rates of short-term cyclic sediment redistribution and net rates of shoreline change. Finally, *White et al.* [2005] concluded that physical processes ultimately decide the fate of residual oil components persisting decades after the West Falmouth spill.

Degradation is chemical change in the chemical composition of the oil mixture, including proportional changes, and the processes that cause them. Processes that degrade oil include dissolution/water washing, evaporation, biodegradation, photo-oxidation/photodegradation, emulsification, and adsorption/sedimentation [*Rashid*, 1974; *Ward et al.*, 1980; *DeLaune et al.*, 1990; *Bence et al.*, 1996; *Wolfe et al.*, 1994; *Wang et al.*, 1999; *Prince et al.*, 2003; *NOAA*, 2006; *Owens*, 2008; *Atlas and Hazen*, 2011; *Liu et al.*, 2012]. These processes generally affect the chemical composition of the oil mixture by the preferential removal of specific groups of compounds and the conversion of certain compounds into other types of compounds.

The relative importance of the different weathering processes can vary depending on the specific environment, but previous studies indicate that evaporation and biodegradation are the degradative processes that most alter the chemical composition of oil in the environment [*Rashid*, 1974; *DeLaune et al.*, 1990; *Wolfe et al.*, 1994; *Prince et al.*, 2003; *Owens*, 2008; *Atlas and Hazen*, 2011]. For the 1989 Exxon Valdez oil spill in Prince William Sound, Alaska, *Wolfe et al.* [1994] estimated that ~20% of the oil evaporated and ~50% biodegraded. Evaporation can convert as much as 30% of oil into the gas phase, effectively removing that fraction from the local environment. This is

likely the dominant weathering process to act on spilled oil over approximately the first ten days [*Strain*, 1986; *Wolfe et al.*, 1994; *Bence et al.*, 1996]. Oil evaporation is controlled by various factors including the composition of the oil, the area and thickness of the oil slick on water, wind speed, and most importantly, temperature, with greater temperatures resulting in greater oil evaporation for any given oil [*Atlas*, 1975; *Wolfe et al.*, 1994]. Temperature is also a critical factor influencing biodegradation (the consumption of oil by microbes), which also depends on the availability of nutrients (nitrogen, and phosphorus), oxygen, and pH [*Bence et al.*, 1996; *DeLaune et al.*, 1990]. In laboratory experiments, *Atlas* [1975] demonstrated greater biodegradation at 20°C than at 10°C. Due to the fact that temperature strongly influences the two major oil degrading processes (biodegradation and evaporation), the location of an oil spill, in particular its latitude, influences the degradation rate of the oil and the timescale of its persistence.

The understanding of oil degradation has been compiled by employing bulk and compound specific analytical techniques. In general, degradation of oil in the environment removes the more reactive compounds (short chain alkanes) as the more refractory compounds (high molecular weight PAHs, resins, and asphaltenes) resist degradation and persist [*Wolfe*, 1994]. Bulk techniques analyze oil as a whole whereas compound specific techniques examine the individual components of the bulk oil, with both approaches utilizing isotopic techniques. The stable carbon isotopic composition of bulk oil is particularly useful for studying oil in the environment because it remains constant through time and weathering [*NOAA*, 1980; *Macko et al.*, 1981]. Investigating how oil in the environment changes over time implies measuring those characteristics

that change. However, if the goal is to detect oil in the environment, a constant oil signal, such as $\delta^{13}\text{C}$, is desirable.

Compound specific techniques are employed to yield more-detailed information on how oil degrades in the environment. Compounds commonly studied include saturated hydrocarbons, especially normal alkanes (n-alkanes, unbranched chains $\text{C}_8\text{-C}_{40}$), the isoprenoids pristane and phytane, BTEX (benzene, toluene, ethyl-benzene, and xylenes), polycyclic aromatic hydrocarbons (PAHs), and biomarkers (molecules used in geochemical applications to ancient sediments that are also found in oil and are resistant to degradation) [Wang *et al.*, 1999; Munoz *et al.*, 1997]. Degradative processes preferentially affect oil hydrocarbons according to chain length. In general, evaporation, dissolution in water, and biodegradation all remove small (C_{27}) compounds [Arey *et al.*, 2007]. More specifically, evaporation results in the loss of methane to C_{13} n-alkanes, $\text{C}_5\text{-C}_6$ benzenes, methyl naphthalenes, C_3 -substituted naphthalenes, ace-naphthalenes and potentially n- $\text{C}_{14}\text{-C}_{16}$ alkanes [Wolfe *et al.*, 1994]. Biodegradation causes partial or total removal of n-alkanes, then subsequent loss of some branched alkanes, cycloalkanes, and aromatics [Sofer, 1984]. Finally, dissolution extracts water soluble components from the oil, thus removing the more polar compounds [Sofer, 1984].

PAHs have been used extensively in studies concerning oil contamination in the environment [Youngblood and Blumer, 1975; Teal *et al.*, 1992; Wang *et al.*, 1999; White *et al.*, 2005; Liu *et al.*, 2012] due to their toxicity to biota [Neff, 1979] and persistence in the environment [Teal *et al.*, 1992; Kennish, 1996; Boehm *et al.*, 2008]. PAHs are some of the more persistent compounds found in oil, therefore they are useful for detecting oil residues in environments years to decades after spills. However, PAHs also degrade,

which involves first the loss of the more volatile, soluble, and biodegradable naphthalenes followed by slower degradation of larger PAHs (3+ rings) and those with higher degrees of alkylation, with chrysene being particularly recalcitrant [Arey *et al.*, 2007; Boehm *et al.*, 2008]. PAH degradation is attributed to evaporation, biodegradation, photodegradation, and dissolution in water [Neff, 1979; Kennish, 1996; Arey *et al.*, 2007].

Changes in biomarker concentrations and gas chromatography mass spectrometry (GC-MS) chromatograms are used to assess degree of oil degradation [Wang *et al.*, 1994; Munoz *et al.*, 1997]. Biomarkers commonly measured for oil degradation include isoprenoids, steranes, hopanes, terpanes, and steroids [Wang *et al.*, 1994; Munoz *et al.*, 1997]. The measurement of biomarkers can indicate which weathering processes acted on oil found in the environment [Munoz *et al.*, 1997]. Over a dozen biomarker concentration ratios have been proposed and are generally most effective at diagnosing biodegradation [Arey *et al.*, 2007]. Compound ratios measure the concentration of a compound with respect to another and may employ biomarkers. The analysis of structural isomers, which are molecules with the same molecular formula but with different bond connections, is also employed in oil degradation studies. Structural isomers of a hydrocarbon compound may evaporate and dissolve into water identically, but often do not biodegrade the same. Thus, sterane isomer concentration ratios are useful in measuring oil biodegradation despite varying evaporation and dissolution effects. It is for this reason that differential degradation of sterane isomers indicates biodegradation [Munoz *et al.*, 1997]. Structural isomers can also yield information on other weathering processes. The ratio of two norhopane isomers can be used to estimate the extent of photodegradation for a given spill oil [Munoz *et al.*, 1997].

As weathering changes the concentration, form, and chemical composition of oil in the environment, the toxicity of the oil is also affected [NRC, 2003]. Like persistence, the toxicity of oil is determined by both the composition of the oil and the natural processes that act on oil in the environment. The most significant way in which toxicity changes over time is by mixing and degradative processes decreasing the concentration of the oil at the impacted location, thus decreasing overall toxicity. Also, many of the more toxic compounds in oil, such as one and two ringed aromatics including BTEX (benzene, toluene, ethyl benzene, and xylenes), tend to be some of the first components removed by degradation [Sanders *et al.*, 1980; Lee and Page, 1997; NRC, 2003]. However, degraded oil remains toxic because some toxic compounds persist, such as PAHs [Reddy *et al.*, 2002; Short *et al.*, 2007; Boopathy *et al.*, 2012; Sanders *et al.*, 1980; Kennish, 1996; Lee and Page, 1997; NRC, 2003]. Therefore although some compounds in oil that persist are also toxic, oil's toxicity generally decreases over time as some toxic components are removed and the concentration of oil is reduced.

Although much is known about the weathering of oil in the environment, there are still gaps to fill in the knowledge. This study applies a ramped pyrolysis (RP) isotope technique to gain new insight into oil degradation and mixing in the environment. The technique is detailed in Rosenheim *et al.* [2008] where it was applied to yield radiocarbon age spectra for Antarctic sediments devoid of datable carbonate minerals. The method has also constrained petrogenic particulate organic carbon (POC) in the Ganges River [Rosenheim and Galy, 2012], generated radiocarbon age spectra for POC from the lower Mississippi-Atchafalaya River system [Rosenheim *et al.*, 2013a], and improved on radiocarbon dating of Antarctic sediment from the Hugo Island Trough [Rosenheim *et al.*,

2013b]. This was accomplished by exploiting thermochemical differences amongst sample components within a mixture. As oil itself is a mixture of compounds and subsequently forms a mixture with background organic material when it enters the environment, the ramped-pyrolysis technique was implemented to investigate oil in the environment. Whereas many methods that are implemented to study oil in the environment extract information from the finest of chemical detail, a broader approach is taken here by implementing a bulk technique to observe qualitative changes in oil related to weathering.

The ramped pyrolysis (RP) isotopic technique separates organic material into fractions based on differences in thermochemical stability. Factors that determine thermochemical stability include chemical composition and age [*Rosenheim et al.*, 2008]. The RP technique is distinct from earlier pyrolysis and variable temperature combustion methods [*McGeekin et al.*, 2001, 2004; *Wang et al.*, 2003; *Maharaj et al.*, 2007a, 2007b; *Plante et al.*, 2009] generates characteristic reaction profiles depicting thermochemically distinct components of a mixture of organic material. Thermochemical differences observed in reaction profiles imply chemical differences amongst the components. Evolved CO₂ from the oxidation of pyrolysis products can be collected as a series of aliquots and analyzed for carbon isotopes to reveal information on the composition and age of sample fractions.

Isotopic analyses in this study are primarily implemented to detect oil in the bulk samples. Radiocarbon analysis is particularly useful in studying oil in the environment due to its high degree of sensitivity and the fact that oil has no measureable ¹⁴C. This contrasts sharply with the young, relatively ¹⁴C-enriched background organic matter of

coastal environments. Therefore, radiocarbon analysis can easily distinguish the two carbon sources. In studies not involving oil, coupling radiocarbon data to the RP data has provided detailed age distributions and new insight into sample composition, thus improving on singular bulk radiocarbon ages [*Rosenheim et al.*, 2008; *Rosenheim and Galy*, 2012]. The ramped pyrolysis technique also employs stable carbon isotopic analysis to identify oil in samples. Stable carbon isotopic signatures can be used to identify oil in coastal Louisiana because the $\delta^{13}\text{C}$ of oil differs from values commonly found in the environments studied [*Smith and Epstein*, 1971; *Haines*, 1976; *Macko and Parker*, 1983; *Chmura et al.*, 1987; *Sharp*, 2007] and is constant through time and weathering [*NOAA*, 1980; *Macko et al.*, 1981; *Rosenheim et al.*, 2013c].

Here I test the hypothesis that thermochemical changes in organic material from oil impacted coastal environments will reflect mixing of the oil with background organic material. A ramped pyrolysis isotopic technique was applied to samples collected over 881 days from beach and marsh environments impacted by DwH. Coupling thermochemical and isotopic data provides evidence of the oil mixing into the environment, as well as signs of oil degradation. In addition, different weathering trends are observed depending on sample type and environment.

Chapter 2. Methods

2.1 Geological setting and sample collection

Sampling occurred at Grand Isle and Bay Jimmy in subtropical Southeastern Louisiana over a period of 881 days after the Macondo well explosion that caused DwH (Figure 2.1). Both sites are parts of the Barataria basin, an interlobe basin which includes physiographic regions of forested swamp in its least saline northwestern extremity, with a southeast progression of fresh, intermediate, brackish, and salt marshes to its barrier islands along the Gulf of Mexico [*Hatton et al.*, 1983; *Chmura*, 1987; *Kosters*, 1989]. Grand Isle is one of the barrier islands forming the seaward boundary of Barataria Bay and is adjacent to the largest inlet to the bay on the NE end of the island. The sampling site at Grand Isle is a sandy, gently sloping marine beach, which is typical in low latitudes. It is affected by minor, diurnal tidal fluctuations, moderate wave energy, and high energy storms, including hurricanes. Bay Jimmy is located within the brackish marsh region of the Barataria basin. Brackish-intermediate marsh sediment is characterized by a 0.1-0.2 m thick vegetative mat with muck, which overlies a fibrous peat layer 0.3-3.1 m in thickness, on top of blue-gray clay or silty clay containing lenses rich in organic matter [*Hatton et al.*, 1983]. The progression towards the Gulf of Mexico from freshwater to salt marshes is characterized by an increasing average grain size

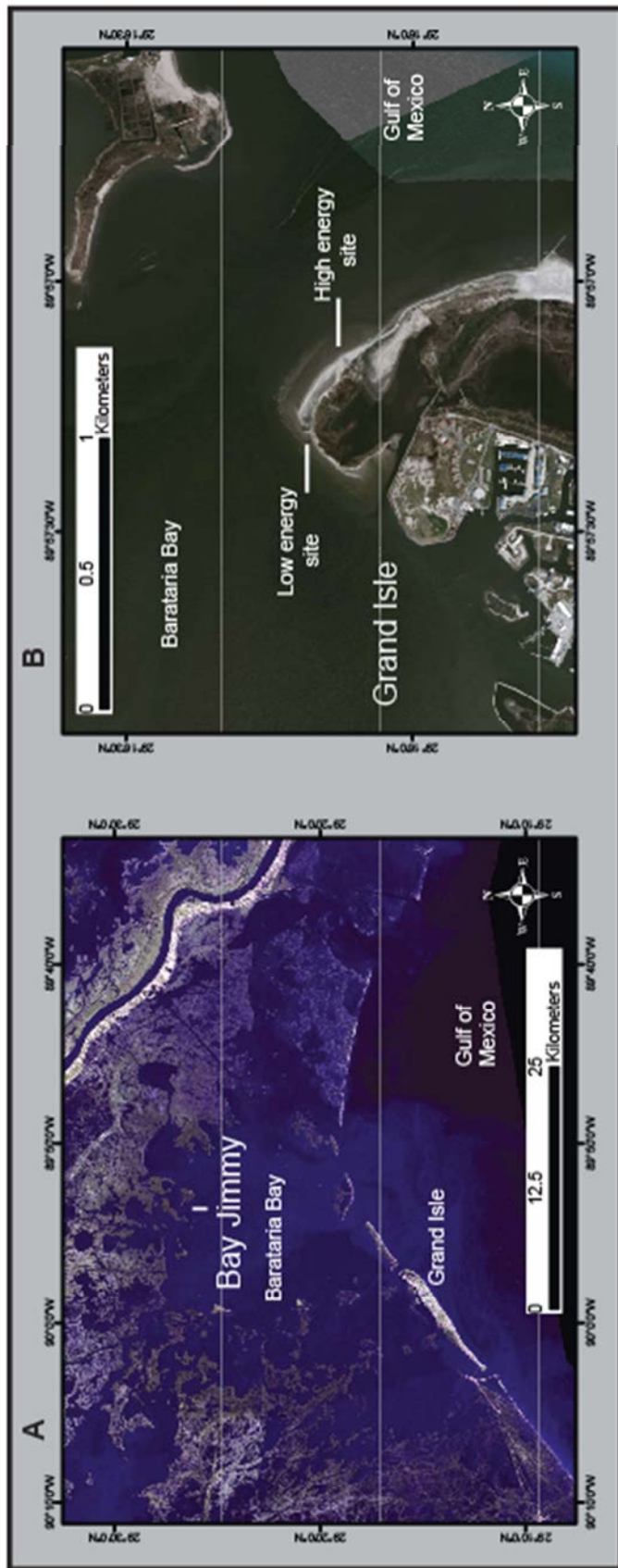


Figure 2.1. A. Sampling locations of Bay Jimmy and Grand Isle, within the Barataria Basin. **B.** High energy and low energy beach sampling sites at the NE end of Grand Isle.

[*Hatton et al.*, 1983]. Being at the seaward extreme of this progression, Grand Isle differs from Bay Jimmy by presenting a larger average grain size.

Two fixed locations were repeatedly sampled for sediment at Grand Isle: a high energy beach site on the channel between Barataria Bay and the Gulf of Mexico, and a low energy beach site located on the lagoon side of the island that faces Barataria Bay. The high energy site is more exposed to wave action and is representative of the ocean-facing side of the barrier island, dominated by the marine environment. The low energy site represents the more protected, salt marsh influenced backside of the barrier island. In general, Grand Isle is a higher energy environment with sediment lower in organic matter, higher oxygen availability, and higher salinity compared to Bay Jimmy. Although an erosive marsh with ~10's of km of southerly fetch, the Bay Jimmy site is considered a lower energy environment compared to the two barrier island sites. For all three locations, higher shoreline energy implies a greater rate of mixing of oil and sediments and higher availability of nutrients and oxygen. Oxygen availability is likely lowest at Bay Jimmy, as marsh sediments are oxygen-limited [*Shin et al.*, 2000] and primary production is highest of the three sampling sites.

Sampling at Grand Isle consisted of digging trenches at these two sites and collecting sediment at different depths, specifically targeting dark bands (Figure 2.2). The trench bottom was also sampled, as an oily sheen was often observed there, along with a petrochemical odor within the trenches. Other samples collected at Grand Isle included: 1. oil slicks from the water surface and oil from the beach surface at earlier sampling dates; 2. tar adhered to a rocky groin; and 3. tar balls. These samples were collected in the vicinity of the high and low energy sites and are categorized as tar



Figure 2.2. Sediment samples from Grand Isle were collected by digging trenches and sampling from dark bands and the trench bottom. An oil sheen was often observed on the water at the trench bottom, as well as an odor similar to that of oil. *Image courtesy of B. Rosenheim.*

samples. Samples collected from Bay Jimmy are categorized as marsh samples and included 1. oil deposits; 2. vegetation with and without visible oil; and 3. a 50 cm surface core collected with a hand auger. The sampling period spanned 881 days after the Macondo well explosion (Figure 2.3), with the first day of sampling (46 d) at Grand Isle occurring on the first day of heavy oiling at that location. Bay Jimmy is less accessible than Grand Isle, therefore sampling there was less frequent than at Grand Isle.

Samples were collected in radiocarbon clean glass jars precombusted at 525°C for ≥ 2 hours to remove organic contaminants. Sampling jars were capped with precombusted aluminum foil and samples were stored under nitrogen gas. A few samples

were collected in Whirlpak® and Ziploc® bags, when precombusted glassware was not available, and all samples were stored below 0°C.

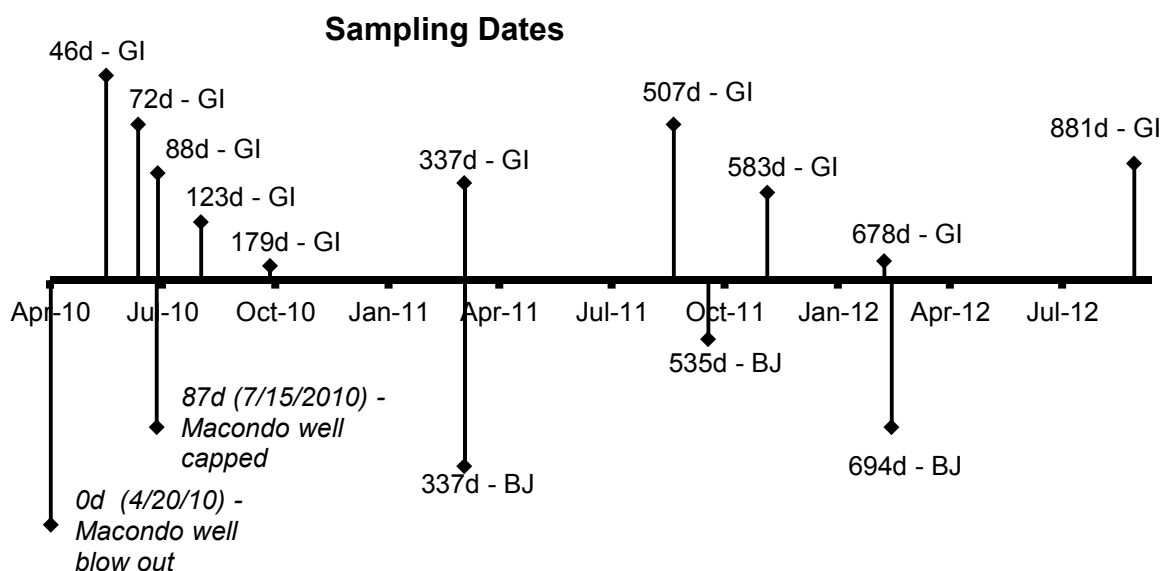


Figure 2.3. Sampling timeline, in days after the Macondo well blow out. *Note - Months marked at month midpoints.

2.2 Addressing remediation

Oil spill remediation efforts were conducted at the locations of this study and during the sampling period, yet they likely did not affect the thermochemical characteristics of the oil. After the testing of various remediation techniques, remediation at Bay Jimmy consisted of manual and mechanical removal of oiled marsh by raking, cutting, and collection [Zengel and Michel, 2013]. In some cases loose organic sorbent material (e.g. bagasse and kenaf plant fibers) was applied and then recovered along with the oiled marsh vegetation [Zengel and Michel, 2013]. These remediation techniques are not suspected to affect the chemical composition of the oil because their relatively simple

manual and mechanical nature. Oil remediation at the Grand Isle study area involved a singular event of surface sediment cleaning that is also not suspected to have affected the thermochemical properties of the oil that remained. In January of 2011 the top ~6.4 cm (2.5 in) of beach sediment at Grand Isle State Park (where sampling occurred) was collected and subjected to a washing process involving heat, then deposited back onto the beach. Processed sediment was analyzed and showed no indications of oil. Considering this and that the washing was not performed *in situ*, it is likely that all oil was removed from all sediment that was processed, and oil in unprocessed sediment was not affected. In sum, at both the Bay Jimmy and Grand Isle study locations, remediation during the sampling period may have decreased the oil concentration but did not affect the thermochemical stability of the oil that remained.

2.3 Sample processing

Prior to analysis, samples from Grand Isle were ground using a mortar and pestle, first picking out shell fragments with tweezers, and then acidified with 10% HCl to remove inorganic carbon. Samples were repeatedly rinsed with Milli-Q deionized water, centrifuged, and decanted until a pH ~6 was reached. Samples were then dried at 60°C for 24 hours or until completely dry. Heavily-oiled samples were dried for < 24 h when possible in order to minimize heat-driven evaporation of volatile compounds. Samples from Bay Jimmy were inspected for shell fragments, which were removed if found, then dried similarly to the Grand Isle samples.

2.4 Analyses

Organic carbon content (%OC) and bulk stable carbon isotopic composition ($\delta^{13}\text{C}$) were determined using an Elementar vario MICRO cube elemental analyzer interfaced to an Isoprime dual inlet isotope ratio mass spectrometer in continuous flow mode (EA-IRMS). Stable carbon isotopic composition is expressed in conventional delta notation, on the per mil (‰) scale, relative to the Vienna Pee Dee Belemnite standard, according to the following equation:

$$(2.1) \quad \delta^{13}\text{C}, \text{‰} = \left(\frac{R_x - R_{std}}{R_{std}} \right) \times 1000$$

where R is the ratio $^{13}\text{C}/^{12}\text{C}$, x denotes the sample, and std denotes the standard [Sharp, 2007]. %OC values were used to determine proper sample size for reliable ramped-pyrolysis isotopic analysis and to calculate expected ramped-pyrolysis yields in order to evaluate for complete carbon recovery. %OC and $\delta^{13}\text{C}$ data were used to screen samples for oil prior to analysis by ramped-pyrolysis. $\delta^{13}\text{C}$ values significantly different than that of DwH oil were considered a strong indication of a lack of oil, which was helpful in determining the identity of samples of questionable appearance collected at Grand Isle.

Samples were analyzed using a ramped-pyrolysis (RP) isotope technique as detailed in [Rosenheim *et al.*, 2008]. Processed samples were placed between precombusted quartz wool and loaded into the RP reactor. The reactor was flushed with ultra-pure helium gas as it was heated at 5°C min^{-1} from ambient laboratory temperature up to 1000°C . Most samples needed to be heated only to $\sim 750^\circ\text{C}$ until all OC was pyrolyzed. Downstream from the reactor, an 800°C combustion chamber with $\sim 8\%$

oxygen concentration and copper, nickel, and platinum wires allowed combustion of moieties from the reactor. The resulting CO₂ circulated through a Sable Systems CA-10 infrared gas analyzer, producing a live readout of CO₂ concentration and allowing photometric quantification of CO₂ during the reaction. CO₂ was collected cryogenically as sequential aliquots that were purified on a vacuum line and sealed in precombusted Pyrex® tubes with copper oxide and silver wire. Radiocarbon and stable carbon analyses on the CO₂ aliquots was accomplished at the National Ocean Sciences Accelerator Mass Spectrometer Facility (NOSAMS) at the Woods Hole Oceanographic Institution. Radiocarbon data are based on measurements of ¹⁴C/¹²C in the sample relative to ¹⁴C/¹²C of 1950 wood (fraction modern, f_m) and are expressed as radiocarbon deficiency ($\Delta^{14}\text{C}$):

$$(2.2) \quad \Delta^{14}\text{C} \cong \delta^{14}\text{C} = (F_m - 1) \times 1000$$

where a short period of time (≤ 3 y) between sampling and measurement renders $\delta^{14}\text{C}$ equal to $\Delta^{14}\text{C}$ relative to analytical uncertainty [*Stuiver and Polach, 1977*]. Subsampling of CO₂ was based on reaction profile, with the objective of collecting individual peaks representing thermochemically distinct fractions of the sample. One adjustment to the RP procedure that was made for this experiment was ensuring a combustion chamber temperature of 800°C prior to heating any sample that may contain volatile compounds, in order to avoid pyrolysis without subsequent combustion. In addition, samples were first analyzed without collecting CO₂ in order to obtain a reaction profile. The reaction profiles were used to determine optimal sample collection points and the sample was re-analyzed with CO₂ collection for isotopic analysis.

Chapter 3. Linking ramped pyrolysis isotope data to oil content through PAH analysis

Manuscript of the author related to this chapter:

Pendergraft M.A., Dincer Z., Sericano J.L., Wade T., Kolasinski, J. and Rosenheim B.E. 2013. Linking ramped pyrolysis isotope data to oil content through PAH analysis. *In review* (submitted to *Environmental Research Letters*)

Abstract

Coupling ramped pyrolysis isotope (^{13}C and ^{14}C) and polycyclic aromatic hydrocarbon (PAH) analyses demonstrates the utility of ramped pyrolysis in screening for oil content in sediments. Here, PAH content and ramped pyrolysis isotope data are coupled to determine relationships between oil contamination, pyrolysis profiles, and isotopic composition of sediments from Barataria Bay, Louisiana, that were contaminated by oil from the 2010 BP Deepwater Horizon spill. Sediment samples with low PAH concentrations are thermochemically stable until higher temperatures, while samples containing high concentrations of PAH pyrolyze at low temperatures. High PAH samples are also depleted in radiocarbon (^{14}C), especially in the fractions that pyrolyze at low temperatures. This lack of radiocarbon in low temperature pyrolysates is indicative of volatile, ^{14}C -free oil content. This study presents a proof-of-concept that oil contamination can be identified by changes in thermochemical stability in organic material and isotope analysis of pyrolysates.

3.1 Introduction

The 2010 BP Deepwater Horizon oil spill (DwH) is the largest accidental oil spill to date, having released from the Macondo well roughly ten times the oil as the *Exxon Valdez* spill [Crone and Tolstoy, 2010]. Besides causing various immediate problems including the loss of life, the oiling of wildlife, and oil deposition in coastal areas, this large spill will have environmental repercussions on longer time scales. Incorporation of this oil into natural environments (marshes, beaches, inland waterways) already undergoing high rates of geomorphologic change [Couvillion *et al.*, 2011] poses challenges to recognizing additional stress from the oil. Chemical or isotopic identification of oil in these environments is necessary to determine the relationship between oil contamination and geomorphologic stress.

Oil contamination in coastal environments, as well as the associated toxicity, can be estimated by measuring polycyclic aromatic hydrocarbons (PAHs), a component of oil [Boehm and Farrington, 1984; Colombo *et al.*, 1989; Wang *et al.*, 1999; Alimi *et al.*, 2003]. PAHs are considered one of the most valuable hydrocarbon classes for detecting oil in the environment because many persist longer than aliphatic hydrocarbons [Wang *et al.*, 1999 and references therein; Alimi *et al.*, 2003 and references therein]. The various forms of oil contamination (a petrogenic PAH source) constitute the largest source of PAHs into the environment [Neff, 1979; Iqbal *et al.*, 2008]. Other PAH sources include the combustion of fossil fuels and organic material (pyrogenic); biological processes (biogenic); and chemical and biological alteration of natural organic material (diagenetic)

[Neff, 1979; Iqbal *et al.*, 2008]. The petrochemical activities of catalytic cracking and coke combustion (both pyrogenic sources) are particularly large PAH sources [Colombo *et al.*, 1989]. PAH concentrations and distributions are usually measured by various gas chromatography (GC) techniques, with GC coupled to mass spectrometry (GC-MS) and flame ionization detection (GC-FID) the two most common methods [Wang *et al.*, 1999]. Short *et al.* [2007] employed PAH analysis to detect oil in Gulf of Alaska beach sediments 16 years after the 1989 *Exxon Valdez* spill and concluded that oil would likely persist there for decades. White *et al.* [2005] measured PAHs in marsh sediment in West Falmouth, Massachusetts 30 years after the 1969 *Florida* spill and found that oil weathering had stopped or was occurring at a very slow pace. These studies have shown that PAH analysis can detect oil in the environment on decadal timescales. PAHs have also been shown to be toxic to marine organisms [Neff, 1979] and are considered possible or probable human carcinogens [Menzie *et al.*, 1992].

This study uses PAHs as a proxy for oil and investigates relationships between PAH content, thermochemical stability, and isotopic composition of sediment from an oil impacted marsh. A sample set with PAH concentrations spanning three orders of magnitude was analyzed with a ramped pyrolysis (RP) isotope technique. Whereas PAH analysis detects a specific compound group present in oil, the RP technique analyzes the entirety of organic carbon (OC) in a sample, yielding a thermochemical profile and an isotopic spectrum of organic material [Rosenheim *et al.*, 2008; Rosenheim and Galy, 2012; Rosenheim *et al.*, 2013a; Rosenheim *et al.*, 2013b] that would include depleted stable carbon and radiocarbon isotopic signatures if oil is present in the sample. Oil has a different chemical composition than the background organic matter found in oil-free

environments and contains compounds that are more volatile than sedimentary organic matter. Using RP, multiple isotopic measurements on a single sample are accomplished by the subsampling of aliquots of CO₂ evolved over continuous temperature intervals of the thermochemical reaction. Stable carbon (¹³C) and radiocarbon (¹⁴C) isotopic measurements for each aliquot of CO₂ provide information on carbon source apportionment and age in a mixture of organic carbon [Rosenheim *et al.*, 2008; Rosenheim and Galy, 2012; Rosenheim *et al.*, 2013a; Rosenheim *et al.*, 2013b]. Isotopic data employed in a binary mixing model can identify oil because oil is isotopically distinct from marsh biomass [Haines, 1976; Chmura *et al.*, 1987; Graham *et al.*, 2010]. Detection of oil using radiocarbon and stable carbon isotopes is advantageous because oil's isotopic signatures are unaffected by weathering [Macko *et al.*, 1981]. Here we compare PAH concentrations in sediment samples to RP reaction profiles and isotopic composition to establish relationships between an organic chemical proxy for oil contamination, thermochemical decomposition trends, and carbon source.

3.2 Methods

Sampling occurred within a brackish marsh environment in Northern Barataria Bay in Southeastern Louisiana. The area from which samples were collected was located between 29.4690°N, 89.9283°W and 29.4411°N, 89.8999°W. Sediment samples (n=4) from the surface (0-2cm) and subsurface (20-21cm) were collected from subtidal and intertidal zones. Sampling occurred 535 days after DwH began releasing oil and oil was

confirmed within the sampling area by survey teams [*Silliman et al.*, 2012; *SCAT*, 2013]. Samples collected ranged in degree of oiling, from obvious to not visible to the sampler.

Sediment samples were analyzed for PAHs using a technique based on NOAA NS&T Methods and validated by 15+ years of interlaboratory comparisons [*Wade et al.*, 2008]. Deuterated surrogate standards (d_8 -naphthalene, d_{10} -acenaphthene, d_{10} -phenanthrene, d_{12} -chrysene, and d_{12} -perylene) were added to 3g of freeze dried sediment and used to calculate analyte concentrations. Samples were extracted with methylene chloride using an accelerated solvent extractor (ASE). Extracts were fractionated by partially deactivated silica/alumina column chromatography by eluting with a 1:1 mixture of pentane and methylene chloride. PAHs were quantitatively analyzed by gas chromatography-mass spectrometry (GC-MS; HP-5890 and HP-5970-MSD) in the selected ion mode (SIM). The GC-MS was calibrated by the injection of standards at five concentrations. Samples were injected in the splitless mode into a 30 m x 0.25 mm i.d. (0.25 μ m film thickness) DB-5 fused silica capillary column (J&W Scientific, Inc.) at an initial temperature of 60°C, then ramped at 12°C min⁻¹ to 300°C and held for 6 min. The mass spectral data were acquired and the molecular ions for each of the PAH analytes were used for quantification. Analyte identification was based on the retention time of the quantitation ion for each analyte and a series of confirmation ions. Twenty-seven different PAH analytes were measured, twenty-one of which are US EPA priority PAHs.

Analysis of the sediment samples and crude oil by ramped pyrolysis was accomplished using the same settings as in previous RP investigations [*Rosenheim et al.*, 2008; *Rosenheim and Galy*, 2012; *Rosenheim et al.*, 2013a; *Rosenheim et al.*, 2013b]; these settings consisted of a smooth temperature ramp of 5°C min⁻¹, 0% O₂ in the

reaction chamber, and ~8% O₂ in the combustion chamber. The crude oil, provided by BP, was sampled directly from the Macondo well head and stored at -4°C. Aliquots of CO₂ were collected at inflection points in the reaction profiles. Two to four CO₂ subsamples from each sediment sample were collected and sent to the National Ocean Sciences Accelerator Mass Spectrometer Facility (NOSAMS) for $\Delta^{14}\text{C}$ and $\delta^{13}\text{C}$ determination. Radiocarbon data, reported in Δ notation and per mil (‰) units, were calculated using:

$$(3.1) \quad \Delta^{14}\text{C} = (F_m e^{(1950-y)/8267} - 1) \times 1000$$

where F_m denotes fraction modern and y represents the year the sample was collected [Stuiver and Pollach, 1977]. Radiocarbon data from the RP analyses were corrected for 9.5 (± 3.8) μg of “modern” blank and 0.05 (± 0.025) μg of ^{14}C -free blank over an entire run, divided equally amongst the aliquots, following recommendations of Santos et al. [2010]. Thus, the system’s blank results in greater (more positive $\Delta^{14}\text{C}$) values depending on sample size and number of subsamples taken – correction for this blank will result in less radiocarbon than measured (more negative $\Delta^{14}\text{C}$). Stable carbon isotopic composition is expressed in δ notation and ‰ units, relative to the Pee Dee Belemnite (PDB) standard, according to:

$$(3.2) \quad \delta^{13}\text{C} = \left(\frac{R_x - R_{std}}{R_{std}} \right) \times 1000$$

where R is the ratio $^{13}\text{C}/^{12}\text{C}$, x denotes the sample, and std denotes the standard [Sharp, 2007].

3.3 Results and discussion

Total PAH concentrations in the sediment (108 to 390,835 ng/g dry weight (dw); Table 1) vary significantly, spanning three orders of magnitude. In comparison, uncontaminated estuarine and marine sediments commonly have total PAH concentrations on the scale of 0-50 ng/g [Neff, 1979; Kennish, 1996]; deep ocean sediments were measured to have a total PAH concentration of 100 ng/g [Windsor and Hites, 1979]; and PAH are acutely toxic to marine organisms at concentrations of 200-10,000 ng/g [Neff, 1979].

At a relatively simplistic interpretation of PAHs in sediment, concentrations indicate a broad range of oil contamination with a strong oil signal in half of the samples. In comparison to values from literature [Neff, 1979; Windsor and Hites, 1979; Kennish, 1996], PAH concentrations of 108 and 120 ng/g (Table 3.1) are considered relatively low and demonstrate possible low-level oil contamination or minor non-petrogenic PAH input. PAH concentrations of 263,870 and 390,835 ng/g (Table 3.1) are considered relatively high and strongly indicative of oil contamination.

Table 3.1. Sediment sample PAH concentration, temperature of maximum CO₂ production, and geometric mean isotopic data.

Sample ID	RP run	Total PAH, ng/g	T _{max} , °C	$\Delta^{14}\text{C}_{\text{cb}}$ *, ‰	$\delta^{13}\text{C}_{\text{cb}}$ *, ‰
Z0055	DB482	108	514	-185	-24.2
Z0094	DB490	120	511	-124	-18.9
Z0149	DB491	390835	201	-857	-27.0
Z0177	DB509	263870	224	-817	-26.4

* geometric mean value

Total PAH concentrations are used in this study, with the inclusion of perylene. Perylene is a PAH with non-petrogenic sources [Aizenshtat, 1973; Venkatesan, 1988 and references therein; Colombo *et al.*, 1989 and references therein], however Neff [1979] reports that South Louisiana crude oil contains a significant concentration of perylene (34.8 ppm). In this sample set, perylene does not account for more than 5% of total PAH, therefore its inclusion or exclusion can be considered inconsequential. It is included in our calculations as a conservative approach, but overall it is a small contribution (0.3%) to the total PAH concentrations measured in the high PAH samples.

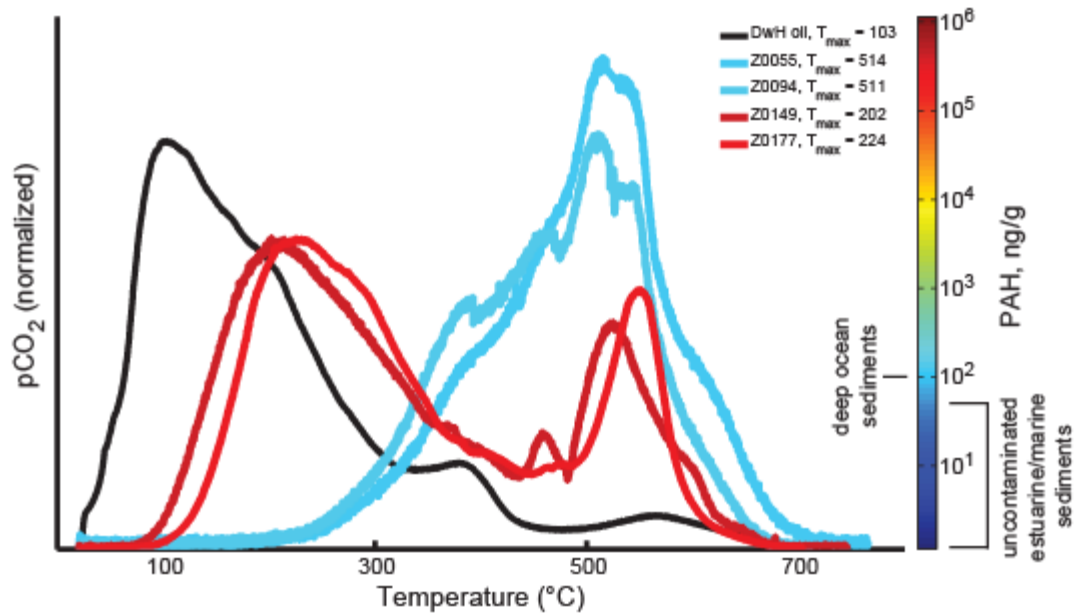


Figure 3.1. Ramped pyrolysis reaction profiles for marsh sediment samples with known PAH content. Evolution of CO₂ (oxidized pyrolysates; ordinate) is plotted over temperature (abscissa). Profile colors are scaled to the sample's total PAH concentration, in ng/g dw.

RP reaction profiles vary with PAH concentration and suggest the presence of oil in high PAH samples (Figure 3.1). Low PAH samples pyrolyze at temperatures above 300°C and are largely devoid of pyrolysis at lower temperatures. In contrast, high PAH samples present a majority of pyrolysis below 300°C. The RP profile of the Macondo

crude oil demonstrates oil's relatively low thermochemical stability (Figure 3.1).

Therefore, the pyrolysis at low temperatures observed in high PAH samples and lacking in low PAH samples can be interpreted as thermochemical indication of oil contamination. The temperature of maximum CO₂ evolution (T_{\max}) can be used to characterize thermochemical reaction profiles. For this sample set, T_{\max} is inversely proportional to PAH concentration, with high PAHs corresponding to low T_{\max} (Figure 3.2). The inverse correlation between PAHs and T_{\max} further supports oil contamination revealing itself at low temperatures in RP.

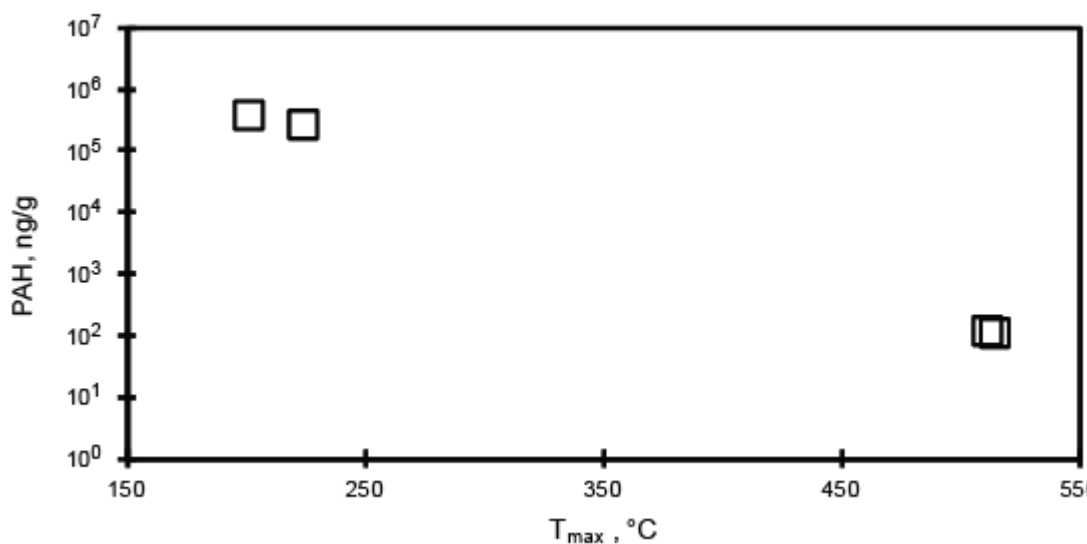


Figure 3.2. PAH concentration (ordinate) versus T_{\max} (abscissa). PAH content is inversely proportional to T_{\max} , with high PAH samples yielding maximum CO₂ production at < 250°C.

Radiocarbon data differ significantly between low and high PAH samples and confirm the presence of oil in high PAH samples. High PAH samples are much more depleted in $\Delta^{14}\text{C}$ (-993 to -560‰) than low PAH samples (-222 to -99‰; Table 3.2). For the high PAH samples, CO₂ produced at low temperatures yields $\Delta^{14}\text{C}$ values very near

Table 3.2. CO₂ aliquot temperatures, sample sizes, isotopic data, and compositional data.

CO ₂ aliquot	Temp. interval	μmol C	F _m ^r	F _m ^c	1σ F _m	Δ ¹⁴ C, ‰ ^c	1σ Δ ¹⁴ C	δ ¹³ C, ‰	1σ δ ¹³ C	f _{oil}	f _{OCb} [†]
DB482-1	amb-518	28.70	0.8465	0.8465	0.0026	-159.8	2.6	-24.2	0.1	0.22	0.78
DB482-2	518-764.5	20.09	0.7838	0.7838	0.0031	-222.1	3.1	-24.1	0.1	0.28	0.72
DB490-1	amb-392	13.13	0.9060	0.9060	0.0033	-100.7	3.3	-19.7	0.1	0.17	0.83
DB490-2	392-469	15.59	0.9077	0.9077	0.0035	-99.1	3.5	-18.8	0.1	0.18	0.82
DB490-3	469-521	13.63	0.8768	0.8768	0.0031	-129.7	3.1	-18.4	0.1	0.20	0.80
DB490-4	521-692	16.81	0.8468	0.8468	0.0032	-159.5	3.2	-18.9	0.1	0.23	0.77
DB491-1	amb-198	24.02	≤ 0.0066 [‡]	≤ 0.0066 [‡]	0.0033	≤ -993.4 [‡]	3.3	-27.7	0.1	0.99	0.01
DB491-2	198-371	50.09	0.0579	0.0579	0.0018	-942.5	1.8	-27.5	0.1	0.95	0.05
DB491-3	371-480	15.91	0.1083	0.1083	0.0047	-892.5	4.7	-27.4	0.1	0.86	0.14
DB491-4	480-676	28.17	0.4365	0.4365	0.0025	-566.8	2.5	-25.3	0.1	0.59	0.41
DB509-1	amb-202	22.52	≤ 0.0071 [‡]	≤ 0.0071 [‡]	0.0035	≤ -992.9 [‡]	3.5	-28.2	0.1	0.99	0.01
DB509-2	202-378	71.11	0.0980	0.0980	0.0018	-902.7	1.8	-27.2	0.1	0.91	0.09
DB509-3	378-460	15.61	0.1806	0.1806	0.0045	-820.7	4.5	-26.6	0.1	0.83	0.17
DB509-4	460-692	39.20	0.4429	0.4429	0.0023	-560.4	2.3	-23.9	0.1	0.59	0.41

^r raw data not subjected to blank correction; ^c blank-corrected data; amb - ambient laboratory temperature; [†] OC_b - background organic carbon

[‡] measured value and uncertainty less than process blank for AMS; age limit and corresponding Δ¹⁴C reported instead.

that of oil, while high temperature CO₂ appears to contain a mixture of ¹⁴C depleted petrogenic carbon and ¹⁴C enriched modern biogenic carbon. Oil has a hypothetical Δ¹⁴C value of -1000‰ (due to blank contamination in sample and graphite preparation and in accelerator mass spectrometric ¹⁴C/¹²C determination, it is not possible to actually measure a value of -1000‰; Table 2). The lowest temperature CO₂ aliquot collected from each high PAH sample resulted in a 2-sigma error after blank correction that was greater than the measured fraction modern (Table 3.2). In these cases, we use an age limit of 2-sigma to calculate the reported fraction modern and Δ¹⁴C values. These values represent limits and the true values are less than the reported fractions modern and Δ¹⁴C, but not measureable using the RP system coupled with AMS analysis. Low PAH samples differ considerably from oil in Δ¹⁴C, with values much closer to the modern end of the radiocarbon spectrum. However, the Δ¹⁴C values from low PAH samples are lower than expected for modern marsh biomass, which we estimate to have a radiocarbon signature of Δ¹⁴C = 77‰ (Table 3.2) based on a measurement of surface sediment from a marsh within the Barataria Basin where oil did not reach. Lower than expected radiocarbon content for low PAH samples could be further evidence of background oil contamination, or attributed to admixture of aged terrigenous carbon depleted in ¹⁴C and low in PAH. Molar quantities and isotopic values are used to calculate a geometric mean isotopic value (comparable to a bulk isotopic value) for the sample analyzed by RP using:

$$(3.3) \quad \delta_{cb} = \sum_{i=1}^n f_i \delta_i ; \text{ where } \sum_{i=1}^n f_i = 1$$

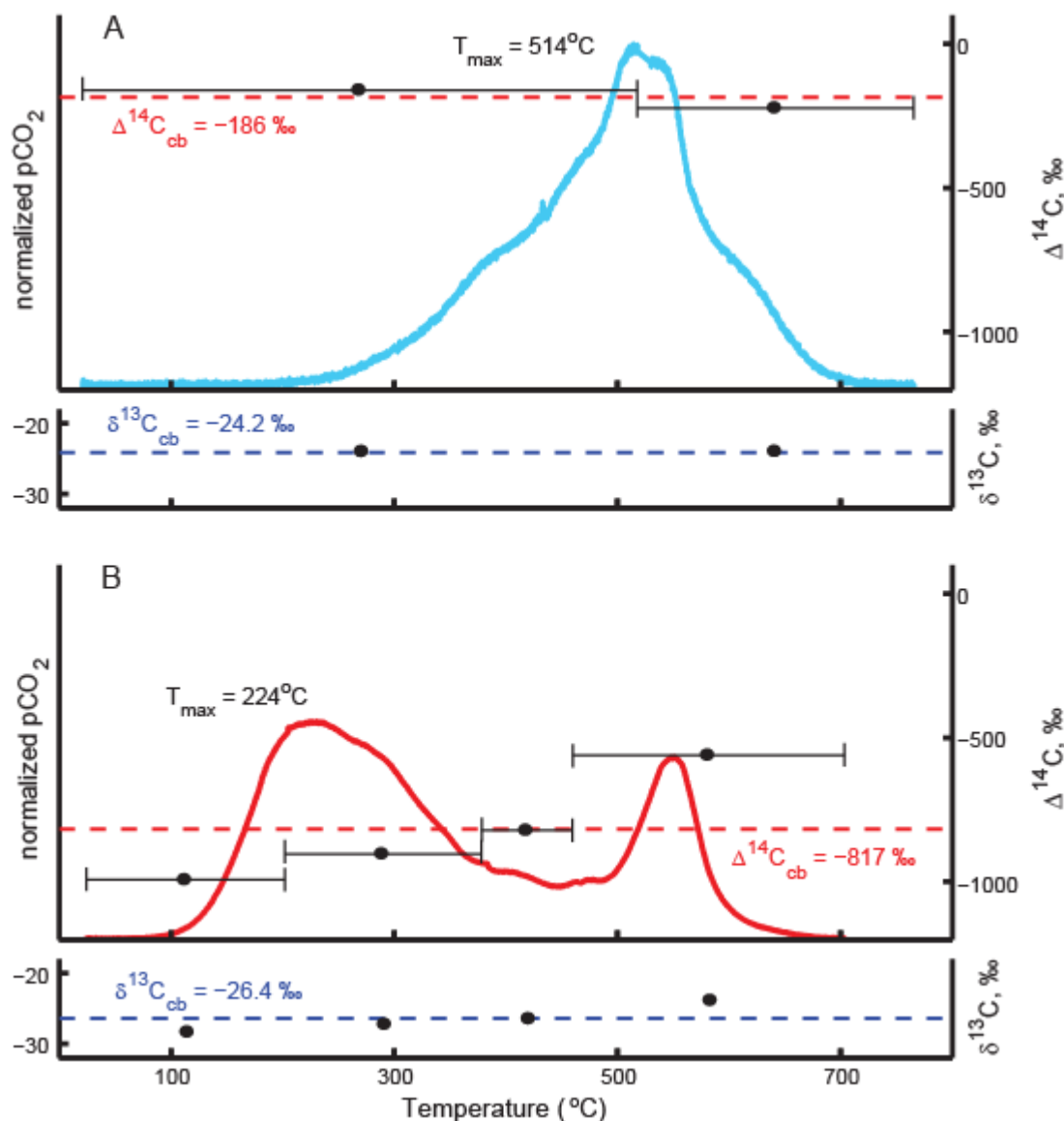


Figure 3.3. Thermochemical and isotopic data for low and high PAH samples (A and B, respectively) plotted over temperature. In the top panel, normalized and unitless CO₂ evolution plots along the left ordinate. Radiocarbon data for CO₂ aliquots (data points at centers of temperature intervals) plot on the right ordinate. Stable carbon isotopic data for the same aliquots is presented in the bottom panel. Geometric mean isotopic data were calculated from the subsamples and are presented in red (radiocarbon) and blue (stable carbon).

where δ_{cb} represents the geometric mean isotopic value, f_i represents the fraction of CO₂ from the whole sample in each aliquot, and δ_i represents the associated isotopic ratios.

Geometric mean $\Delta^{14}\text{C}_{\text{cb}}$ values range between -185 and -124‰ for low PAH samples and between -857 and -817‰ for high PAH samples (Table 3.1).

Assuming sample composition to be a binary mixture of oil and background organic carbon (OC_b), a Bayesian multi-source isotope mixing model was employed to estimate component fractions [Parnell *et al.*, 2010]. The mixing model has the same conventional formula as Equation 3.3, but δ_{cb} is replaced by δ (the measured isotopic composition from a sample comprised of a mixture of endmembers). The model is able to incorporate known variability in endmembers and analytical error associated with the isotopic measurements. Applying the model to radiocarbon data, low PAH samples yield low oil composition and high PAH samples yield high oil composition. Calculated fractions oil (f_{oil}) of 0.17 to 0.28 indicate low, but significant, oil composition in the OC of low PAH samples. Use of our measured endmember likely produces a maximum of f_{oil} in these cases; OC_b with less radiocarbon would decrease these fractions, as discussed in more detail below. Calculated f_{oil} values of 0.59 to 0.99 demonstrate the prevalence of oil in the OC of the high PAH samples. The four high PAH CO_2 aliquots collected below 380°C yield $f_{\text{oil}} > 0.91$, confirming oil as the source of the low temperature pyrolysis in these samples. The highest temperature CO_2 aliquot collected from each high PAH sample both yield f_{oil} values of 0.59, reflecting a mixture of oil and OC_b .

Stable carbon data show further indication of oil in high PAH samples, with calculated bulk values near that of oil and the most depleted values corresponding to low temperature pyrolysis. DwH oil has a $\delta^{13}\text{C}$ value of -27.3‰ (Table 3.3) and the OC_b of the study area can be characterized by the stable carbon isotopic signatures of the

dominant plant species, *S. alterniflora*, and Barataria Bay brackish marsh sediments ($\delta^{13}\text{C}$ = -12.5‰ and -17‰, respectively; Table 3.3) [Haines, 1976; Chmura *et al.*, 1987].

Stable carbon isotopic signatures for low PAH samples (full range of individual aliquots = -24.2 to -18.4‰, range of geometric mean $\delta^{13}\text{C}_{\text{cb}}$ = -24.2 to -18.9‰) differ from those

Table 3.3. Isotopic values for assumed endmembers.

Carbon source	$\Delta^{14}\text{C}$, ‰	$\delta^{13}\text{C}$, ‰
Macondo oil	-1000 ^a	-27.3 ^d
Brackish marsh OC	77 ^b	-17 ^e
<i>Spartina alterniflora</i>	77 ^c	-12.5 ^f

^a theoretical value; ^b measured

^c assumed equal to brackish marsh OC

^d avg. value from measurements and [Graham *et al.*, 2010]

^e [Chmura *et al.*, 1987]; ^f – [Haines, 1976]

for high PAH samples (full range of individual aliquots = -28.2 to -23.9‰, range of geometric mean $\delta^{13}\text{C}_{\text{cb}}$ = -27.0 to -26.4‰), which are indicative of oil. Stable carbon isotope values below that for oil may be due to fractionation during the RP reaction or inclusion of C_3 terrigenous carbon ($\delta^{13}\text{C}$ = -34 to -23‰) [Smith and Epstein, 1971].

Stable carbon isotope data from samples low in PAHs (Figure 3.3A; Table 3.2), whereas more enriched than high PAH samples, are more depleted than the assumed endmember range of -17 to -12.5‰ [Haines, 1976; Chmura *et al.*, 1987]. This could be interpreted as minor inclusion of oil ($\delta^{13}\text{C}$ = -27.3‰) or more evidence of terrigenous carbon from C_3 vegetation. The difference in stable carbon data between the two low PAH samples is likely due to them having been collected from different sediment depths. The surface sample (0-1cm) yields enriched $\delta^{13}\text{C}$ values, likely due to a higher fraction of plant

organic material. A deeper sample (20-21cm sediment depth) shows more depleted $\delta^{13}\text{C}$ values, indicative of sedimentary organic carbon [Chmura *et al.*, 1987].

The OC_b endmember radiocarbon value of our binary mixing model ($77 \pm 38.5\%$) was measured to represent authigenic input of carbon into these sediments which likely comprises the largest amount of sedimentary OC. Other endmember values are possible, but unlikely. At the most basic level, the mineral fraction of wetland soil can be considered to be delivered by fluvial processes in the Mississippi River-Atchafalaya River system (MARS), and this fraction is deposited with existing particulate organic carbon (POC). Values of $\Delta^{14}\text{C}$ of such sediments have been shown to range between -216 and -118‰ [Rosenheim *et al.*, 2013a], and these values would become more enriched in ^{14}C due to continued incorporation of authigenic carbon from primary production in the marsh. Only three of six low PAH ramped pyrolysis aliquots show $\Delta^{14}\text{C}$ within the range of MARS POC and the other three fell on either side of this range. Stable carbon isotope values of the RP aliquots support a high degree of authigenic OC coming from C_4 photosynthesis (Table 3.2), supporting our use of modern *S. alterniflora* as an endmember. Use of the MARS POC as an endmember would reduce the calculated fractions oil for low PAH samples, but would have a negligible effect on most high PAH f_{oil} values because the oil endmember is considerably less than both POC and modern marsh biomass endmembers. A value of 77‰ is a better estimate for OC_b radiocarbon than using the measured MARS POC radiocarbon data because some $\Delta^{14}\text{C}$ values from the present study are higher (-99‰ max) than the POC values and thus a binary mixing model using POC and oil endmembers would be unsolvable. Also used in the mixing model was the most negative $\Delta^{14}\text{C}$ value achieved for oil using RP AMS after having

been corrected for error ($-998.2 \pm 1.8\%$), as well as the error associated with each $\Delta^{14}\text{C}$ measurement (mean(\pm SD) of $3.1(\pm 0.9)$). The model was run with 500,000 iterations in order for its outputs to be robust despite the variability. The average(\pm SD) amount of resulting uncertainty (maximum possible fraction value minus minimum) in the calculated oil and OC_b fractions for any given CO_2 aliquot was $0.16(\pm 0.15)$ at the 95% confidence level.

A Keeling plot (technique similar to that first used by Keeling [1958]) allows independent calculation of an endmember when a range of binary mixtures has been measured. Plotting stable carbon isotopic ratios against the reciprocal of calculated fractions oil (Figure 3.4A) produces a Keeling-like plot. When linearly regressed, the data yield an estimate for the $\delta^{13}\text{C}$ value of the DwH oil ($\delta^{13}\text{C} = -27.2\%$ where $1/f_{\text{oil}}=1$) within measurement error ($1\sigma=0.1\%$) of the measured value (-27.3% , Table 3.3). Using one data point to represent each of the four bulk samples, radiocarbon data was plotted against the reciprocal of total PAH concentration (Figure 3.4B). The most negative radiocarbon value was used from each high PAH sample's CO_2 aliquots to represent the oil endmember, while the least negative radiocarbon value from each low PAH sample's CO_2 aliquots was used to characterize the OC_b endmember. A linear regression yields a y-intercept that serves as an approximation ($\Delta^{14}\text{C} = -990\%$) of the radiocarbon signature of the DwH oil. DwH oil analyzed by RP AMS yields radiocarbon data between -998 and -986% after having been corrected for instrument background and process blank. Therefore an estimate of -990% from Figure 4B can be considered acceptable. A background (oil-free) $\Delta^{14}\text{C}$ value of 77% corresponds to a PAH concentration of 91

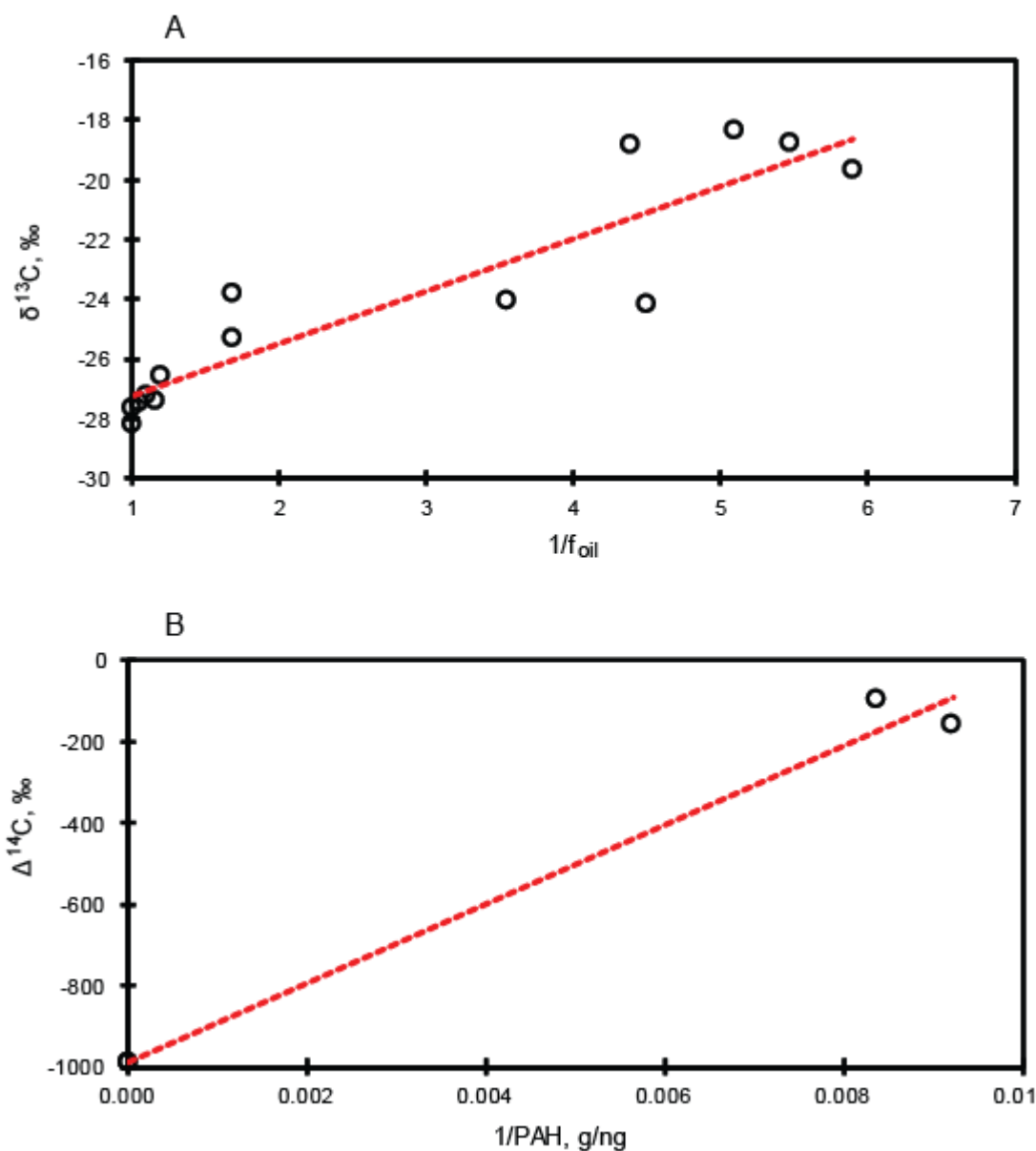


Figure 3.4. **A.** Stable carbon isotopic data for ramped pyrolysis subsamples (ordinate) against the reciprocal of the subsample's calculated fraction oil (abscissa). A linear regression yields the line $y=1.76x-29.0$, $R^2=0.8397$. Calculating at $1/f_{oil}=1$, where sample composition is 100% oil, produces a DwH oil $\delta^{13}C$ estimate of -27.2‰ , which is accurate when compared to direct measurements. **B.** The most negative radiocarbon value from the CO_2 aliquots from high PAH samples and the least negative radiocarbon value from the low PAH CO_2 aliquots (ordinate, $n=4$), are plotted against $1/PAH$ (abscissa) for the four samples. A linear regression yields $y=97445x-990$, $R^2=0.9861$. The y-intercept corresponds to very high PAH levels, implying a sample of pure oil, and yields a radiocarbon estimate of -990‰ , comparable to the theoretical value of -1000‰ . At a radiocarbon value for modern marsh biomass of 77‰ , a background PAH concentration of 91 ng/g dw is produced, near what is expected for a background (uncontaminated) level.

ng/g, which is a reasonable background estimate when compared to values from the literature of < 100 ng/g [Neff, 1979; Kennish, 1996; Windsor and Hites, 1979].

3.4 Conclusions

We show that oil contamination can be isolated by a bulk-partitioning organic carbon technique, ramped pyrolysis, whereby components are separated based on thermochemical stability. Two proxies for oil content, PAH concentration and $\Delta^{14}\text{C}$ of the organic carbon, relate to T_{max} and RP pyrolysis profile, demonstrating the utility of RP analysis for identification of oil contamination. RP reaction profiles differ significantly depending on PAH content: samples with high levels of PAHs produce significant pyrolysis at low temperatures, whereas samples with low PAH levels did not pyrolyze at low temperatures. Subsamples comprising almost entirely of oil (calculated fraction oil of 0.99) highlight the ability of RP isotope analysis to separate the different carbon sources within an oil-contaminated sediment sample. Stable carbon isotopic data further support the correlation between oil content, high PAH concentration, and pyrolysis at low temperatures. Perhaps most importantly, coupling the rather straightforward pyrolysis reaction with new generations of isotope analyzers (e.g. laser cavity ring-down flow-through $\delta^{13}\text{C}$ analyzers and gas-accepting continuous flow AMS systems [Roberts *et al.*, 2007]) may increase the utility of RP isotope analysis as a screening method for oil contamination in sediments for future spills and continued monitoring of the DwH catastrophe.

Chapter 4. Investigating oil degradation and mixing in coastal environments using ramped pyrolysis

The following chapter is written in the form of a manuscript to be submitted to a scientific journal for publication.

Abstract

Oil degradation involves change in oil's chemical composition caused by various environmental factors and can be affected by other processes, such as the mixing of the oil into the environment. Here, a ramped pyrolysis isotope technique is employed to investigate thermochemical and isotopic changes in organic material from coastal environments contaminated with oil from the 2010 BP Deepwater Horizon oil spill. Beach sediment, tar, and marsh samples subjected to various rates of mixing were collected from a barrier island and a brackish marsh in Southeast Louisiana over a period of 881 days. Stable carbon (^{13}C) and radiocarbon (^{14}C) isotopic data demonstrate a predominance of oil in the organic material. Ramped pyrolysis data show thermochemical evidence of oil degradation rates that differ depending on the rate at which oil is mixed into the environment.

4.1 Introduction

On average, spills account for 7% of the estimated 9.5 million barrels (1.3×10^6 metric tons) of oil that enters the ocean each year [NRC, 2003]. The 2010 BP Deepwater Horizon oil spill (DwH) released 4.9 million barrels (6.7×10^5 metric tons) of oil into the Gulf of Mexico from the Macondo well, an equivalent of 51% of the average annual amount of oil released into the ocean [Ramseur, 2010; Crone and Tolstoy, 2010; Griffiths, 2012]. DwH is the largest accidental oil spill to date, having released roughly ten times the quantity of oil as the 1989 *Exxon Valdez* spill in the Gulf of Alaska [Crone and Tolstoy, 2010]. In addition, DwH affected an ecologically and economically important region already at risk: the Mississippi River Delta ecosystem. This region constitutes about 37% of the coastal wetlands of the 48 conterminous United States [Couvillion *et al.*, 2011; Mendelssohn *et al.*, 2012]. These wetlands support roughly 30% of the total United States fishing industry and protect a network of infrastructure responsible for an equal proportion of the country's oil and gas supply [Mendelssohn *et al.*, 2012]. The Mississippi River Delta also suffers from significant land loss, estimated at 4877 km² during 1932 to 2010 [Couvillion *et al.*, 2011] and expected to reach 10,000+ km² by the year 2100 if measures are not taken [Blum and Roberts, 2009].

Oil is toxic and can have deleterious effects to biota [Sanders *et al.*, 1980; Kennish, 1996; Lee and Page, 1997; NRC, 2003], including marsh vegetation [Hester and Mendelssohn, 2000 and references within; Mendelssohn *et al.*, 2012], which stabilizes sediment within the Mississippi River Delta [Day *et al.*, 2011]. Oil is removed from the environment by weathering, which includes mixing and degradation. Mixing is the incorporation of oil into the environment through physical transport. Degradation refers

to chemical changes in the chemical composition of the oil mixture, including proportional changes, and the processes that cause those changes. In general, degradation of oil in the environment removes the more reactive compounds (e.g. short chain alkanes) as the more refractory compounds (e.g. high molecular weight PAHs, resins, and asphaltenes) resist degradation and persist [Wolfe, 1994]. Previous studies indicate that evaporation and biodegradation are the degradative processes that most alter the chemical composition of oil in the environment [Rashid, 1974; DeLaune *et al.*, 1990; Wolfe *et al.*, 1994; Prince *et al.*, 2003; Owens, 2008; Atlas and Hazen, 2011].

Due to the fact that the oil weathering factors vary according to location, oil persists for different lengths of time and degrades at different rates depending on the environment where it is deposited and the oil's physical form [Kingston, 2002; Reddy *et al.*, 2002; Peacock *et al.*, 2005; White *et al.*, 2005; Short *et al.*, 2007]. Kingston [2002] emphasized that oil tends to persist for longer periods on protected coastlines. This has been confirmed by the extensive work conducted on oil from the 1969 *Florida* spill in West Falmouth, Massachusetts, which has shown oil to have persisted in a salt marsh for three decades [Reddy *et al.*, 2002; Peacock *et al.*, 2005; White *et al.*, 2005].

Environmental factors also influence the form in which oil is deposited onto coastlines, which can, in turn, influence degradation rate and persistence of the oil [Irvine *et al.*, 1999; Irvine *et al.*, 2006; Short *et al.*, 2007]. Oil in the form of mousse persisted for 5+ years after the *Exxon Valdez* spill [Irvine *et al.*, 1999]. Other research conducted following that same spill identified tar balls from a separate source that had likely persisted for 25 years [Kvenvolden *et al.*, 1995]. Bence *et al.* [1996] summarized that oil

degraded much faster rate when finely dispersed in an oxygenated shoreline than when sequestered in large, subsurface accumulations.

Applying a ramped pyrolysis (RP) isotopic technique to oil in the environment aims to provide a thermochemical assessment of the degradation state of the oil. The RP technique, detailed in *Rosenheim et al.* [2008], separates bulk organic material into fractions based on differences in thermochemical stability. Factors that determine thermochemical stability include chemical composition and age [*Rosenheim et al.*, 2008]. By analyzing the entirety of organic carbon (OC) in a sample, the RP technique yields a stability profile of organic material [*Rosenheim et al.*, 2008; *Rosenheim and Galy*, 2012; *Rosenheim et al.*, 2013a; *Rosenheim et al.*, 2013b]. Oil has a different chemical composition than the background organic matter found in oil free environments and contains compounds that are more volatile than sedimentary organic matter. Multiple isotopic measurements on a single sample are accomplished by the subsampling of aliquots of CO₂ evolved over continuous temperature intervals of the thermochemical reaction. Stable carbon (¹³C) and radiocarbon (¹⁴C) isotopic measurements for each aliquot of CO₂ provide information on carbon source apportionment and age in a mixture of organic carbon [*Rosenheim et al.*, 2008; *Rosenheim and Galy*, 2012; *Rosenheim et al.*, 2013a; *Rosenheim et al.*, 2013b]. The resulting isotopic spectrum will include lighter stable carbon isotopes and near zero radiocarbon if oil is present in the sample. Isotopic data employed in a binary mixing model can estimate the oil portion of the OC because oil is isotopically distinct from coastal organic material [*Haines*, 1976; *Chmura et al.*, 1987; *Graham et al.*, 2010; *Pendergraft et al.*, 2013].

The purpose of this study is to test the hypothesis that the rate of oil degradation is independent of the rate of oil mixing into the environment. To test this hypothesis, samples from oil-impacted coastal environments subject to different rates of mixing were collected during a period of 881 days. Ramped pyrolysis isotope analysis was employed to produce a thermochemical assessment of the relative rates of degradation of beach sediment, tar, and marsh samples. Additionally, an attempt is made to connect specific oil degradation processes to changes in thermochemical profiles. Isotopic data are used to connect pyrolysis data to oil content and isotopic signals of oil degradation versus fractionation are discussed.

4.2 Methods

4.2.1 Sample locations, types, and processing

Grand Isle and Bay Jimmy in Southeastern Louisiana were sampled over the course of 881 days following the Macondo well blow out that initiated DWH (Figures 2.1, 2.3). Grand Isle, a barrier island at the convergence of Barataria Bay and the Gulf of Mexico, is a low latitude, sandy beach affected by moderate wave energy and seasonal, high energy storms, including hurricanes. Two locations at Grand Isle were repeatedly sampled for sediment: a relatively high energy beach site, exposed to wave energy from the Gulf of Mexico, and a relatively low energy beach site located on the protected lagoon side of Grand Isle facing Barataria Bay. The sampling location of Bay Jimmy lies within the brackish marsh region of the Barataria Basin [*Chmura et al.*, 1987]. Although an erosive marsh with ~10's of km of southerly fetch, the Bay Jimmy site is considered a

lower energy environment compared to the two barrier island sites. For all three locations, higher shoreline energy implies a greater rate of mixing of oil and sediments and higher availability of nutrients and oxygen. Oxygen availability is likely lowest at Bay Jimmy, as marsh sediments are oxygen-limited [*Shin et al.*, 2000] and primary production is highest of the three sampling sites.

Sediment sampling at Grand Isle involved digging trenches near the shoreline at the two fixed sites and collecting sediment from dark bands observed in the trench walls (Figure 2.2). Sediment was also collected from the trench bottom, which often presented an oily sheen, along with an odor of petrochemicals within the trench. Other samples collected at Grand Isle included oil on the water and beach surface at early sampling dates; oil/tar coating on a rocky groin; and conglomerates on the beach surface resembling tar balls. These samples were collected near the fixed high and low energy sites and were categorized as tar samples. Samples from Bay Jimmy are categorized as marsh samples and include oil deposits; vegetation with and without visible oil; and a 50 cm surface core collected with a hand auger. Samples were collected in glassware capped with aluminum foil (both precombusted at 525°C for ≥ 2 hs) and a plastic lid, and stored at $\leq 0^\circ\text{C}$ under nitrogen gas. Some samples from Bay Jimmy were collected in sealed bags (Whirlpack®/Ziploc®) when precombusted glassware was unavailable.

Samples from Grand Isle were ground with a mortar and pestle, acidified with 10% HCl to remove inorganic carbon, then repeatedly rinsed with deionized water, centrifuged, and decanted until a pH~6 was reached, then finally dried at 60°C for 24 hs or until completely dry. Samples from Bay Jimmy were inspected for shell fragments, which were removed when found, then dried similarly to the Grand Isle samples.

4.2.2 Analyses

Organic carbon content (%OC) and bulk stable carbon isotopic composition ($\delta^{13}\text{C}$) were measured on 127 beach sediment, tar, and marsh samples at the Stable Isotope Laboratory at Tulane University (SILTU) using an Elementar vario MICRO cube elemental analyzer interfaced to an Isoprime dual inlet isotope ratio mass spectrometer in continuous flow mode (EA-IRMS). %OC values were used to calculate sample size and expected yields for RP analysis in order to evaluate for complete carbon recovery. A subset of the 127 samples was screened for reaction profiles using RP without the collection of CO_2 for isotopic analysis. Based on this screening, 16 representative samples were re-analyzed by RP with collection and subsequent isotopic analysis of CO_2 aliquots. The same RP procedure was used as in previous studies [Rosenheim *et al.*, 2008; Rosenheim and Galy, 2012; Rosenheim *et al.*, 2013a; Rosenheim *et al.*, 2013b] and more details of the analysis can be found in Rosenheim *et al.* [2008]. Briefly, samples were heated at 5°C min^{-1} in anoxic conditions until all OC pyrolyzed ($\sim 750^\circ\text{C}$). Pyrolysis products were continually flushed from the reaction chamber (0% O_2) as they formed and then oxidized in a combustion chamber ($\sim 8\% \text{O}_2$). The evolving CO_2 was continually measured with an infrared gas analyzer, then cryogenically collected in continuous aliquots. Subsampling was conducted with the objective of collecting individual pyrolysis peaks representing thermochemically distinct fractions of the sample. Radiocarbon and stable carbon analyses of the CO_2 aliquots was accomplished at the National Ocean Sciences Accelerator Mass Spectrometer Facility (NOSAMS) at the Woods Hole Oceanographic Institution. Radiocarbon data, reported in Δ notation and per mil (‰) units, were calculated using:

$$(4.1) \quad \Delta^{14}\text{C} \cong \delta^{14}\text{C} = (F_m - 1) \times 1000$$

where F_m is fraction modern. We assume $\Delta^{14}\text{C}$ to be equivalent to $\delta^{14}\text{C}$ [Stuiver and Pollach, 1977] because less than one year passed between sample collection and measurement. Stable carbon isotopic composition is expressed in δ notation and ‰ units, relative to the Pee Dee Belemnite (PDB) standard, according to:

$$(4.2) \quad \delta^{13}\text{C} = \left(\frac{R_x - R_{std}}{R_{std}} \right) \times 1000$$

where R is the ratio $^{13}\text{C}/^{12}\text{C}$, x denotes the sample, and std denotes the standard [Sharp, 2007].

4.3 Results

Compositional (%OC) and bulk stable carbon isotopic ($\delta^{13}\text{C}$) data for 127 beach sediment, tar, and marsh samples show varying trends. Beach sediment samples collected at Grand Isle, Louisiana after the Macondo well blow out decrease in %OC (range of 0.1 to 14.0%, mean($\pm 1\sigma$) of 1.7(± 3.0)%) over a span of 881 days (Figure 4.1A). No such trend is observed for tar samples from Grand Isle (range of 0.2 to 86.0%, mean($\pm 1\sigma$) of 22.0(± 25.1)%) collected during the same period (Figure 4.1B). Compositional data for marsh samples collected from Bay Jimmy (range of 3.6 to 74.9%, mean($\pm 1\sigma$) of 23.8(± 21.2)%) over 694 d post DwH show a range of values for the first date with a subsequent decreasing trend (Figure 4.1C). Stable carbon isotopic data are most depleted on average for tar samples (mean($\pm 1\sigma$) of -26.5(± 2.1)‰), less depleted for

beach sediment samples (mean($\pm 1\sigma$) of -24.8(± 1.7)‰), and the least depleted for marsh samples (mean($\pm 1\sigma$) of -22.1(± 3.8)‰).

Time series of RP data present varying thermochemical trends amongst the different sample types and locations (Figure 4.2). The evolution of CO₂ over the pyrolysis ramp estimates decomposition reaction rates $\left(\frac{d[Reactants]}{dt}\right)$ for the mixture of compounds comprising the OC because temperature is linear with time [Rosenheim *et al.*, 2013a]. RP data of CO₂ concentration versus temperature are normalized to allow for comparison between samples with different amounts of carbon. As a result, the areas under reaction profiles are equal and reaction profiles should be interpreted by considering what fraction of the sample pyrolyzes at which temperatures. The ramped pyrolysis technique heats samples to as high as 1000°C and this study uses the following temperature distinctions: temperatures < 300°C are considered low; temperatures 300-500°C are considered mid-range; and temperatures > 500°C are considered high. Grand Isle sediment from both high and low energy sites at experience a majority of pyrolysis at lower temperatures 88 d, but at 678 d pyrolyze almost entirely at mid-to-high temperatures (Figure 4.2A and B). Tar samples from Grand Isle differ from the sediment samples in their RP data (Figure 4.2C) by continuing to yield a majority of pyrolysis below 300°C through 881 d. Additionally, a tar ball from 678 d presents an anomalous reaction profile. RP data for marsh samples from Bay Jimmy are characterized by low temperature pyrolysis persisting through 535 d, a mid-temperature peak at 337 d that shifts to higher temperatures at 535 d, and a sample at 694 d largely devoid of pyrolysis below 300°C (Figure 4.2D).

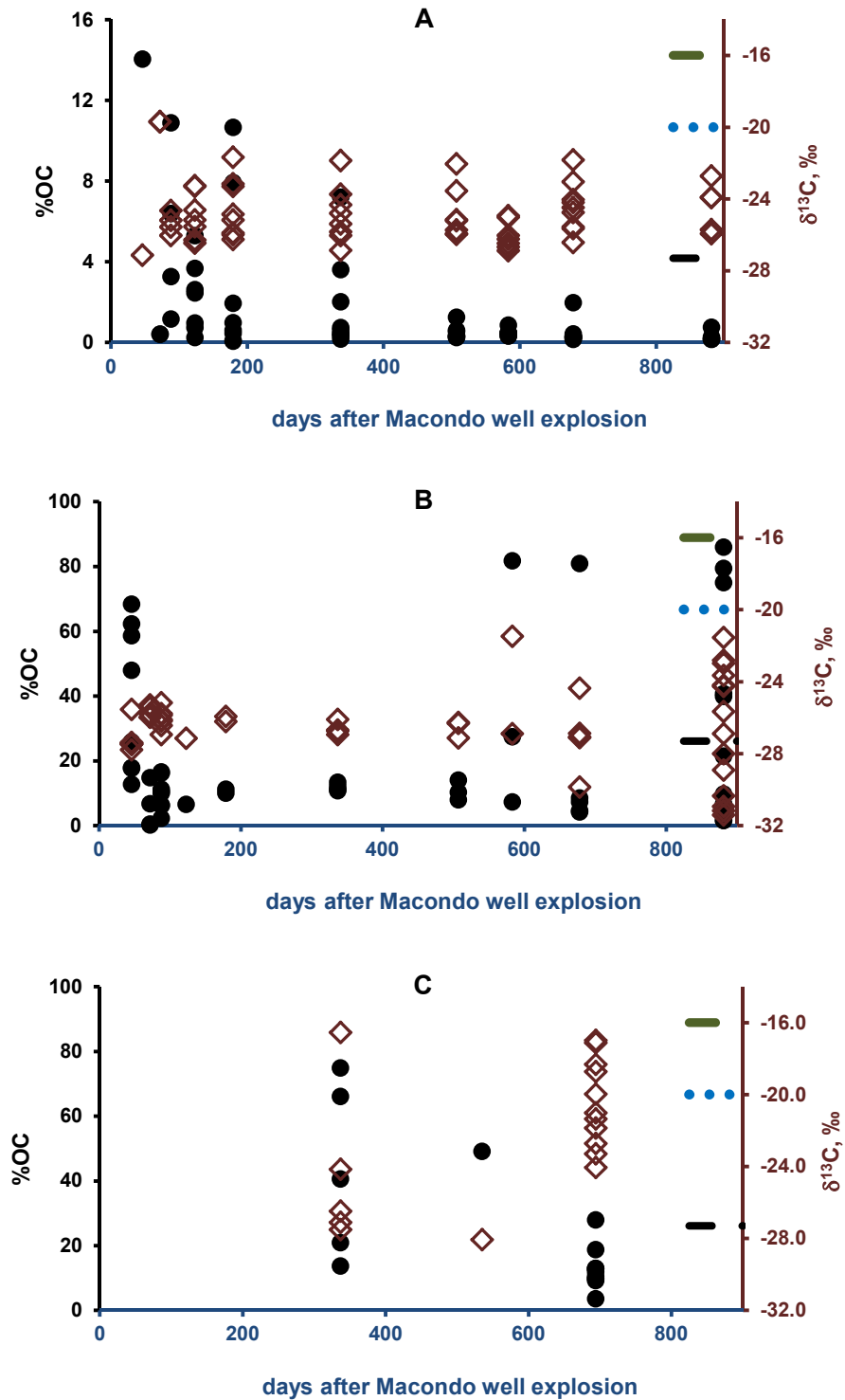


Figure 4.1. %OC, plotted as black circles scaled to the left axis, and $\delta^{13}\text{C}$, plotted as red diamonds scaled to the right axis, over time. Data are for the 127 beach sediment, tar, and marsh samples. **A.** Beach sediment. **B.** Tar. **C.** Marsh samples. Right axis marked at $\delta^{13}\text{C}$ values for Macondo oil (-27.3‰, black), marine organic carbon (-20‰, blue), and brackish marsh (-16‰, green). $\delta^{13}\text{C}$ on VPDB scale.

Isotopic data for CO₂ aliquots collected during ramped pyrolysis (Tables 4.1 and 4.2, Figure 4.3) indicate the source of the carbon in the CO₂ presented in the ramped pyrolysis data. Very negative radiocarbon values (mean($\pm 1\sigma$) of -892(± 215)‰) dominate the aliquots of CO₂ collected during RP, with the exception of the Bay Jimmy 694 d sample. Stable carbon isotopic signatures (mean($\pm 1\sigma$) of -27.4(± 2.0)‰ PDB) were also depleted on average. CO₂ aliquot quantities and isotopic values are used to calculate a geometric mean isotopic value (equivalent to a bulk isotopic value) using:

$$(4.3) \quad \delta_{cb} = \sum_{i=1}^n f_i \delta_i ; \text{ where } \sum_{i=1}^n f_i = 1$$

where δ_{cb} represents the geometric mean isotopic value, f_i represents the fraction of CO₂ from the whole sample in each aliquot, and δ_i represents the associated isotopic ratios. $\Delta^{14}\text{C}_{cb}$ (range of -995 to 0, mean($\pm 1\sigma$) of -874(241)‰) and $\delta^{13}\text{C}_{cb}$ (range of -28.8 to -20.5; mean($\pm 1\sigma$) of -27.4(± 2.0)‰) can be compared to bulk isotopic data, such as the $\delta^{13}\text{C}$ data generated by EA-IRMS in this study (Table 4.1). Assuming sample composition to be a binary mixture of oil and background organic carbon (OC_b), a mixing model was employed to estimate component fractions. The mixing model has the same conventional formula as Equation 4.3, but δ_{cb} is replaced by δ (the measured isotopic composition from a sample comprised of a mixture of endmembers). Calculated fraction oil (f_{oil}) values from radiocarbon data and Equation 4.2

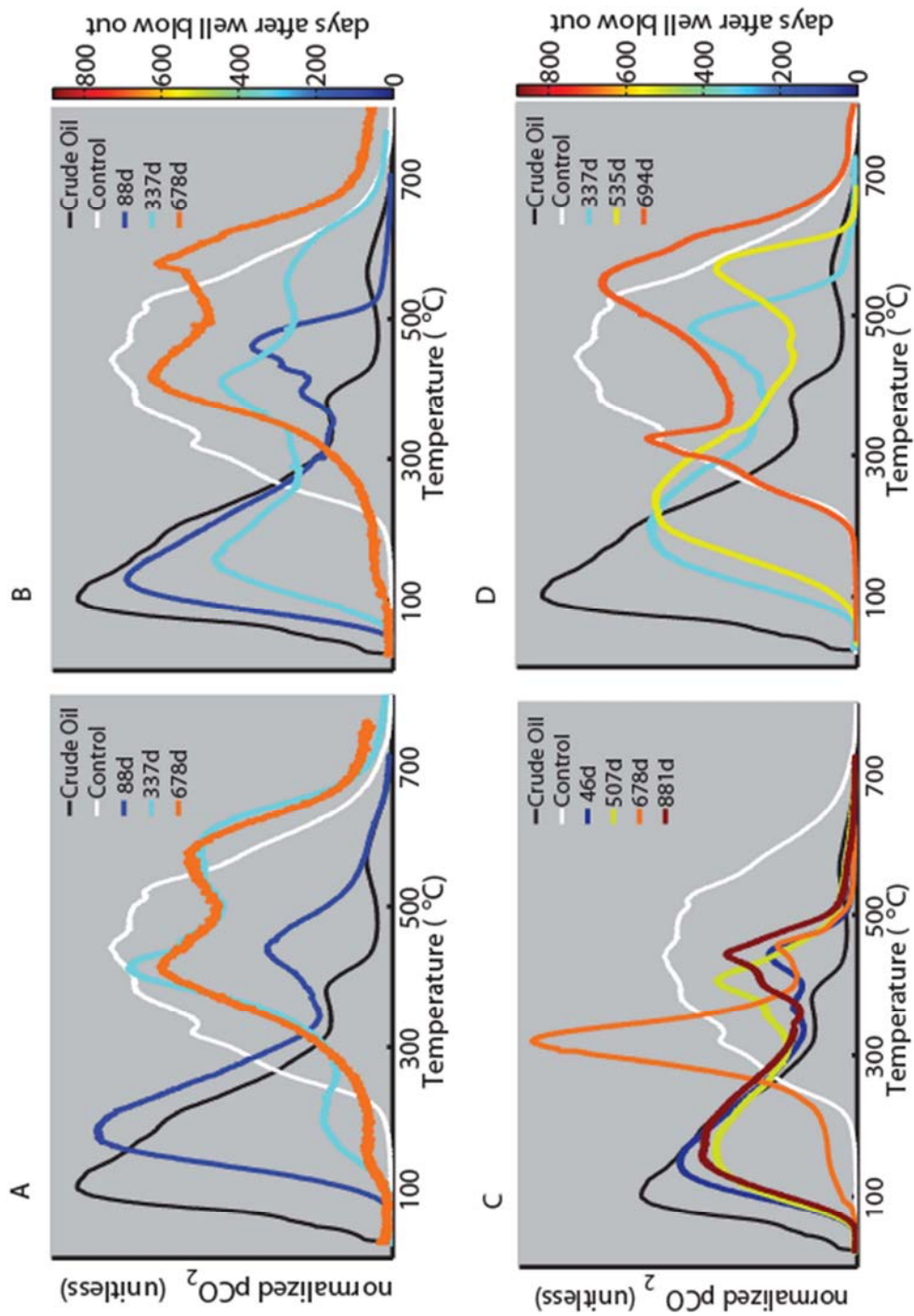


Figure 4.2. RP reaction profile trends over time for four samples types. Individual plots display evolution of CO_2 over a smooth temperature ramp to 800°C. **A.** Grand Isle beach sediments from the high energy site. **B.** Grand Isle beach sediments from the low energy site. **C.** Marsh samples from Bay Jimmy within Barataria Bay. Profiles for Macondo crude oil (black) and a control sample from unopened marsh (white) given for reference.

quantify oil in the CO₂ aliquots (Tables 4.1 and 4.2) and show high portions of OC comprised of oil (mean($\pm 1\sigma$) of 0.900(± 0.199)). Applying to the mixing model geometric mean isotopic data calculated using Equation 4.3 yields calculated bulk fraction oil ($f_{\text{oil-cb}}$) values that quantify oil for entire beach sediment, tar, and marsh samples (mean($\pm 1\sigma$) of 0.88(± 0.22); Table 4.1).

Plotting isotopic data together with thermochemical data connects isotopic values with the corresponding reaction profile intervals (Figures 4.5 - 4.8). Thermochemical and radiocarbon data are presented together on a plot with two ordinate axes, normalized CO₂ concentration on the left and $\Delta^{14}\text{C}$ on the right, and a panel below containing $\delta^{13}\text{C}$ values for the same subsamples, all plotted over a single temperature abscissa. The temperature of maximum CO₂ evolution (T_{max}) is useful to compare reaction profiles. Radiocarbon data are plotted as points centered on horizontal lines that encompass the temperature interval over which CO₂ was evolved and collected. The vertical position of the points corresponds to $\Delta^{14}\text{C}$ values (right y-axis). Data points near the bottom of the plot show radiocarbon values approaching -1000‰ and thus indicate a high fraction oil in the OC. Stable carbon isotopic data for the same aliquots are presented in the bottom panel, with lower values being indicative of oil. Geometric mean isotopic values are presented as dotted lines labeled with the associated values.

sample	day	%OC	$\Delta^{14}\text{C}_{\text{cb}}$, ‰	$f_{\text{oil-cb}}$	$\delta^{13}\text{C}$, ‰*	$\delta^{13}\text{C}_{\text{cb}}$, ‰*	$\delta^{13}\text{C}_{\text{cb}} - \delta^{13}\text{C}$, ‰*
GI-A-20100716-4-sed	88	3.26	-985	0.986	-25.2	-	-
GI-A-20110322-3-sed	337	0.46	-854	0.865	-25.8	-27.9	-2.0
GI-A1-20120226-2-sed	678	0.27	-890	0.898	-25.6	-28.4	-2.8
GI-A2-20120226-2-sed	678	0.31	-792	0.807	-24.0	-27.3	-3.2
GI-B-20100716-7-sed	88	10.88	-992	0.993	-25.6	-28.8	-3.2
GI-B-20110322-3-sed	337	3.61	-954	0.957	-25.4	-28.5	-3.1
GI-B-20120226-2-sed	678	0.14	-884	0.892	-24.2	-27.9	-3.8
GI-A-20100604-1-oil	46	25.83	-994	0.994	-27.5	-28.5	-1.0
GI-B-20110908-1-tar	507	14.04	-983	0.985	-26.3	-28.4	-2.1
GI-20120226-1-tar	678	4.54	-976	0.978	-26.9	-26.7	0.2
GI-20120226-3-tar	678	80.87	-995	0.995	-29.9	-28.5	1.4
GI-A-20120916-1-tar	881	6.72	-980	0.982	-25.7	-28.6	-2.9
GI-20120916-3-tar	881	3.16	-893	0.900	-22.8	-26.4	-3.6
BBB-1-20110322-1-tar	337	40.56	-940	0.944	-28.7	-27.7	0.9
BB-A-3-20111006-1-tar	535	49.07	-867	0.876	-28.5	-27.3	1.2
BJ-20120313-2-plant	694	12.88	0	0.072	-20.0	-20.5	-0.5
min			-995	0.072	-29.9	-28.8	-3.8
max			0	0.995	-20.0	-20.5	1.4
mean			-874	0.883	-25.7	-27.4	-1.6
1 σ			241	0.224	2.4	2.0	1.8

* $\delta^{13}\text{C}$ wrt PDB

Table 4.1. EA-IRMS compositional and isotopic data and NOSAMS isotopic data for samples analyzed by both techniques. The “cb” subscript indicates the geometric mean calculated from CO_2 subsamples measured at NOSAMS. $\delta^{13}\text{C}$ on PDB scale.

Sample (RP analysis ID)	day	Upper Temp. Limit	$\Delta^{14}\text{C}$, ‰	1σ $\Delta^{14}\text{C}$	$\delta^{13}\text{C}$, ‰	1σ $\delta^{13}\text{C}$	f_{oil}	f_{ocb}
GI-A-20100716-4-sed (DB475)	88	162	-987	1.4	-28.4	0.1	0.988	0.012
		205	-994	1.3	-28.1	0.1	0.994	0.006
		362	-986	1.8	-27.9	0.1	0.987	0.013
		446	-976	1.4	-27.6	0.1	0.978	0.022
		714	-976	1.4	-	-	0.978	0.022
GI-A-20110322-3-sed (DB639)	337	272	-936	1.5	-29.8	0.1	0.941	0.059
		500	-783	1.6	-27.2	0.1	0.799	0.201
		824	-911	1.1	-28.0	0.1	0.917	0.083
GI-A1-20120226-2-sed (DB643)	678	503	-846	1.3	-28.4	0.1	0.857	0.143
		752	-953	1.1	-28.6	0.1	0.956	0.044
GI-A2-20120226-2-sed (DB661)	678	501	-711	1.5	-26.8	0.1	0.731	0.269
		780	-903	2.3	-28.0	0.1	0.910	0.090
GI-B-20100716-7-sed (DB658)	88	336	-995	0.4	-29.3	0.1	0.996	0.004
		418	-988	1.0	-28.8	0.1	0.989	0.011
		702	-983	0.6	-26.8	0.1	0.984	0.016
GI-B-20110322-3-sed (DB670)	337	285	-979	0.8	-29.3	0.1	0.980	0.020
		499	-917	1.5	-27.7	0.1	0.923	0.077
		763	-968	1.1	-28.2	0.1	0.971	0.029
GI-B-20120226-2-sed (DB665)	678	487	-838	1.6	-27.6	0.1	0.850	0.150
		824	-935	1.1	-28.4	0.1	0.940	0.060
GI-A-20100604-1-oil (DB649)	46	347	-995	1.0	-28.9	0.1	0.996	0.004
		401	-992	1.0	-29.4	0.1	0.992	0.008
		661	-988	0.5	-26.5	0.1	0.989	0.011
GI-B-20110908-1-tar (DB646)	507	315	-991	0.4	-28.9	0.1	0.991	0.009
		700	-974	0.6	-27.6	0.1	0.975	0.025
GI-20120226-1-tar (DB341)	678	334	-981	0.5	-27.7	0.1	0.983	0.017
		722	-972	0.6	-25.8	0.1	0.974	0.026
GI-20120226-3-tar (DB653)	678	199	-994	1.0	-26.2	0.1	0.994	0.006
		410	-996	0.3	-29.2	0.1	0.997	0.003
		626	-987	0.6	-26.6	0.1	0.988	0.012
GI-A-20120916-1-tar (DB654)	881	337	-990	0.4	-29.4	0.1	0.991	0.009
		710	-963	0.8	-27.2	0.1	0.966	0.034
GI-20120916-3-tar (DB656)	881	238	-965	1.4	-27.5	0.1	0.967	0.033
		356	-882	1.6	-27.2	0.1	0.890	0.110
		676	-880	1.4	-25.8	0.1	0.888	0.112
BBB-1-20110322-1-tar (DB657)	337	400	-970	1.4	-28.7	0.1	0.972	0.028
		676	-877	1.5	-25.8	0.1	0.886	0.114
BB-A-3-20111006-1-tar (DB659)	535	329	-954	0.8	-28.5	0.1	0.958	0.042
		441	-863	1.4	-27.9	0.1	0.873	0.127
		681	-695	1.8	-24.5	0.1	0.717	0.283
BJ-20120313-2-plant (DB662)	694	376	-4.2	3.5	-20.0	0.1	0.075	0.925
		804	1.9	3.8	-20.7	0.1	0.070	0.930
min			-996		-29.8		0.070	0.003
max			1.9		-20.0		0.997	0.930
mean			-892		-27.4		0.900	0.100
1σ			215		2.0		0.199	0.199

Table 4.2. Isotopic data for CO₂ aliquots from 16 samples analyzed by RP. $\delta^{13}\text{C}$ wrt PDB

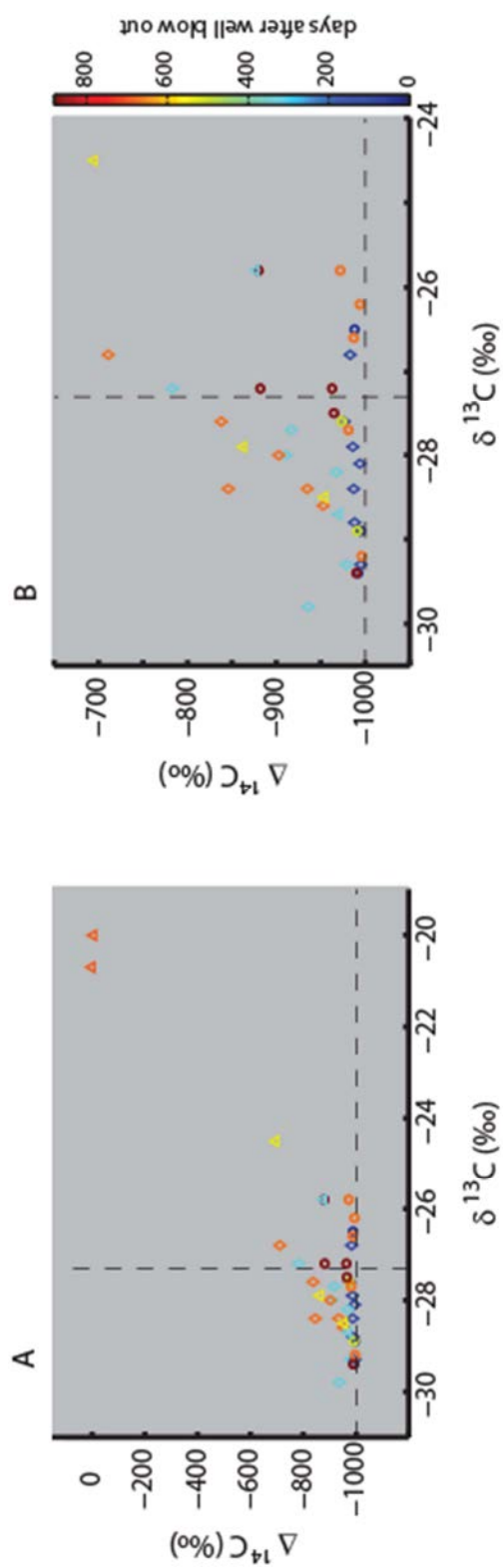


Figure 4.3. $\Delta^{14}\text{C}$ vs. $\delta^{13}\text{C}$ for CO_2 aliquots generated during ramped pyrolysis. Diamonds – Beach sediment; Circles – Tar samples; Triangles – Marsh samples. Marker color scaled to sampling date with respect to well head blow out. Black dotted lines at $\Delta^{14}\text{C}$ and $\delta^{13}\text{C}$ values for Macondo oil. **A.** All data. **B.** Main data cluster, excluding potential outliers at top right in A. The congregation of data near oil's isotopic signatures (the intersection of the dotted lines) indicates the majority of OC in those samples.

4.4 Discussion

4.4.1 %OC and $\delta^{13}\text{C}$ of sediment, tar, and marsh samples

Compositional (%OC) and bulk stable carbon isotope ($\delta^{13}\text{C}$) analyses of 127 beach sediment, tar, and marsh samples present trends of oil weathering that vary according to sample type. In general, high %OC values and low $\delta^{13}\text{C}$ values are indicative of oil content. Thus, the decrease in %OC in Grand Isle sediment samples (Figure 4.1A) demonstrates a decrease in oil due to the general process of oil weathering. $\delta^{13}\text{C}$ data (mean($\pm 1\sigma$) of $-24.8(\pm 1.7)\text{‰}$) are more depleted than an expected marine signature of -20‰ , indicating the presence of oil within the beach sediment. For the marsh samples (Figure 4.1C), the earliest sampling date shows high %OC values and low $\delta^{13}\text{C}$ values that are indicative of oil. By the last sampling date, the data separate into relatively low %OC and relatively high $\delta^{13}\text{C}$ values, showing a reduction in oil proportion due to weathering. Thus a weathering trend is apparent in the marsh data, although the scarcity of data prevents robust comparisons to the beach sediment. Compositional data for tar samples from Grand Isle (Figure 4.1B) show no decrease over time, with values as high as 86% at 881 d. These data indicate preservation and persistence of oil in the form of tar balls and tar coatings on rocks, and minimal incorporation of background organic carbon (OC_b). Tar sample $\delta^{13}\text{C}$ data (mean($\pm 1\sigma$) of $-26.5(2.1)\text{‰}$) display a strong oil influence through 881 d, with greater variability at the last sampling date likely due to a greater diversity of samples collected. Although %OC and bulk $\delta^{13}\text{C}$ data indicate oil weathering, they provide little insight into specific changes to oil resulting from degradation.

4.4.2 Conceptual model of ramped pyrolysis profiles for oiled sediment

Changes in thermochemical data can result from changes in the relative quantities of oil and background organic material (OM_b), as occurs in mixing, or from changes in the chemical composition of each component, as in oil degradation. Thus, interpretation of the ramped-pyrolysis data is dependent upon identifying the source(s) of OC observed in the thermochemical data, which is accomplished using isotopic measurements [Pendergraft *et al.*, 2013]. Oil content was shown to affect the pyrolysis profile of OC in Barataria Bay [Pendergraft *et al.*, 2013]. Focusing on certain mixing and degradation scenarios, I propose different types of ramped pyrolysis profiles using Gaussian curves (Figure 4.4). A bimodal RP reaction profile is expected for a mixture of oil and OC_b without chemical interaction (Figure 4.4A). Mixing is expected to result in a diminished oil peak from effective dilution of oil with admixture of OC_b (Figure 4.4B). Degradation, which changes the chemical composition of oil, is expected to change the shape of the oil RP profile to higher temperatures due to the loss of more volatile components and conversion of other components into more stable molecules [Sofer, 1984; Wolfe *et al.*, 1994; Arey *et al.*, 2007; Boehm *et al.*, 2008] (Figure 4.4C). By extension, degraded oil mixed with OC_b (Figure 4.4D) is expected to result in a reaction profile distinct from any combination of undegraded oil and OC_b . Therefore, an RP profile with an attenuated low-temperature peak with respect to the OC_b peak will be interpreted as mixing, whereas other changes in reaction profiles will be interpreted as degradation. This conceptual model facilitates interpretation of RP data from mixtures that lie between the endmembers presented in Chapter 3 and Pendergraft *et al.* [2013].

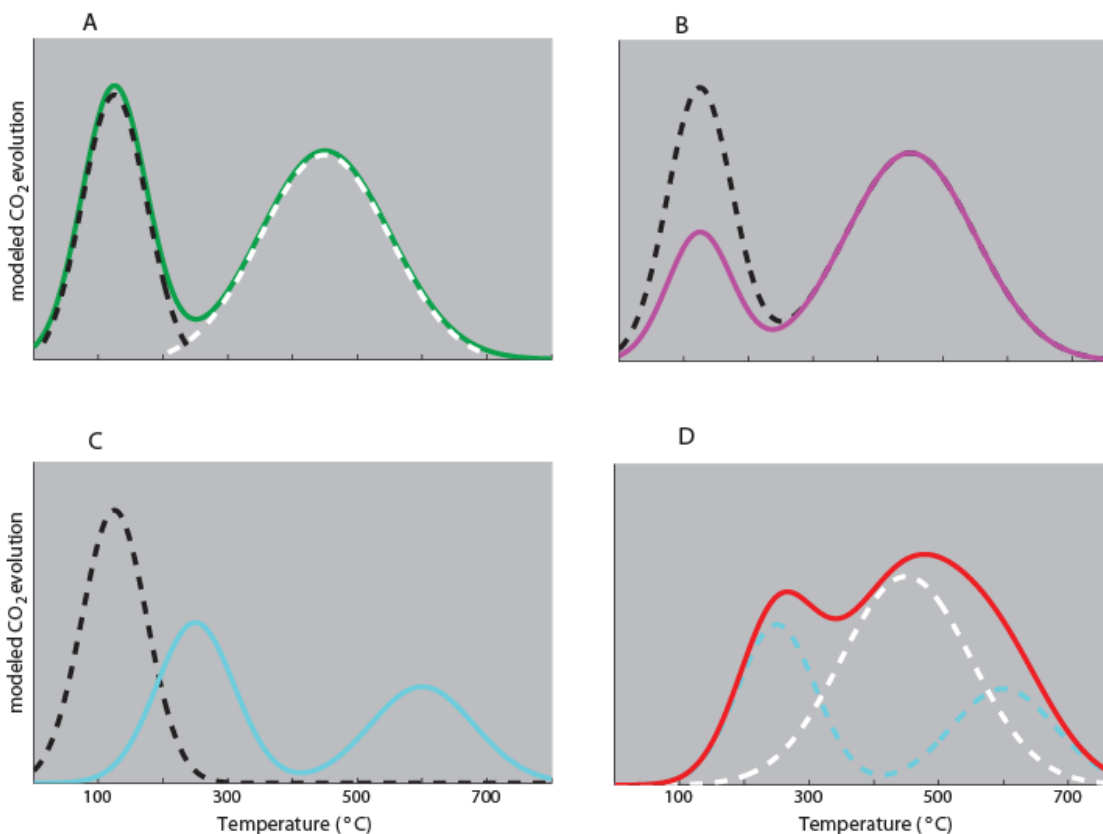


Figure 4.4. Modeling of possible changes in RP data. The black dotted curve represents an initial reaction profile for oil prior to mixing and degradation. **A.** The green profile is the theoretical result of a mixture of oil (black) and OC_b (white). **B.** Mixing is expected to decrease the oil signal (black) while not affecting the OC_b profile. The resulting profile (purple) resembles the initial composite curve (green) but has a decreased oil peak. **C.** Degradation is expected to change the shape of the oil itself, resulting in a profile for degraded oil (blue) that differs from that of undegraded oil (black). **D.** The composite profile (red) of degraded oil + OC_b is expected to differ significantly from the composite profile of undegraded oil + OC_b (green). In the red profile, oil no longer exists as one, easily identifiable peak, and therefore must be detected separately from OC_b.

4.4.3 Isotopic data for RP CO₂ aliquots

Radiocarbon and stable carbon isotopic data demonstrate oil to be the major source of OC in the 16 samples subjected to RP isotopic analysis. The expected sources of carbon for these samples and their associated $\delta^{13}\text{C}$ values are oil (-27.3‰), marine organic material (-20‰), and brackish marsh organic material (-17 to -12.5‰) [Haines, 1979; Chmura *et al.*, 1987; Sharp, 2007]. Stable carbon isotopic data for the samples analyzed by RP (mean($\pm 1\sigma$) for CO₂ aliquots = -25.7(± 2.4)‰; mean($\pm 1\sigma$) for $\delta^{13}\text{C}_{\text{cb}}$ = -

27.4 (± 2.0)‰) indicate significant levels of oil in all the samples, yielding a mean $\delta^{13}\text{C}_{\text{cb}}$ value within measurement error ($1\sigma=0.1$ ‰) of the Macondo oil. However, the fact that 64% of the RP CO_2 aliquots yield $\delta^{13}\text{C}$ data below the lowest expected endmember (Figure 4.3) indicates that stable carbon isotopes are likely fractionated during RP, as previously observed [Rosenheim and Galy, 2012; Rosenheim et al., 2013b]. In addition, geometric mean values for the CO_2 aliquots measured at NOSAMS are consistently below bulk values measured at SILTU, by -1.6‰ on average (Table 4.1). Though this may be further indication of fractionation during RP, analytical differences between two laboratories using separate techniques to measure $\delta^{13}\text{C}$ is another possible reason. Radiocarbon data also show that oil is the major OC source in the RP samples (Figure 4.3), yielding high calculated fraction oil values (mean($\pm 1\sigma$) for CO_2 aliquots = 0.900(± 0.199); mean($\pm 1\sigma$) for $f_{\text{oil-cb}} = 0.88(\pm 0.22)$). The ability of the RP technique to separate oil from OC_b is supported by aliquots with very negative radiocarbon values (minimum of -996‰) and correspondingly high calculated fraction oil values (maximum of 0.997). A maximum $\Delta^{14}\text{C}$ value of -880‰, corresponding to a minimum f_{oil} value of 0.888, for tar samples from Grand Isle confirm a petrogenic composition.

4.4.4 Interpretation of reaction profiles

Considering that isotopic data demonstrate the OC is dominated by oil for nearly all samples, changes in thermochemical stability for this dataset (Figure 4.2) can generally be interpreted as evidence of oil degradation. Therefore, Figure 4.2 presents varying trends of oil degradation in high and low energy beach sediment, tar, and, marsh

samples. Oil degradation in the pyrolysis profiles is most apparent in a decrease in low temperature pyrolysis over time.

In this study, oil degradation occurs fastest in beach sediments, with high energy beach sediments presenting a faster rate of oil degradation than low energy beach sediments. RP data for sediment from the Grand Isle high and low energy sites (Figure 4.2A and B, respectively) display similar trends of a decrease in low temperature pyrolysis and a relative increase in high temperature pyrolysis. Isotopic data for each reaction profile shows oil to be the major source of OC for both sites (Figures 4.5, 4.6). Reaction profiles for the two sites vary somewhat at 88 d, with differing offsets from the crude oil peak (Figure 4.2A, B) suggesting differential weathering. The degradative processes that would have acted on the oil during this period are dissolution of water-soluble compounds as oil travelled from the wellhead through the water column, evaporation and photo-oxidation/photodegradation when on the surface, and biodegradation along the entire path through mixing into the barrier island sediments. RP data from sediment at the high and low energy beach sites differ most at 337 d, with relatively more low temperature pyrolysis persisting at the low energy site (Figure 4.2A, B). This suggests a faster degradation rate at the high energy location, in agreement with *Rashid's* [1974] conclusion that mechanical energy is a significant factor in oil weathering. Greater wave energy at the high energy site resulted in faster dispersion of the oil, a higher supply of oxygen for oil-consuming microbes, and a resulting quicker degradation rate than at the sheltered low energy site. Additionally, at 337 d the $\Delta^{14}\text{C}_{\text{cb}}$ value for the low energy site is 100‰ lower than at the high energy site, corresponding to a higher $f_{\text{oil-cb}}$ value (+0.092) at the low energy location. This is further evidence of more

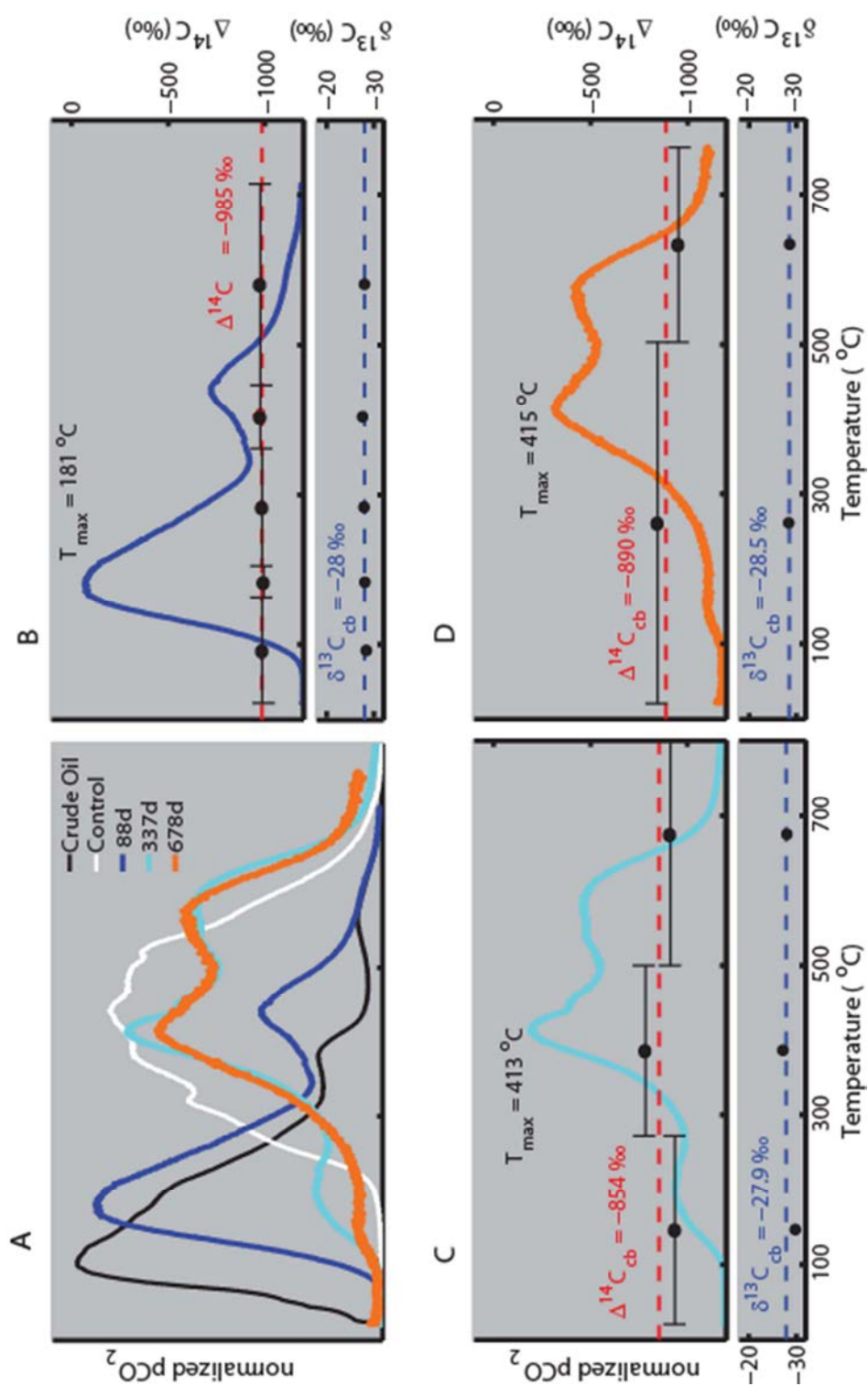


Figure 4.5. RP isotopic data for high energy beach sediment samples. Profiles for Macondo crude oil (black) and a control sample from unoiled marsh (white) given for reference. **A.** Trend in profiles over time. **B.-D.** Profiles with isotopic data for samples at 88, 337, and 678 d. Left axis in top panel is CO_2 evolution. Right axis is $\Delta^{14}\text{C}$. Horizontal bars indicate temperature intervals over which the aliquots of CO_2 were collected. Bottom panel plots $\delta^{13}\text{C}$ for the same intervals. T_{max} is temperature at which maximum pyrolysis occurs. Calculated bulk isotopic values and dashed lines in red ($\Delta^{14}\text{C}$) and blue ($\delta^{13}\text{C}$).

oil remaining at the low energy location at 337 d, suggesting a slower overall weathering rate than at the high energy site. By 678 d, sediment from the high and low energy locations presents similar reaction profiles, both devoid of low temperature pyrolysis, indicating parity in their respective oil degradation states.

Ramped pyrolysis profiles indicate that tar balls and deposits are the most persistent form of oil and some tar balls may exist from previous spills or natural seepage (Figures 4.2C, 4.6). Unlike the beach sediment samples, the tar samples produce a majority of pyrolysis at low temperatures through 881 d. This is evidence of thermochemically unstable oil being preserved in the form of tar balls and tar coating on rocks. A greater portion of a tar sample at 881 d pyrolyzes at $< 300^{\circ}\text{C}$ than does a sediment sample from the high energy site at 337 d, implying a significantly slower degradation rate for tar than for oil in high energy beach sediments. Tar balls and tar coatings on rocks degrade at a relatively slow rate because the oil they contain is not mixed into the environment. Oil in these forms maintains a high surface area to mass ratio. Microbes, oxygen, and nutrients are restricted to the outer surface, while the majority of the oil remains largely isolated from degradative processes [Bence et al., 1996]. The sample at 678 d that presents a unique RP profile (Figure 4.7D) could be suspected of having a composition other than oil, but very depleted radiocarbon data ($\Delta^{14}\text{C}_{\text{cb}} = -995\text{‰}$) yield f_{oil} of 0.966-0.991. This tar ball may have been subjected to a unique set of degradative processes and/or may be from a source other than DwH.

Marsh RP isotopic data (Figures 4.2D, 4.8) indicate slower degradation in comparison to the beach sediments, yet faster degradation when compared to the tar samples. Low temperature pyrolysis persists through 535 d, shifting to slightly higher

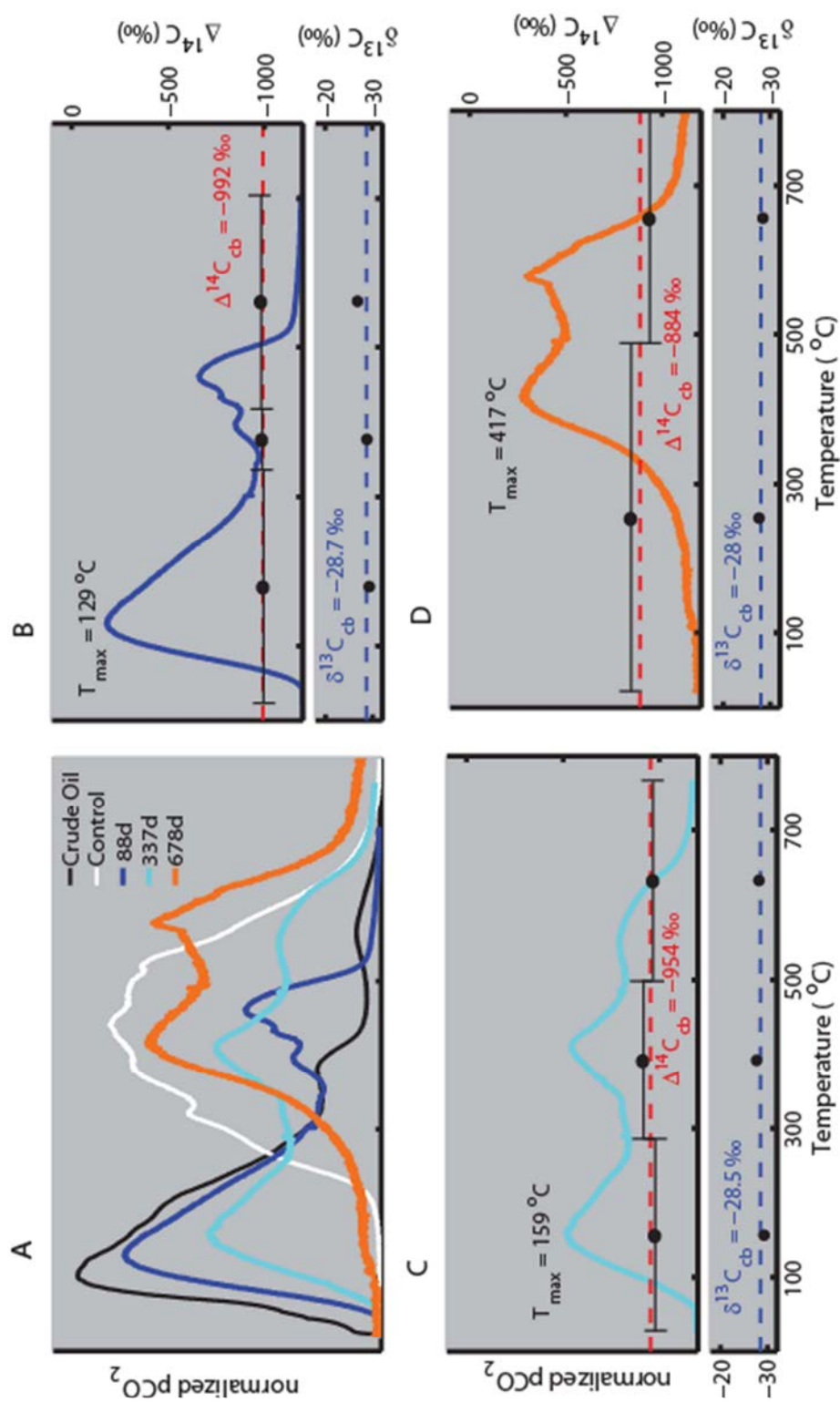


Figure 4.6. RP isotopic data for low energy beach sediment samples. Profiles for Macondo crude oil (black) and a control sample from unoiled marsh (white) given for reference. **A.** Trend in profiles over time. **B.-D.** Profiles with isotopic data for samples at 88, 337, and 678 d. Left axis in top panel is CO_2 evolution. Right axis is $\Delta^{14}C$. Horizontal bars indicate temperature intervals over which the aliquots of CO_2 were collected. Bottom panel plots $\delta^{13}C$ for the same intervals. T_{max} is temperature at which maximum pyrolysis occurs. Calculated bulk isotopic values and dashed lines in red ($\Delta^{14}C$) and blue ($\delta^{13}C$).

temperatures over time. The low temperature peak at 535 d is more prominent than the low temperature peak for the low energy beach sediment at 337 d, implying a slower weathering rate in the marsh. This agrees with there being less mechanical energy and sediment transport at the marsh site than at the low energy beach site. Also evident in the marsh thermochemical data is a shift to higher temperatures between the second peak at 337 d and the second peak at 535 d. The second peak at 535 d has a higher OC_b content (0.283) compared to the second peak at 337 d (0.114), which could alone account for the shift in temperature, or it could be a factor in addition to oil degradation resulting in stabilization of oil components. The trend in radiocarbon data at 337 d and 535 d shows lower values at lower temperatures and higher values at higher temperatures, in agreement with the assumption that oil pyrolyzes at low temperatures and OC_b pyrolyzes at higher temperatures. The sample at 694 d is *Juncus* grass that had no visible oil, and it yielded f_{oil} of 0.075 and 0.070 for its lower and higher temperature peaks. A $\delta^{13}C_{cb}$ value of -20.5‰ is significantly enriched compared to the majority of $\delta^{13}C$ data in this study and further confirms a lack of oil in this sample. A tar sample at 507 d and a marsh sample at 535 d present relatively similar reaction profiles, with both displaying low temperature pyrolysis. However, the low temperature marsh peak occurs at a higher temperature ($T_{max} = 234^{\circ}C$ (marsh) vs. $T_{max} = 157^{\circ}C$ (tar)), indicating the oil is more degraded in the marsh. This is interpreted as evidence of faster mixing of oil in the marsh as compared to the slower rate of the incorporation into the environment of oil in tar balls and tar coatings. The difference in sampling dates may have an influence, as the marsh sample was collected from a later date than the tar sample, but the difference in time (28 d) is considered relatively small on the 881 d timescale of the study. Beyond these two

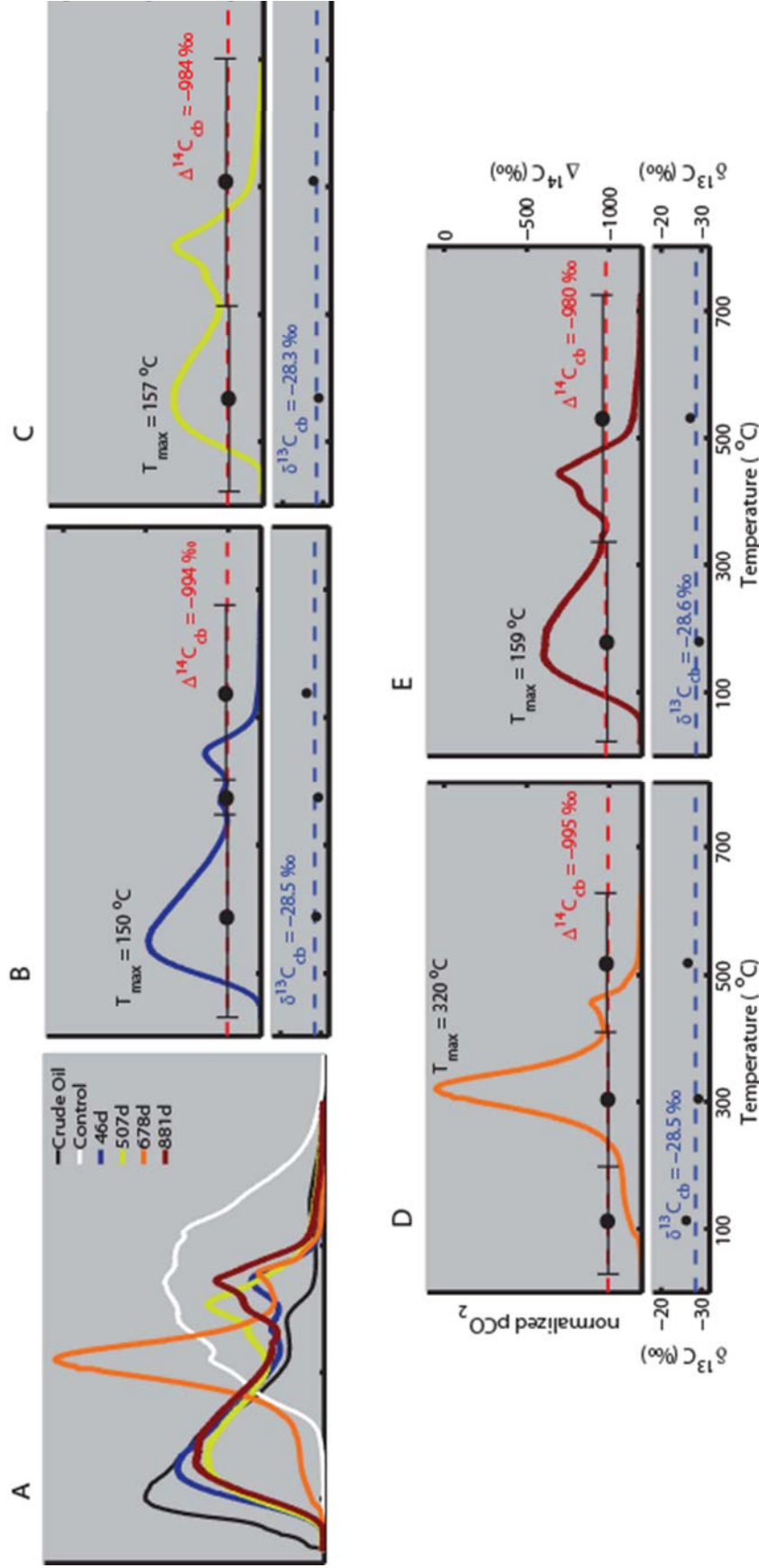


Figure 4.7. RP isotopic data for tar samples. Profiles for Macondo crude oil (black) and a control sample from un-oiled marsh (white) given for reference. **A.** Trend in profiles over time. **B.-E.** Profiles with isotopic data for samples at 46, 507, 678, and 881 d. Left axis in top panel is CO_2 evolution. Right axis is $\Delta^{14}\text{C}$. Horizontal bars indicate temperature intervals over which the aliquots of CO_2 were collected. Bottom panel plots $\delta^{13}\text{C}$ for the same intervals. T_{max} is temperature at which maximum pyrolysis occurs. Calculated bulk isotopic values and dashed lines in red ($\Delta^{14}\text{C}$) and blue ($\delta^{13}\text{C}$).

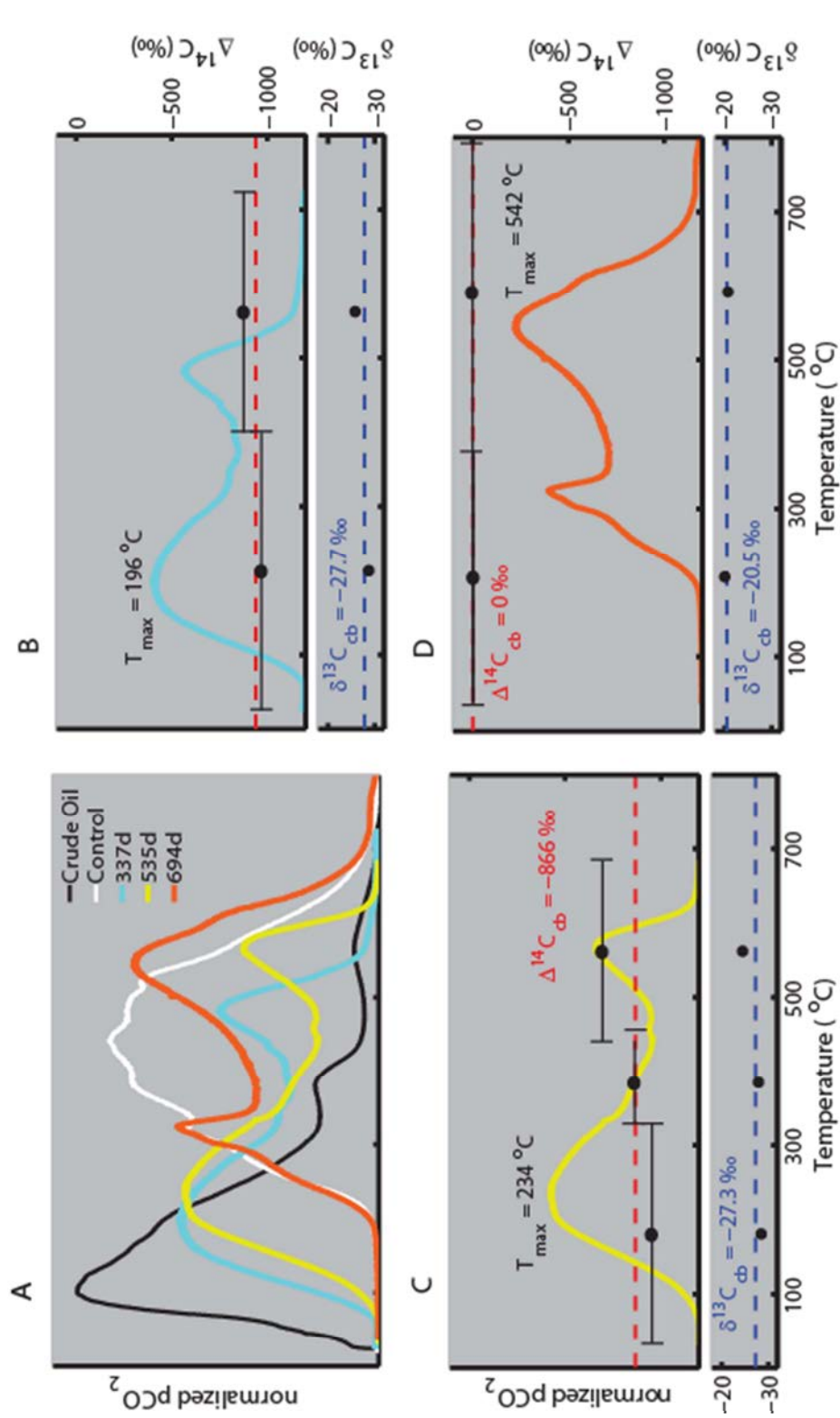


Figure 4.8. RP isotopic data for marsh samples. **A.** Trend in profiles over time. Profiles for Macondo crude oil (black) and a control sample from unooled marsh (white) given for reference. **B.-D.** Profiles with isotopic data for samples at 337, 535, and 694 d. Left axis in top panel is CO_2 evolution. Right axis is $\Delta^{14}C$. Horizontal bars indicate temperature intervals over which the aliquots of CO_2 were collected. Bottom panel plots $\delta^{13}C$ for the same intervals. T_{max} is temperature at which maximum pyrolysis occurs. Calculated bulk isotopic values in red ($\Delta^{14}C$) and blue ($\delta^{13}C$).

sampling dates, the marsh and tar data diverge further, with the 694 d marsh sample lacking oil, whereas oil persists in the tar samples through 881 d.

4.4.5 Thermochemical signs of specific degradation processes

It is not possible to ascertain exactly which type(s) of degradation produced the changes in thermochemical stability in Figures 4.2 and 4.5-4.8, however oil evaporated in the laboratory and oil from a rocky groin provide some constraint on the evaporation and biodegradation signatures in RP. Previous studies have stated evaporation and biodegradation to be the degradation processes that most affect oil in the environment [Rashid, 1974; DeLaune *et al.*, 1990; Wolfe *et al.*, 1994; Prince *et al.*, 2003; Owens, 2008; Atlas and Hazen, 2011]. In a previous experiment, crude oil sampled from the Macondo well head was left to evaporate at 60°C for 310 hs and it was confirmed that the oil's stable carbon isotopic composition did not significantly change (Figure 4.9, from Rosenheim *et al.* [2013c]). The remaining residue was analyzed by RP to investigate a thermochemical change in the oil specific to evaporation. The reaction profiles of the crude oil and the evaporation residue are similar except that the profile of the evaporation residue profile is shifted to higher temperatures (Figure 4.10). Therefore, evaporation resulted in the loss of crude oil compounds that pyrolyze below ~100°C. The reaction profile of the day 88 sediment sample from the high energy site at Grand Isle (Figures 4.2A, 4.5B) presents a reaction profile similar to that of the evaporated oil residue. This is interpreted as thermochemical evidence of evaporative degradation in that sample and in other samples showing similar shifts in prominent, low temperature pyrolysis peaks.

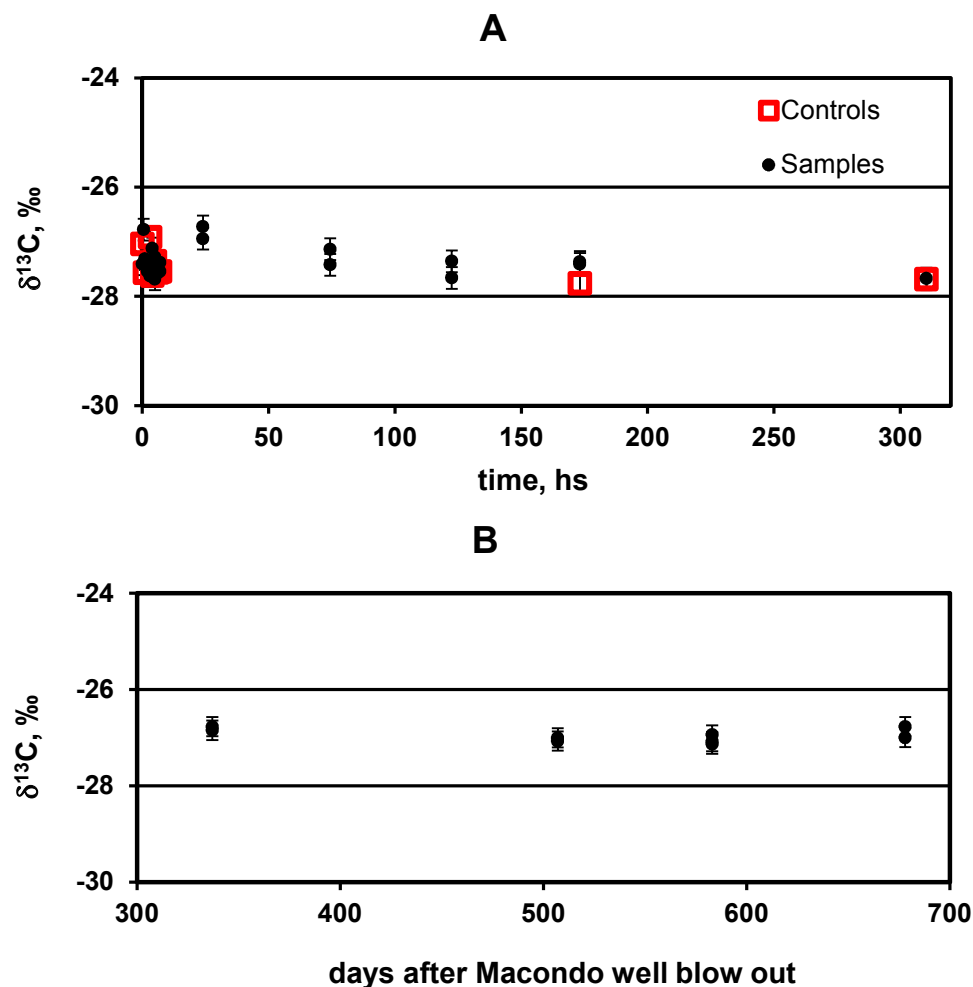


Figure 4.9. A. Stable carbon isotopic composition of Macondo well head crude oil evaporated at 60°C and sampled at intervals. Controls were prepared at outset, stored at <0°C, and analyzed at intervals. **B.** Stable carbon isotopic composition of oil from rocky groin subject to evaporation and photodegradation but limited microbial degradation due to a lack of moisture. Samples measured in duplicate. [Rosenheim *et al.*, 2013c]

Evaporation at temperatures exceeding those experienced by DwH did not account for the more pronounced loss of low temperature (< 300°C) pyrolysis indicated in the conceptual model (Figure 4.4B) and observed to an even greater degree in the beach sediment and marsh samples (Figure 4.2 A, B and D).

The disappearance of low temperature pyrolysis may be due to biodegradation, as indicated by tar deposits collected from a rocky groin (Figure 4.11). One of the samples

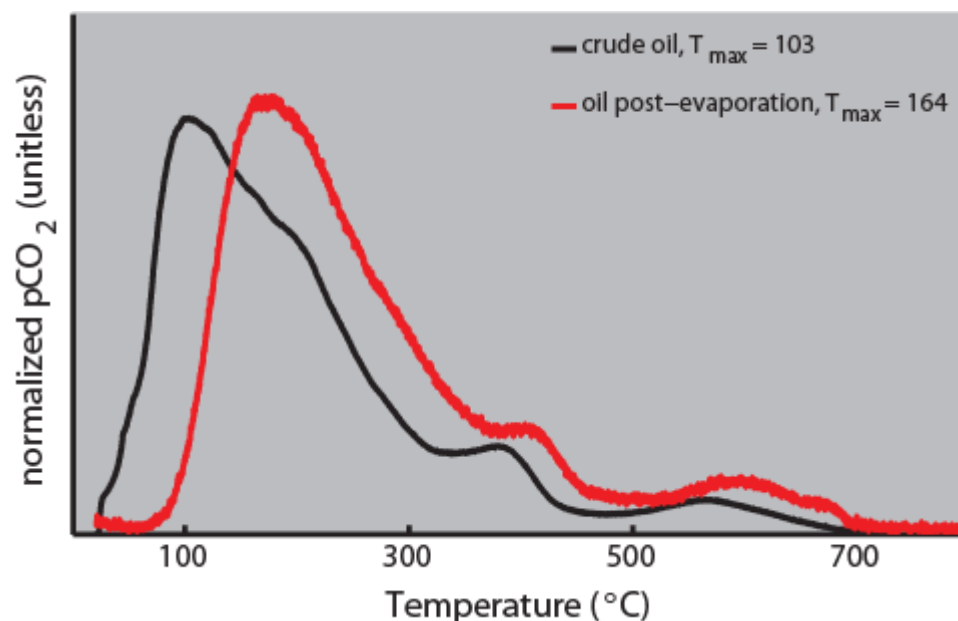


Figure 4.10. evaporation's effect on crude oil's RP reaction profile. Crude oil was evaporated at 60°C for 310 hs. The reaction profile of the remaining residue (red) resembles that of the crude oil (black) but is shifted to higher temperatures, exhibiting a loss of compounds that pyrolyze at low temperatures. High temperature thermochemical species appear to remain unchanged. The reaction profile of the day 88 sediment sample from the high energy site at Grand Isle (Figures 4.2A, 4.5B) presents a reaction profile similar to that of the evaporated oil residue.

was taken from the top of the rocky groin and it is assumed that it had been continually exposed to sunlight and kept dry most of the time. The other sample was collected from within the rocky groin and it is assumed that this sample had remained out of direct sunlight and was often wet from wave and tidal action. Solar radiation and a lack of moisture are likely to result in conditions inhospitable to oil degrading microbes. A damp environment protected from solar radiation is likely to be a more hospitable environment to microbes. Tar deposits from these two environments present significantly different pyrolysis profiles (Figure 4.11). It is hypothesized that the oil components that

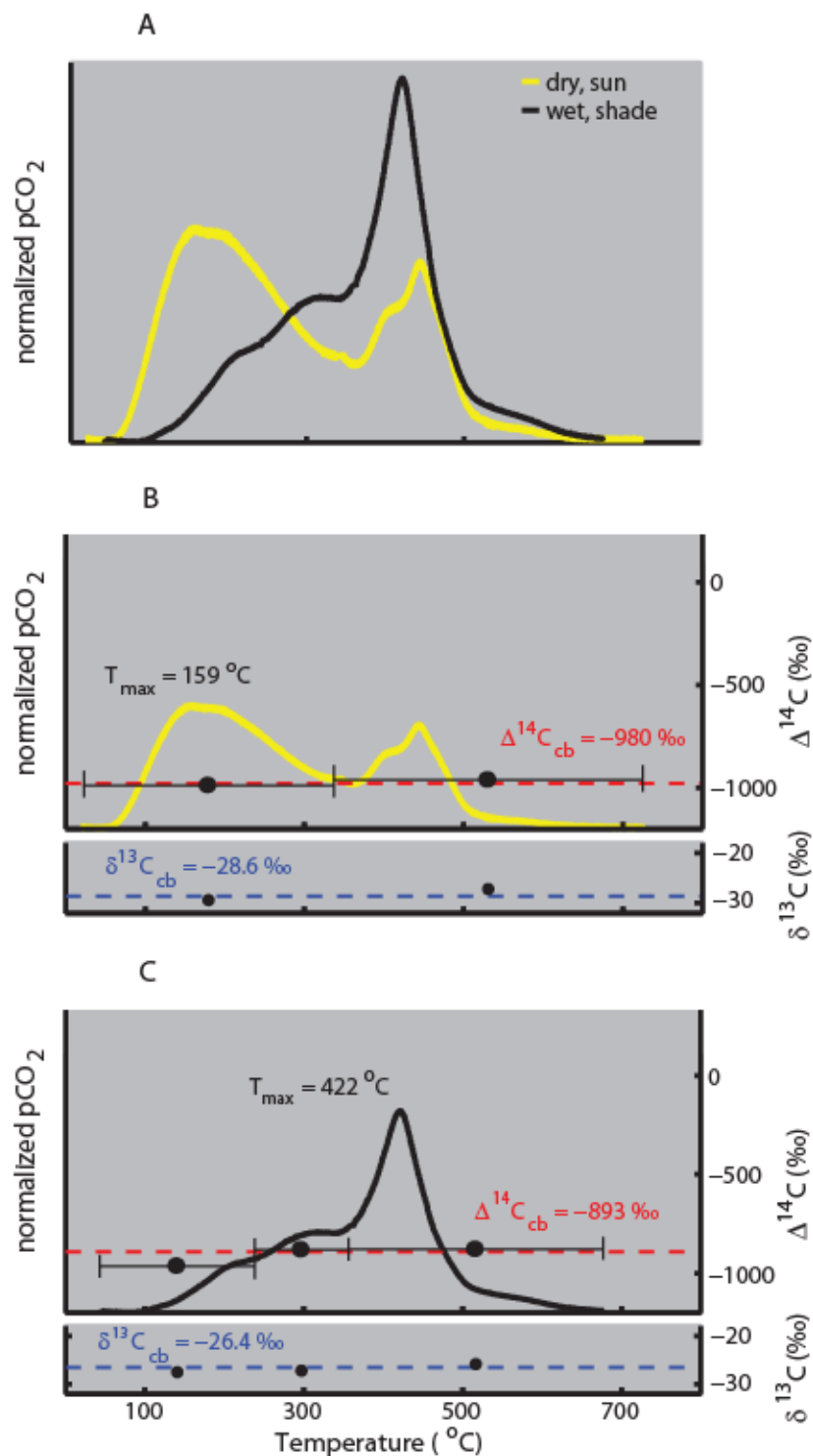


Figure 4.11. A. A comparison of profiles from a tar deposit that remained dry and exposed to sunlight and a tar deposit that remained wet and out of direct sunlight. It is hypothesized that the wet, shaded environment was conducive to microbes. The microbes may have consumed portions of the oil that are apparent in the reaction profile from the tar deposit kept dry and in the sun and that are lacking in the profile of the sample kept wet and in the shade. **B.** Isotopic data confirm an oil source of the OC in the samples. Less negative isotopic values in the wet, shade sample may indicate incorporation of marine OC.

pyrolyzed at low temperatures in the dry, exposed tar were consumed by microbes in the wet, shaded tar deposit. The lack of pyrolysis at low temperatures displayed by the wet, shaded sample is similar to that presented by the beach sediment and marsh samples (Figure A, B and D). Isotopic data for both samples confirms their compositions to be mostly oil. The less negative $\Delta^{14}\text{C}$ and $\delta^{13}\text{C}$ values for the wet, shaded tar deposit may be a result of incorporation of marine OC as a result of the sample having been in regular contact with sea water.

4.4.6 Isotopic trends

Despite the crude oil reaction profile exhibiting a majority of pyrolysis at low temperatures and minimal pyrolysis at mid-to-high temperatures, the RP isotopic data is dominated by very negative radiocarbon and stable carbon values at all temperatures. In some samples, aliquots produced at higher temperatures yielded calculated f_{oil} values that are higher than f_{oil} values for samples at low-mid temperatures (Figure 4.12). In these cases, not only was oil present in the high temperature pyrolysis products, but also a greater fraction of the pyrolysis products at high temperatures was comprised of oil than at the low-mid temperature range. The crude oil RP profile displays some oil compounds pyrolyzing at temperatures above 500°C. The oil that pyrolyzed at higher temperatures in samples is either those oil compounds or compounds that pyrolyzed at lower temperatures in the crude oil but were degraded in a way which increased their thermochemical stability and resulted in them pyrolyzing at higher temperatures in the samples. The presence of OC_b in samples can explain why a greater fraction of high

temperature pyrolysis products were comprised of oil than pyrolysis products at low-mid temperatures. The control sample RP profile, shown repeatedly in white, demonstrates that OC_b pyrolyzes in the mid-temperature range. This, in conjunction with some oil components pyrolyzing at higher temperatures, could explain f_{oil} values greater than calculated bulk f_{oil} values at high temperatures. For the five high temperature aliquots where $f_{oil} > f_{oil-cb}$, the $\delta^{13}C$ values range from -28.6 to -28.0‰, which are indicative of oil. However, aged, recalcitrant C_3 terrigenous carbon could yield $\delta^{13}C$ values [Smith and Epstein, 1971].

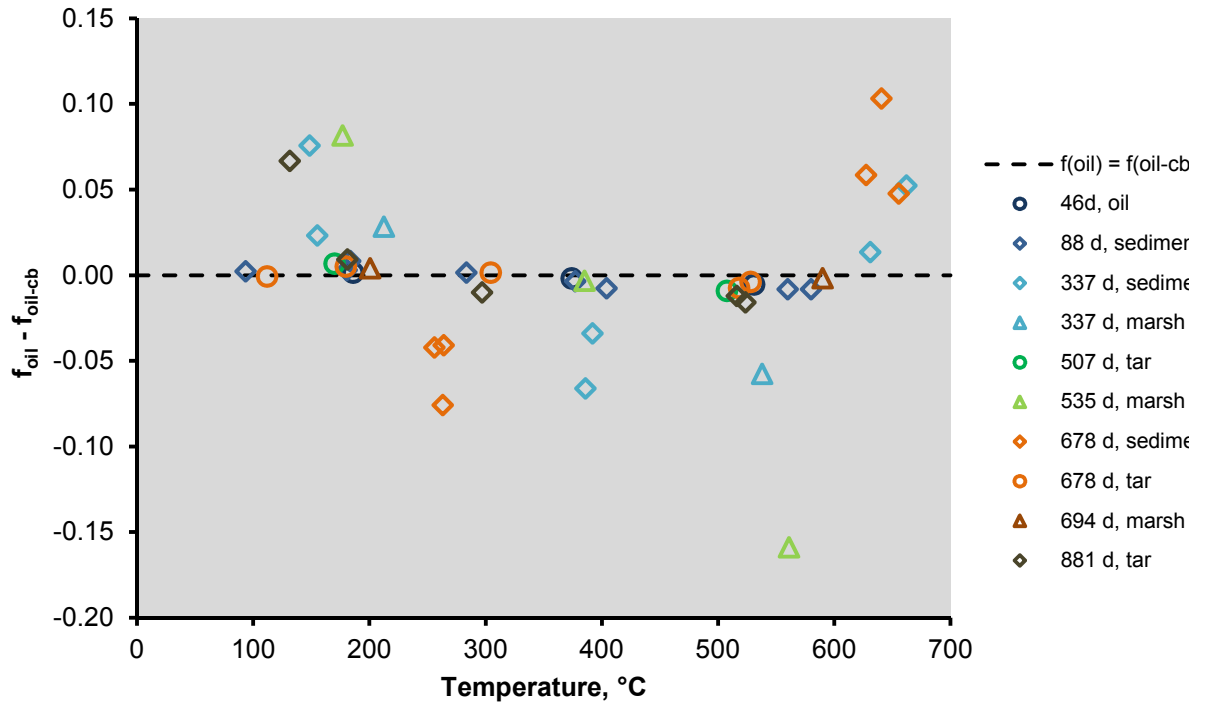


Figure 4.12. For each aliquot, the difference between individual calculated fraction oil and the calculated bulk fraction oil, plotted at temperature interval midpoints. Deviation from the black dotted line at zero, where $f_{oil} = f_{oil-cb}$, is the fraction oil amount that an aliquot differs from the geometric mean of all the aliquots collected during RP of a given sample. Points > 0 in the low temperature range coincide with the assumption that oil pyrolyzes at low temperatures. Points < 0 in mid temperatures demonstrate OC_b pyrolysis. Points > 0 at high temperatures demonstrate pyrolysis of thermochemically stable oil compounds and a lack of pyrolysis of OC_b .

Isotopic data show evidence of fractionation at highest f_{oil} values and mixing at lower f_{oil} values. At high f_{oil} there is no mixing because there is just one carbon source (oil). But oil is a mixture of compounds and the pyrolysis reactor succeeds in showing more isotopic variation amongst the various oil compounds than is observed in the bulk oil in nature [Macko *et al.*, 1981] and in the laboratory (Figure 4.9, from Rosenheim *et al.* [2013c]). This is interpreted as RP causing chemical fractionation of oil components that are isotopically and thermochemically different. Stable carbon isotope fractionation has been observed before in RP [Rosenheim and Galy, 2012; Rosenheim *et al.*, 2013b], however it is important to note that radiocarbon measurements, on which the oil fraction is calculated, are corrected for stable carbon isotope composition [Stuiver and Pollach, 1977; Rosenheim *et al.*, 2008]. As more OC_b is mixed into the oil, the stable isotope values for any one fraction oil value show less variance. This is because mixing with OC_b has a more significant effect on isotopic composition than chemical fractionation of oil in RP due to there being greater isotopic difference between oil and OC_b than between the various oil components. Therefore, as isotopically distinct species are mixed into this system, this type of plot becomes more effective at showing the OC endmembers mixing in the environment.

$\Delta^{14}C$ is plotted against $\delta^{13}C$ for sediment and tar samples (Figure 4.13) to highlight the isotopic effects of chemical fractionation from RP and the mixing of oil with OC_b . Data were linearly regressed according to sampling date and the steepness of the respective slopes is interpreted as an indication of degree of mixing. Aliquots from sediment samples from 88 d show little variance in $\Delta^{14}C$, due to all oil components having the same $\Delta^{14}C$ signature and the samples being comprised almost entirely of oil.

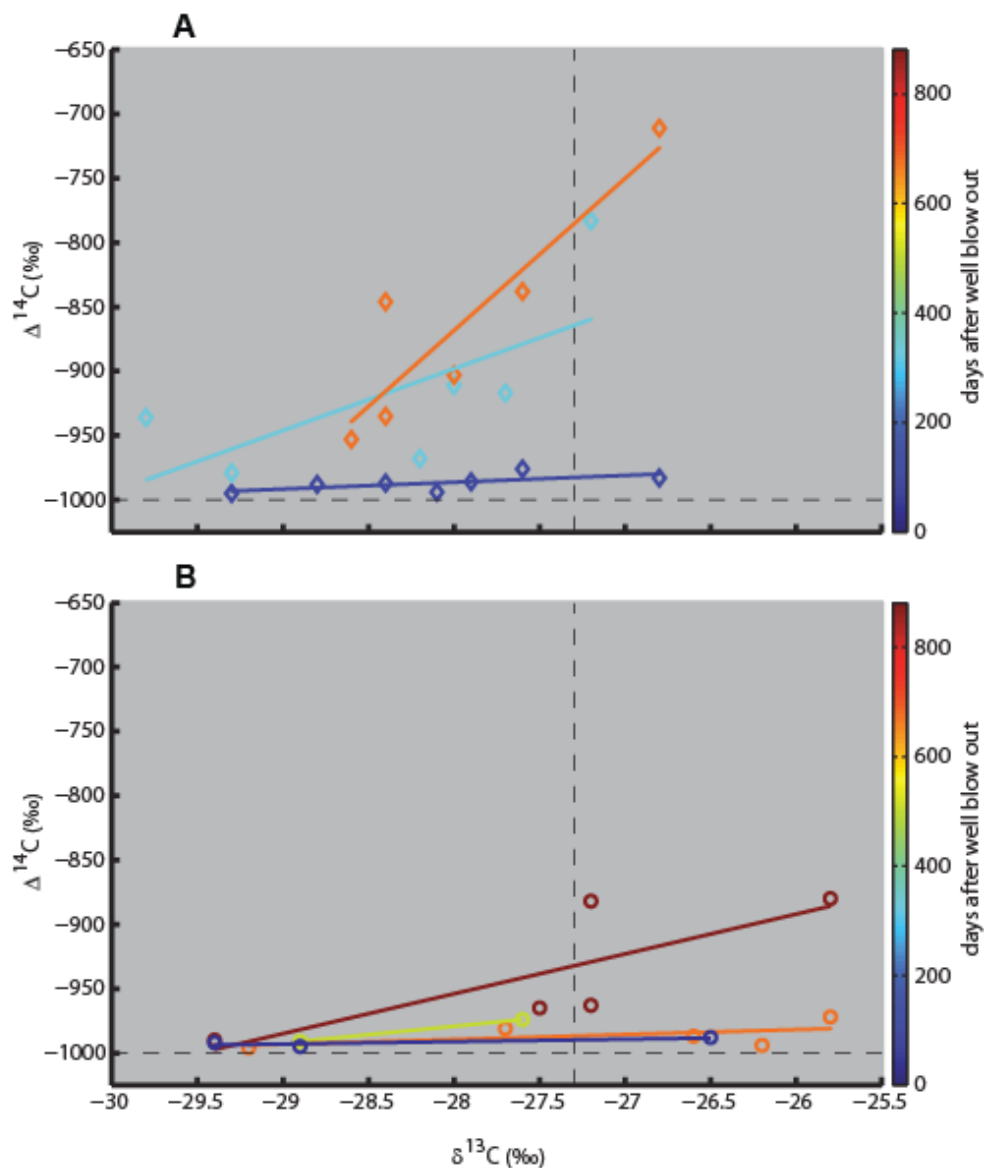


Figure 4.13. A. Carbon isotopic compositions of aliquots of sediment samples produced on the RP system. Dark blue – 88 d; light blue – 337 d; orange – 678 d. The dotted lines are at isotopic values for Macondo crude oil. Slopes of linear regressions for each date are interpreted to be proportional to degree of mixing (addition of OC_b to the oil). At 88 d, variation in $\delta^{13}\text{C}$ data with minimal variation in $\Delta^{14}\text{C}$ data is interpreted as evidence of fractionation. At 337 d and 678 d, increasing variation in $\Delta^{14}\text{C}$ with respect to variation in $\delta^{13}\text{C}$ is interpreted as an increasing degree of incorporation of OC_b . **B.** When treated similarly, data from tar samples produce less steep slopes, implying less incorporation of OC_b and less mixing of oil into the environment when in the form of tar balls and tar accumulations of rocks. Dark blue – 46 d; yellow – 507 d; orange – 678 d; maroon – 881 d.

However, the same aliquots show significant variance in $\delta^{13}\text{C}$, due to RP fractionation of oil compounds that vary in $\delta^{13}\text{C}$. Through days 337 and 678 a mixing signal becomes dominant over the fractionation signal and implies increasing incorporation of OC_b . Data from tar samples show a similar trend but at a slower rate, indicating a slower mixing rate of oil in the form of tar balls and tar accumulations on rocks (Figure 4.13B).

4.5 Conclusions

Oil degradation, defined as chemical change in the oil mixture, is affected by non-degradative processes, such as the mixing of the oil with background organic carbon. Ramped pyrolysis isotopic analysis of beach sediment, tar, and marsh samples shows oil degraded most rapidly where mixing of the oil into the environment likely occurred fastest. Oil degradation rates, observed in changes in thermochemical data over time, were greatest for oil dispersed in high energy beach sediments and smallest in accumulations of oil in the forms of tar balls and tar coating on rocks. Relative oil degradation rates for the four sample types is as follows: high energy beach sediments > low energy beach sediments > marsh samples > tar samples. Isotopic data revealed that oil dominated the organic carbon in coastal Louisiana after the 2010 Deepwater Horizon oil spill and persisted, especially in tar balls and tar coatings on rocks, for 881 d. Comparing stable carbon data versus radiocarbon data provides an isotopic perspective on the mixing of oil with OC_b over time.

Chapter 5. Conclusions

For as long as the global economy is fueled by oil, spills will likely continue to be an undesirable side effect. Once an oil spill has occurred, various environmental processes begin to change the physical form and chemical composition of the oil. Mixing is a physical process of distribution and dilution of oil that can indirectly affect oil degradation. Despite extensive research having been conducted on oil weathering, there is still much to learn on the interaction between oil and the environment. This thesis presents a thermochemical and isotopic perspective of oil mixing and degradation.

The first part of this research provides a proof-of-concept that oil contamination can be identified by changes in thermochemical stability in organic material and isotopic analysis of pyrolysates. A ramped pyrolysis (RP) isotope technique was applied to marsh sediment samples in which oil was identified using the chemical proxy of polycyclic aromatic hydrocarbons (PAHs). RP reaction profiles differ significantly according to PAH content, with samples low in PAHs thermochemically stable until higher temperatures, and samples high in PAHs showing relatively low thermochemical stability. A lack of radiocarbon in samples containing high levels of PAHs confirms the presence of oil and its influence on thermochemical stability. Separation of oil from the background organic material (OM) is demonstrated by the evolution of pyrolysates almost completely comprised of petrogenic carbon.

The second part of the work presented here is the application of the RP isotope technique to beach sediment, tar, and marsh samples collected over a period of 881 days after the onset of the 2010 BP Deepwater Horizon oil spill. Stable carbon and radiocarbon isotopic data demonstrate the OM of almost all samples analyzed by RP to be largely comprised of oil. Thermochemical changes in the OM of beach sediment and marsh samples shows evidence of oil degradation, whereas pyrolysis data for tar samples indicate the persistence of oil in the form of tar balls and deposits. Differences in relative rates of degradation are attributed to differences in the rate at which the oil is mixed into the environment. Oil degrades fastest in high energy beach sediments because greater amounts of wave energy and sediment distribution result in fastest dispersion of the oil and a greater supply of oxygen to oil consuming microbes. Oil degradation is slowest in the tar samples because oil in this form mixes the slowest, maintaining a low surface area to mass ratio that severely limits biodegradation. Relative rates of degradation for the four sample types is: high energy beach sediments > low energy beach sediments > marsh samples > tar samples.

As a bulk-partitioning organic carbon isotopic technique whereby OM components are separated based on thermochemical stability, ramped pyrolysis shows promising results for studying oil in the environment. In the future the technique could be applied as a screening method for oil that would simultaneously yield a thermochemical measure of the oil's degradation state. Additionally, the RP technique may be able to yield even higher resolution data if coupled to new generations of isotope analyzers.

Appendix A: A brief description of investigations into isotopic ($\delta^{13}\text{C}$) and thermochemical signals of evaporation

In order to better understand how evaporation changes the stable carbon isotopic composition ($\delta^{13}\text{C}$) and the ramped pyrolysis profile of oil, crude oil sampled from the Macondo well head and provided by BP was placed in a low temperature oven at 60°C for 310 hs. The oil was sampled at intervals and analyzed for $\delta^{13}\text{C}$ using an Elementar vario MICRO cube elemental analyzer interfaced to an Isoprime dual inlet isotope ratio mass spectrometer in continuous flow mode (EA-IRMS). Controls were prepared at the outset of the experiment, stored at -4°C , and analyzed at intervals along with the samples. The stable carbon isotopic composition of the oil proved to remain constant during evaporation. This finding confirms measurements made on field samples by *Macko et al.* [1981] and is presented as Figure 4.9 in *Rosenheim et al.* [2013c]. After the oil had evaporated for 310 hs it was later analyzed by ramped pyrolysis. The resulting thermochemical profile (Figure 4.10) displays a shift to higher temperatures on the scale of the temperature of evaporation (60°C). Similarities with pyrolysis profiles of beach sediment samples (Figures 4.5 A,B and 4.6 A,B) indicate evaporation degraded those samples from early sampling dates. Perhaps more importantly, the data also show that evaporation alone cannot account for the nearly total disappearance over time of low temperature pyrolysis (Figure 4.2 A, B and D), indicating that other degradation processes must have acted on the oil.

Appendix B: Compiled elemental and isotopic data from EA-IRMS

Sample Name	day #	$\delta^{13}\text{C}$, ‰	%OC	$\delta^{15}\text{N}$, ‰	%N	C:N
GI-A-20100604-1-oil.raw	46	-27.49	25.83	-44.68	0.34	75.19
GI-040610-A2-1.raw	46	-27.44	24.48	-	-	-
GI-040610-A2-2.raw	46	-27.44	41.59	-	-	-
GI-A-20100604-2-tar.raw	46	-189.63	74.38	-8.73	0.43	171.47
GI-A-20100604-2-tar-rep.raw	46	-27.76	71.93	-74.15	0.62	115.17
GI-A-20100604-2-oil.raw	46	14.93	39.82	-10.74	0.17	234.21
GI-A-20100604-2-oil-rep.raw	46	-27.01	35.19	-28.03	1.01	34.68
use		-27.41	47.90			
GI-040610-A4-1.raw	46	-27.40	57.15	-	-	-
GI-040610-A4-2.raw	46	-27.30	48.65	-	-	-
GI-A-20100604-4-oil.raw	46	128.82	68.25	-16.74	0.23	295.41
GI-A-20100604-4-oil-rep.raw	46	-27.77	60.25	-243.96	0.90	66.66
use		-27.49	58.58			
GI-040610-A5-1.raw	46	-27.33	93.54	-	-	-
GI-040610-A5-2.raw	46	-27.31	77.33	-	-	-
GI-A-20100604-5-oil.raw	46			-6.29	0.34	
GI-A-20100604-5-oil-rep.raw	46	-27.57	63.62	50.30	0.78	81.96
GI-A-20100604-5-tar-rep.raw	46	-27.66	61.00			
use		-27.47	62.31			
GI-B-20100604-1-oil.raw	46	-25.55	17.86			
GI-B-20100604-2-sed.raw	46	-36.79	16.20	3.64	0.13	125.43
GI-B-20100604-2-sed-rep.raw	46	-27.12	14.04	-22.70	0.36	38.73
GI-B-20100604-3-oil.raw	46	-27.78	12.73	-29.46	0.13	99.36
GI-040610-B4-1.raw	46	-27.40	42.64	-	-	-
GI-040610-B4-2.raw	46	-27.38	41.59	-	-	-
GI-B-20100604-5-oil.raw	46	-27.41	17.68			
(missing GI-20100604-1-oil)						
GI-20100604-2-oil.raw	46	-451.18	69.66	-85.57	0.45	154.58
GI-20100604-2-oil-rep.raw	46	-27.38	68.32	-66.53	1.46	46.79
GI-A-20100630-1-tar.raw	72	-25.30	0.46	-92.18	0.07	6.89
GI-A-20100630-2-tar.raw	72	-24.20	0.18	-338.84	0.06	3.18
GI-A-20100630-2-tar-r.raw	72	-25.45	0.05	-22.35	0.01	7.11
GI-A-20100630-5-oil.raw	72	-27.43	6.87	-22.33	0.12	56.98
GI-A-20100630-5-oil-dup.raw	72	-24.55	6.54	-423.94	0.23	27.97
use		-25.99	6.71	-423.94	0.23	27.97
GI-20100630-3-tar.raw	72	-73.27	13.82	-3.42	0.13	109.66
GI-20100630-3-tar-rep.raw	72	-25.79	14.75	-26.41		
GI-20100630-12-sed.raw	72	-19.69	0.40	34.40	0.13	3.09

= GI-20100630-7-SED

GI-A-20100716-1-tar.raw	88	-25.17	6.15	-269.08	0.60	10.24
GI-A-20100716-2-tar.raw	88	-25.77	6.32	-245.12		
GI-A-20100716-4-sed.raw	88	-25.19	3.26	-11.45	0.30	11.03
GI-A-20100716-6-tar	88	-25.86	11.24	-60.26	0.83	13.50
GI-A-20100716-7-tar.raw	88	-26.44	10.00	-5.57	0.52	19.12
GI-B-2010-0716-1-SED.raw	88	-26.23	1.48	-19.80	0.08	18.49
GI-B-20100716-1-tar.raw	88	-23.37	2.27			
GI-B-20100716-1-tar-r.raw	88	-26.94	1.38	14.72	0.03	44.18
GI-B-2010-0716-2-SED.raw	88	-27.17	11.17	-15.77	0.09	128.79
GI-B-20100716-2-tar.raw	88	-26.71	21.95	4037.81	0.63	34.88
use		-26.94	16.56			
GI-B-2010-0716-4-SED.raw	88	-27.03	14.09	-30.00	0.11	133.86
GI-B-20100716-4-tar.raw	88	-25.22	18.24			
use		-26.12	16.16			
GI-B-20100716-5-sed.raw	88	-23.91	1.36	-71.11	0.20	6.69
GI-B-20100716-5-sed-rep.raw	88	-25.38	0.96	-27.46	0.17	5.51
use		-24.65	1.16			
GI-B-20100716-6-sed.raw	88	-26.03	6.39	-265.29	0.29	22.15
GI-B-20100716-7-sed.raw	88	-25.56	10.88	-607.77	0.00	
GI-20100716-1-tar.raw	88	-26.19	10.51	35.44	0.53	19.93

GI-A-20100820-1-sed.raw	123	-25.17	0.24			
GI-A-20100820-2-sed.raw	123	-23.28	2.44	-128.97	0.36	6.88
GI-A-20100820-3-sed.raw	123	-23.26	0.73	-40.47	0.25	2.88
GI-A-20100820-4-TAR.raw	123	-27.15	6.58	-17.14	0.21	31.57
GI-B-2010-0820-1-SED.raw	123	-26.45	5.29	-30.56	0.10	52.35
GI-B-2010-0820-2-SED.raw	123	-26.29	3.66	-25.12	0.02	168.43
GI-B-2010-0820-3-SED.raw	123	-25.54	2.62	-17.22	0.13	19.41
GI-B-2010-0820-4-SED.raw	123	-24.60	0.96	-11.76	0.01	76.77

GI-A-101015-1-water	missing, never analyzed, maybe all went to IU					
GI-A-20101015-2-sed.raw	179	-25.17	0.45	27.96	0.04	10.24
GI-A-20101015-3-sed.raw	179	-23.29	0.09	-20.55	0.10	0.88
GI-A-20101015-4-sed.raw	179	-21.67	0.06	134.48	0.07	0.85
GI-A-20101015-5-sed.raw	179	-23.15	0.60	-173.63	0.18	3.29
GI-B-2010-1015-1-SED.raw	179	-26.69	11.06	-27.60	0.10	105.57
GI-B-2010-1015-1-SED-REP.raw	179	-25.12	10.25	-24.17	0.06	177.61
GI-B-20101015-1-sed.raw	179	-23.68	0.43	-232.52	0.10	4.13
use		-25.90	10.65			
GI-B-2010-1015-2-SED.raw	179	-25.98	1.93	-31.14	0.06	33.18
GI-B-20101015-3-sed.raw	179	-24.87	7.42	-73.73	0.48	15.33
GI-B20101015-3-sed.raw	179	-24.83	8.43	-13.46	0.70	12.07
use		-24.85	7.93			
GI-B-2010-1015-4-SED.raw	179	-26.25	0.97	-23.52	0.11	9.04
GI-20101015-1-TAR.raw	179	-25.93	10.00	-16.58	0.60	16.63
GI-20101015-3-tar.raw	179	-26.22	11.24	-181.34		
GI-101015-2-water	missing, never analyzed, maybe all went to IU					

GI-A-20110322-1-sed.raw	337	-22.68	0.31	-375.96	0.05	5.81
GI-A-20110322-1-sed-r.raw	337	-26.03	0.26	-2.38	0.01	26.67
GI-A-20110322-2-sed.raw	337	-24.29	0.35	-24.09	0.05	6.85

GI-A-20110322-2-sed-rep.raw	337	-24.34	0.45	-63.18	0.05	8.31
use		-24.31	0.40			
GI-A-20110322-3-sed.raw	337	-23.51	0.46	-132.32	0.08	5.39
GI-A-20110322-3-sed-r.raw	337	-25.82	0.32	-1.17	0.01	25.20
GI-A-20110322-4-mud(-sed)	missing					
GI-A-20110322-5-tar.raw	337	-26.10	13.39	-179.78	0.27	49.43
GI-B-2011-0322-1SED.raw	337	-24.80	0.73	4.79	0.04	19.99
GI-B-2011-0322-2SED.raw	337	-26.10	0.65	-34.13	0.04	17.19
GI-B-20110322-2-sed.raw	337	-23.48	0.57	-10.42	0.16	3.67
use		-24.79	0.61			
GI-B-2011-0322-3SED.raw	337	-25.15	0.77	-8.24	0.14	5.53
GI-B-2011-0322-3-SED-REP.raw	337	-24.75	0.44	-16.47	0.04	10.39
GI-B-20110322-3-sed.raw	337	-26.27	9.61	22.27	0.38	25.16
use		-25.39	0.60			
GI-B-20110322-4-sed.raw	337	-21.24	0.09	-38.71	0.07	1.20
GI-B-20110322-4-sed-rep.raw	337	-20.88	0.06	-197.52	0.04	1.63
GI-B-20110322-4-sed-dup.raw	337	-21.87	0.48	-3.55	0.12	3.96
GI-B-20110322-4-sed-r.raw	337	-23.43	0.05			
use avg of all 4 measurements		-21.86	0.17			
GI-B-20110322-5-sed.raw	337	-26.86	7.20			
GI-20110322-1-Tar-1.raw	337	-27.10	11.48	2.86	0.05	254.04
GI-20110322-1-Tar-2.raw	337	-26.75	12.11	-89.27	0.41	29.85
GI-20110322-1-Tar-3.raw	337	-26.94	12.30	-0.84	0.03	432.03
GI-20110322-1-Tar-4.raw	337	-27.23	11.28	-29.87	0.05	238.09
GI-20110322-1-Tar-5.raw	337	-27.26	11.35			
GI-20110322-1-Tar-6.raw	337	-26.50	11.58			
GI-20110322-1-Tar-7.raw	337	-26.85	10.70	-17.03	0.35	30.60
GI-20110322-1-Tar-8.raw	337	-26.77	13.33	-119.29	0.01	968.18
GI-20110322-1-Tar-9.raw	337	-27.00	13.25	-8.53	0.13	102.40
GI-20110322-1-Tar-10.raw	337	-27.07	13.06	-11.23	0.06	205.86
use		-26.95	12.05			
GI-20110322-2-TAR.raw	337	-25.76	3.70	-72.81	0.29	12.75
GI-20110322-2-TAR-sub.raw	337	-27.08	21.62	-138.87	0.33	64.61
GI-20110322-2-tar-rep.raw	337	-27.22	6.94	-152.73	0.15	47.69
use		-26.69	10.75			
GI-20110322-3-TAR.raw	337	-26.40	10.94	8.32	0.61	17.94
GI-20110322-3-tar-rep.raw	337	-27.10	11.33			
use		-26.75	11.14			
GI-20110322-4-sed.raw	337	-22.92	2.62	-14.88	0.29	9.02
GI-20110322-4-sed-rep.raw	337	-24.52	1.42	8.20	0.07	20.88
use		-23.72	2.02			
GI-A-20110908-1-SED.raw	507	-25.21	0.32	-43.14	0.02	16.91
GI-A-20110908-2-SED.raw	507	-25.96	0.29	-13.32	0.00	#DIV/0!
GI-A-20110908-3-SED.raw	507	-25.73	0.53	-182.13	0.05	11.56
GI-A-20110908-4-SED.raw	507	-25.93	0.28	2.50	0.01	40.51
GI-A-20110908-5-TAR.raw	507	-22.77	29.68	1.26	1.09	27.20
GI-A-20110908-6-SED.raw	507	-25.16	0.23	-44.35	0.00	129.11
GI-B-20110908-1-TAR.raw	507	-26.27	7.98	-368.05	0.07	114.04
GI-B-20110908-2-SED.raw	507	-22.04	1.25	-	0.16	7.80
GI-B-20110908-3-SED.raw	507	-23.55	0.60	-210.67	0.18	3.35
GI-20110908-1-TAR.raw	507	-26.32	14.04	-73.99	0.12	116.87

GI-20110908-2-TAR.raw	507	-27.13	10.33	-	0.04	258.37
GI-A-20111123-1-SED.raw	583	-26.47	0.46	-129.99	0.14	3.29
GI-A-20111123-2-SED.raw	583	-27.84	0.32	-48.77	0.13	2.43
GI-A-20111123-2-SED-dup.raw	583	-17.25	1.40	278.22	0.34	4.06
GI-A-20111123-2-sed-r.raw	583	-25.90	0.05	-37.32	0.02	2.21
use	583	-26.87	0.86			
GI-A-20111123-3-SED.raw	583	-26.67	0.32	-98.92	0.06	5.30
GI-A-20111123-4-SED.raw	583	-24.94	0.48	-	0.07	6.91
GI-B-20111123-1-SED.raw	583	-26.89	0.55	-214.99	0.12	4.60
GI-B-2011-1123-1-SED.raw	583	-25.58	0.38	-22.91	0.14	2.77
use		-26.23	0.46			
GI-B-20111123-2-SED.raw	583	-25.87	0.48	-10.96	0.12	3.90
GI-B-2011-1123-2-SED.raw	583	-26.29	0.22	-7.63	0.04	6.38
GI-B-2011-1123-2-SED-REP.raw	583	-25.91	0.28	-12.55	0.16	1.77
use		-26.02	0.33			
GI-B-20111123-3-SED	583	-25.79	0.35	-88.96	0.06	5.86
GI-B-2011-1123-3-SED.raw	583	-24.26	0.38	-37.25	0.04	8.72
use		-25.02	0.37			
GI-20111123-1-TAR-1.raw	583	-27.08	7.44	-3.62	0.04	200.07
GI-20111123-1-TAR-2.raw	583	-26.94	6.51	-36.22	0.06	104.75
GI-20111123-1-TAR-3.raw	583	-27.13	7.47	-11.00	0.03	264.76
GI-20111123-1-TAR.raw	583	-26.46	7.86	7.00	0.03	295.98
use		-26.90	7.32			
GI-20111123-2-TAR.raw	583	-21.49	27.43	1.50	1.25	22.01
GI-20111123-3-TAR.raw	583	-60.71	81.71	-37.31	0.39	207.12
GI-A1-20120226-1-sed.raw	678	-21.81	0.25	-14.54	0.09	2.86
GI-A1-20120226-2-sed.raw	678	-24.38	0.27	47.15	0.00	
GI-A1-20120226-2-sed-r.raw	678	-25.65	0.15	-22.87	0.01	10.91
GI-A1-20120226-3-sed.raw	678	-22.50	1.96	2.65	0.11	17.61
GI-A1-20120226-3-sed-r.raw	678	-24.74	1.51	-0.45	0.07	22.79
GI-A2-20120226-1-sed.raw	678	-21.43	0.27	-47.19	0.05	5.01
GI-A2-20120226-1-sed-r.raw	678	-25.56	0.11	-5.80	0.01	11.57
GI-A2-20120226-2-sed.raw	678	-24.14	0.31	200.33	0.06	4.99
GI-A2-20120226-2-sed-r.raw	678	-24.04	0.24	-6.29	0.02	11.41
GI-B-20120226-1-sed.raw	678	-24.72	0.42	-270.01	0.00	
GI-B-20120226-1-sed-r.raw	678	-26.42	0.35	5.51	0.01	31.71
GI-B-20120226-2-sed.raw	678	-23.10	0.15	69.92	0.11	1.41
GI-B-20120226-2-sed-r.raw	678	-25.27	0.13	-5.87	0.01	11.54
use		-24.19	0.14			
GI-B-20120226-3-sed.raw	678	-20.94	0.18	-355.05	0.04	4.37
GI-B-20120226-3-sed-r.raw	678	-23.05	0.05	8.88	0.01	5.61
GI-B-20120226-4-sed.raw	678	-23.77	0.25	-385.74	0.10	2.43
GI-B-20120226-4-sed-r.raw	678	-24.47	0.08	-6.10	0.01	8.17
GI-20120226-1-TAR-2.raw	678	-26.77	4.80	-8.93	0.03	146.48
GI-20120226-1-TAR-4.raw	678	-27.00	4.28	-25.69	0.05	78.78
use		-26.88	4.54			
GI-2012-226-2-TAR-1.raw	678	-26.90	7.32	-39.67	0.06	118.31
GI-2012-226-2-TAR-2.raw	678	-27.25	7.29	-14.93	0.06	131.14
use		-27.08	7.30			

GI-20120226-3-tar.raw	678	-29.85	80.87	74.76	0.48	167.29
GI-20120226-4-tar.raw	678	-24.36	8.50			
GI-20120226-5-tar.raw	678	-23.25	4.24	775.49	0.23	18.74
GI-20120226-5-tar-r.raw	678	-27.11	3.73	-32.98	0.06	65.22
GI-A-20120916-1-tar.raw	881	-25.66	9.11	259.09	0.00	
GI-A-20120916-2-tar.raw	881	-28.01	39.87	-65.37	0.53	75.47
GI-A-20120916-3-tar.raw	881	-23.54	1.47	-583.24	0.00	
GI-A-20120916-3-tar-r.raw	881	-22.98	1.76	-4.76	0.08	20.98
use			1.62			
GI-A-20120916-4-tar.raw	881	-31.18	74.99	66.69	0.96	77.80
GI-A-20120916-5-sed.raw	881	-22.54	0.27	-33.33	0.06	4.42
GI-A-20120916-5-sed-r.raw	881	-25.92	0.02	-25.57	0.01	2.06
GI-A-20120916-6-sed.raw	881	-24.44	0.16	-276.15	0.03	4.66
GI-A-20120916-6-sed-r.raw	881	-25.71	0.01			
GI-B1-20120916-1-sed.raw	881	-31.07	0.74	-54.37	0.27	2.78
GI-B1-20120916-1-sed-r.raw	881	-23.91	0.09	-101.03	0.03	2.80
GI-B2-20120916-1-sed.raw	881	-28.87	0.15	-1361.54	0.06	2.69
GI-B2-20120916-1-sed-r.raw	881	-22.71	0.03	-8.47	0.01	4.80
GI-B2-20120916-2-sed.raw	881	-29.93	0.16	-185.92	0.03	4.70
GI-B2-20120916-2-sed-r.raw	881	-23.92	0.02	-44.07	0.01	2.77
GI-B-20120916-1-tar.raw	881	-21.56	21.46	7.60	1.10	19.54
GI-20120916-1-tar.raw	881	-24.27	6.72	-407.10	0.40	16.88
GI-20120916-2-tar.raw	881	-23.42	3.98			
GI-20120916-2-tar-r.raw	881	-26.90	3.16	-9.15	0.06	56.00
GI-20120916-3-tar.raw	881	-22.82	3.16	304.66	0.00	
GI-20120916-4-tar.raw	881	-30.35	79.44			
GI-20120916-5-tar.raw	881	-30.93	85.97	99.22	0.00	
GI-20120916-6-tar.raw	881	-31.41	85.92	-186.82	0.63	135.96
GI-20120916-7-tar.raw	881	-28.92	40.70	-407.36	0.55	73.47
GI-20120916-8-tar.raw	881	-24.20	9.69	262.50	0.32	29.89
GI-20120916-9-tar.raw	881	-21.31	1.59	-55.33	0.19	8.32
GI-20120916-9-tar-r.raw	881	-23.66	0.56	-5.98	0.07	7.94
BB-A-20110322-1-plant.raw	337	-28.01	74.85	-86.27	0.60	124.51
BB-A-20110322-1-plant-r.raw	337	-26.48	64.28	3.12	0.67	95.59
BBB-2-20110822-1-plant.raw (BBB-2-20110322-1-plant.raw)	(337) 337	-27.51	66.05	17.73	0.63	105.11
BB-20110322-1-tar.raw	337	-16.54	13.70	-33.45	0.58	23.44
BC1-20110322-2-tar.raw	337	-24.15	20.89	-19.11	0.57	36.85
BBB-1-20110322-1-tar.raw	337	-27.11	40.56	3.92	0.47	86.16
BB-A-3-20111006-1-tar.raw	535	-28.08	49.07	-76.82	0.61	79.91
BJ-20120313-1-plant.raw	694	-21.86	12.73	-29.55	0.74	17.11
BJ-20120313-2-plant.raw	694	-18.73	12.88	-82.78	0.62	20.69
BJ-20120313-1-cor.raw	694	-18.33	9.82	-51.71	0.49	20.01
BJ-20120313-2-cor.raw	694	-17.13	12.88	5.65	0.72	17.80
BJ-20120313-3-cor.raw	694	-17.00	9.70	-27.11	0.71	13.68
BJ-20120313-4-cor.raw	694	-16.79	3.59	-260.63	0.32	11.11
BJ-20120313-4-cor-r.raw	694	-19.98	1.23	-2.22	0.08	14.84
BJ-20120313-5-cor.raw	694	-21.02	11.85	3.46	0.69	17.08
BJ-20120313-6-cor.raw	694	-21.35	9.21	10.78	0.59	15.63

BJ-20120313-7-cor.raw	694	-23.30	18.77	28.12	0.92	20.34
BJ-20120313-8-cor.raw	694	-22.73	10.52	-18.29	0.63	16.65
BJ-20120313-9-cor.raw	694	-24.06	27.92	4.24	1.42	19.70
Macondo Crude-A3.raw	0	-27.05	80.96	-45.15	0.11	723.06
Macondo Crude-A4.raw	0	-27.47	80.09	-5.09	0.48	167.80
Macondo Crude-A5.raw	0	-27.46	82.12	-51.24	0.05	1587.06
Macondo Crude-A6.raw	0	-27.34	81.95	-42.85	1.00	81.58
run 65: use %OC or "below limit"; use isotopic data from EA_CN-66						
run66: use d13C; use %OC if >/= run65 data, then avg 65&66						

Appendix C: Compiled isotopic data from the National Ocean Sciences Accelerator Mass Spectrometer Facility (NOSAMS) for samples analyzed by ramped pyrolysis

*data from Ch. 3 not included as they are provided in Table 3.2

**data are not corrected for blank

sample	$\mu\text{mol CO}_2$	Fm	1 σ	$\Delta^{14}\text{C, ‰}$	1 σ	$\delta^{13}\text{C, ‰}$	1 σ	$\Delta^{14}\text{C}_{\text{cb, ‰}}$	$\delta^{13}\text{C}_{\text{cb, ‰}}$
GI-A-20100716-4-sed, DB-475-1	24.5	0.0131	0.0011	-987.0	1.4	-28.4	0.1	-984.7	-
DB-475-2	29.2	0.0065	0.0010	-993.6	1.3	-28.1	0.1		
DB-475-3	53.3	0.0137	0.0014	-986.4	1.8	-27.9	0.1		
DB-475-4	22.7	0.0238	0.0011	-976.4	1.4	-27.6	0.1		
DB-475-5	25.1	0.0243	0.0011	-975.8	1.4	-	-		
GI-A-20110322-3-sed, DB-639-1	15.8	0.0645	0.0012	-935.9	1.5	-29.8	0.1	-854.3	-27.9
DB-639-2	56.5	0.2186	0.0013	-783.1	1.6	-27.2	0.1		
DB-639-3	48.7	0.0900	0.0009	-910.6	1.1	-28.0	0.1		
GI-A1-20120226-2-sed, DB-643-1	21.5	0.1555	0.0010	-845.7	1.3	-28.4	0.1	-889.7	-28.4
DB-643-2	15.0	0.0476	0.0009	-952.8	1.1	-28.6	0.1		
GI-A2-20120226-2-sed, DB-661-1	14.2	0.2916	0.0012	-710.5	1.5	-26.8	0.1	-792.2	-27.3
DB-661-2	10.4	0.0974	0.0018	-903.4	2.3	-28.0	0.1		
GI-B-20100716-7-sed, DB-658-1	139.3	0.0048	0.0003	-995.2	0.4	-29.3	0.1	-992.0	-28.8
DB-658-2	20.9	0.0119	0.0008	-988.2	1.0	-28.8	0.1		
DB-658-3	41.7	0.0170	0.0005	-983.2	0.6	-26.8	0.1		
GI-B-20110322-3-sed, DB-670-1	31.9	0.0214	0.0006	-978.7	0.8	-29.3	0.1	-953.8	-28.5
DB-670-2	28.9	0.0835	0.0012	-917.2	1.5	-27.7	0.1		
DB-670-3	17.9	0.0319	0.0009	-968.4	1.1	-28.2	0.1		
GI-B-20120226-2-sed, DB-665-1	17.4	0.1629	0.0013	-838.4	1.6	-27.6	0.1	-883.8	-27.9
DB-665-2	15.4	0.0653	0.0009	-935.2	1.1	-28.4	0.1		
GI-A-20100604-1-oil, DB-649-1	133.0	0.0048	0.0008	-995.2	1.0	-28.9	0.1	-993.6	-28.5
DB-649-2	17.1	0.0085	0.0008	-991.6	1.0	-29.4	0.1		
DB-649-3	31.2	0.0123	0.0004	-987.8	0.5	-26.5	0.1		
GI-B-20110908-1-tar, DB-646-1	39.5	0.0094	0.0003	-990.7	0.4	-28.9	0.1	-983.3	-28.4

DB-646-2	29.6	0.0267	0.0005	-973.5	0.6	-27.6	0.1		
GI-20120226-1-TAR, DB-341-1	25.6	0.0186	0.0004	-981.4	0.5	-27.72	0.1	-976.0	-26.7
DB-341-2	32.1	0.0283	0.0005	-971.7	0.6	-25.81	0.1		
GI-20120226-3-tar, DB-653-1	18.5	0.0060	0.0008	-994.1	1.0	-26.2	0.1	-994.8	-28.5
DB-653-2	149.5	0.0036	0.0002	-996.5	0.3	-29.2	0.1		
DB-653-3	28.6	0.0132	0.0005	-986.9	0.6	-26.6	0.1		
GI-A-20120916-1-tar, DB-654-1	49.9	0.0100	0.0003	-990.1	0.4	-29.4	0.1	-980.3	-28.6
DB-654-2	28.6	0.0371	0.0006	-963.1	0.8	-27.2	0.1		
GI-20120916-3-tar, DB-656-1	13.7	0.0358	0.0011	-964.5	1.4	-27.5	0.1	-892.7	-26.4
DB-656-2	26.8	0.1191	0.0013	-881.8	1.6	-27.2	0.1		
DB-656-3	52.6	0.1213	0.0011	-879.6	1.4	-25.8	0.1		
BBB-1-20110322-1-tar, DB-657-1	100.7	0.0303	0.0011	-969.9	1.4	-28.7	0.1	-939.5	-27.7
DB-657-2	49.2	0.1236	0.0012	-877.3	1.5	-25.8	0.1		
BB-A-3-20111006-1-tar, DB-659-1	175.0	0.0460	0.0006	-954.4	0.8	-28.5	0.1	-866.5	-27.3
DB-659-2	50.9	0.1381	0.0011	-862.9	1.4	-27.9	0.1		
DB-659-3	88.7	0.3069	0.0014	-695.3	1.8	-24.5	0.1		
BJ-20120313-2-plant, DB-662-1	70.0	1.0033	0.0028	-4.2	3.5	-20.0	0.1	-0.1	-20.5
DB-662-2	148.5	1.0094	0.0030	1.9	3.8	-20.7	0.1		

List of References

- Aizenshtat Z. 1973. Perylene and its geochemical significance. *Geochimica et Cosmochimica Acta*. 37: 559-567.
- Alimi H., Ertel T. and Schug B. 2003. Fingerprinting of hydrocarbon fuel contaminants: literature review. *Environmental Forensics*. 4(1): 25-38.
- Arey S.J, Nelson R.K. and Reddy C.M. 2007. Disentangling Oil Weathering Using GCxGC. 1. Chromatogram Analysis. *Environmental Science & Technology*. 41: 5738-5746.
- Atlas R.M. and Hazen T.C. 2011. Oil Biodegradation and Bioremediation: A Tale of the Two Worst Spills in U.S. History. *Environmental Science & Technology*. 45: 6709-6715.
- Barron M.G. 2012. Ecological Impacts of the Deepwater Horizon Oil Spill: Implications for Immunotoxicity. *Toxicologic Pathology*. 40: 315-320.
- Bence A.E., Kvenvolden K.A. and Kennicutt II M.C. 1996. Organic geochemistry applied to environmental assessments of Prince William Sound, Alaska, after the Exxon Valdez oil spill - a review. *Organic Geochemistry*. 24(1): 7-42.
- Blum D.M. and Roberts H.H. 2009. Drowning the Mississippi Delta due to insufficient sediment supply and global sea-level rise. *Nature Geoscience*. 2: 488-491.
- Boehm P.D. and Farrington J.W. 1984. Aspects of the polycyclic aromatic hydrocarbon geochemistry of recent sediments in the Georges Bank region. *Environmental Science and Technology*. 18(11): 840-845.
- Chmura G.L., Aharon P., Socki R.A. and Abernethy R. 1987. An inventory of ^{13}C abundances in coastal wetlands of Louisiana, USA: vegetation and sediments. *Oecologia*. 74: 264-271.
- Couvillion B.R., Barras J.A., Steyer G.D., Sleavin W., Fischer M., Beck H., Trahan N., Griffin, B. and Heckman, D. 2011. Land area change in coastal Louisiana from 1932 to 2010: U.S. Geological Survey Scientific Investigations Map 3164, scale 1:265,000, 12 p. pamphlet.

- Crone T.J. and Tolstoy M. 2010. Magnitude of the 2010 Gulf of Mexico Oil Leak. *Science*. 330: 634.
- Day J.W., Kemp G.P., Reed D.J., Cahoon D.R., Boumans R.M., Suhayda J.M. and Gambrell R. 2011. Vegetation death and rapid loss of surface elevation in two contrasting Mississippi delta salt marshes: The role of sedimentation, autocompaction and sea-level rise. *Ecological Engineering*. 37: 229-240.
- Deegan L.A., Johnson D.A., Warren R.S., Peterson B.J., Fleeger J.W., Fagherazzi S. and Wollheim W.M. 2012. Coastal eutrophication as a driver of salt marsh loss. *Nature*. 490: 388-392.
- DeLaune R.D., Gambrell R.P., Pardue J.H. and Patrick W.H. Jr. 1990. Fate of Petroleum Hydrocarbons and Toxic Organics in Louisiana Coastal Environments. *Estuaries*. 13(1):72-80.
- Graham W.M., Condon R.H., Carmichael R.H., D'Ambra I., Patterson H.K., Linn L.J., and Hernandez Jr. F J. 2010 Oil carbon entered the coastal planktonic food web during the Deepwater Horizon oil spill, *Environmental Research Letters*, 5.
- Griffiths S.K. 2012. Oil Release from Macondo Well MC252 Following the Deepwater Horizon Accident. *Environmental Science & Technology*. 46: 5616-5622.
- Haines E.B. 1976. Stable carbon isotope ratios in the biota, soils and tidal water of a Georgia salt marsh. *Estuarine and Coastal Marine Science*. 4: 609-616.
- Hatton R.S, DeLaune R.D. and Patrick Jr. W.H. 1983. Sedimentation, accretion and subsidence in marshes of Barataria Basin, Louisiana. *Limnology and Oceanography*. 28(3): 494-502.
- Hester M.W. and Mendelssohn I.A. 2000. Long-term recovery of a Louisiana brackish marsh plant community from oil-spill impact: vegetation response and mitigating effects of marsh surface elevation. *Marine Environmental Research*. 49: 233-254.
- Iqbal J., Overton E.B. and Gisclair D. 2008. Polycyclic aromatic hydrocarbons in Louisiana rivers and coastal environments: source fingerprinting and forensic analysis. *Environmental Forensics*. 9(1): 63-74.
- Irvine G.V., Mann D.H. and Short J.W. 1999. Multi-year persistence of oil mousse on high energy beaches distant from the Exxon Valdez spill origin. *Marine Pollution Bulletin*. 38(7): 572-584.

- Irvine G.V., Mann D.H. and Short J.W. 2006. Persistence of 10-year old Exxon Valdez oil on Gulf of Alaska beaches: The importance of boulder-armoring. *Marine Pollution Bulletin*. 52: 1011-1022
- Keeling C.D. 1958. The concentration and isotopic abundances of atmospheric carbon dioxide in rural areas. *Geochimica et Cosmochimica Acta*. 13: 322-334.
- Kennish M J. 1997. Practical Handbook of Estuarine and Marine Pollution. (Boca Raton: CRC)
- Kingston P.F. 2002. Long-term environmental impact of oil spills. *Spill Science & Technology Bulletin*. 7(1-2): 53-61.
- Kosters E.C. 1989. Organic-clastic facies relationships and chronostratigraphy of the Barataria interlobe basin, Mississippi delta plain. *Journal of Sedimentary Petrology*. 59(1): 98-113.
- Kvenvolden K.A., Hostettler F.D., Carlson P.R. and Rapp J.B. 1995. Ubiquitous tar balls with a California-source signature on the shorelines of Prince William Sound, Alaska. *Environmental Science and Technology*. 29(10): 2684-2694.
- Lee R.F. and Page D.S. 1997. Petroleum Hydrocarbons and Their Effects in Subtidal Regions after Major Oil Spills. *Marine Pollution Bulletin*. 34(11): 928-940.
- Liu Z., Liu J., Zhu Q. and Wu W. 2012. The weathering of oil after the Deepwater Horizon oil spill: insights from the chemical composition of the oil from the sea surface, salt marshes and sediments. *Environmental Research Letters*. 7: 1-14.
- Macko S.A. and Parker P.L. 1983. Stable Nitrogen and Carbon Isotope Ratios of Beach Tars on South Texas Barrier Islands. *Marine Environmental Research*. 10: 93-103
- Macko S.A., Parker P.L., Botello A.V. 1981. Persistence of Spilled Oil in a Texas Salt Marsh. *Environmental Pollution (Series B)*. 2: 119-128.
- Maharaj S., Barton C.D., Karathanasis T.A.D., Rowe H.D. and Rimmer S.M. 2007a. Distinguishing “new” from “old” organic carbon on reclaimed coal mine sites using thermogravimetry: I. Method development. *Soil Science*. 172(4): 292-301.

- Maharaj S., Barton C.D., Karathanasis T.A.D., Rowe H.D. and Rimmer S.M. 2007b. Distinguishing “new” from “old” organic carbon on reclaimed coal mine sites using thermogravimetry: II. Field validation. *Soil Science*. 172(4): 302-312.
- McGeehin J., Burr G.S., Jull A.J.T., Reines D., Gosse J., Davis P.T., Muhs D., Southon J. 2001. Stepped-combustion ^{14}C dating of sediment: a comparison with established techniques. *Radiocarbon*. 43(2A): 255-261.
- McGeehin J., Burr G.S., Hodgins G., Bennett S.J., Robbins J.A., Morehead N., Markewich H. 2004. Stepped-combustion ^{14}C dating of bomb carbon in lake sediment. *Radiocarbon*. 46(2): 893-900.
- Mendelssohn I.A., Andersen G.L., Baltz D.M., Caffey R.H., Carman K.R., Fleeger J.W., Joye S.B., Lin Q., Maltby E., Overton E.B., Rosas L.P. 2012. Oil Impacts on Coastal Wetlands: Implications for the Mississippi River Delta Ecosystem after the Deepwater Horizon Oil Spill. *BioScience*. 62(6): 562-574.
- Munoz D., Guiliano M., Doumenq P., Jacquot F., Scherrer P. and Mille G. 1997. Long Term Evolution of Petroleum Biomarkers in Mangrove Soil (Guadeloupe). *Marine Pollution Bulletin*. 34(11): 868-874.
- Neff J.M. 1979. *Polycyclic Aromatic Hydrocarbon in the Aquatic Environment: Sources, Fates and Biological Effects*. (London: Applied Science)
- NOAA, 1980. Proceedings of a Symposium on Preliminary Results from the September 1979 Researcher/Pierce Ixtoc-I cruise. NOAA Office of Marine Pollution Assessment.
- NOAA. 2006. Alaska North Slope Crude Blends. NOAA Office of Response and Restoration.
- National Resource Council (NRC). 2003. Oil in the Sea III: Inputs, Fates, and Effects. *The National Academies Press*. Available at <http://www.nap.edu/catalog/10388.html>
- Owens E.H., Taylor E. and Humphrey B. 2008. The persistence and character of stranded oil on coarse-sediment beaches. *Marine Pollution Bulletin*. 56: 14-26.
- Pendergraft, M.A, Dincer, Z., Sericano, J.L., Wade, T., Kolasinski, J. and Rosenheim, B.E. 2013. Linking ramped pyrolysis isotope data to oil content through PAH analysis. *In review* (submitted to *Environmental Research Letters*).

- Prince R.C. et al. 2003. The Roles of Photooxidation and Biodegradation in Long-term Weathering of Crude and Heavy Fuel Oils. *Spill Science & Technology Bulletin*. 2: 145-156.
- Ramseur J.L. 2010. Deepwater Horizon Oil Spill: The Fate of the Oil. Congressional Research Service Report 7-5700. Available at www.crs.gov R41531
- Rashid M.A. 1974. Degradation of Bunker C Oil under Different Coastal Environments of Chedabucto Bay, Nova Scotia. *Estuarine and Coastal Marine Science*. 2: 137-144.
- Reddy C.M., Eglington T.I., Hounshell A., White H.K., Xu L., Gaines R.B. and Frysiner G.S. 2002. The West Falmouth Oil Spill After Thirty Years: The Persistence of Petroleum Hydrocarbons in Marsh Sediments. *Environmental Science & Technology*. 36:4754-4760.
- Rosenheim B.E., Day M.B., Domack E.W., Schrum H., Benthein A. and Hayes J.M. 2008. Antarctic sediment chronology by programmed-temperature pyrolysis: Methodology and data treatment. *Geochemistry, Geophysics, Geosystems*. 9(4).
- Rosenheim B.E. and Galy V. 2012. Direct Measurement of Riverine Particulate Organic Carbon Age Structure. *Geophysical Research Letters*. 39.
- Rosenheim B.E., Roe K.M., Roberts B.J., Kolker A.S., Allison M.A. and Johannesson K.H. 2013a. River discharge influences on particulate organic carbon age structure in the Mississippi/Atchafalaya River System. *Global Biogeochemical Cycles*. 27: 1-13.
- Rosenheim B.E., Santoro J.A., Gunter M. and Domack E.W. 2013b. Improving Antarctic sediment ^{14}C dating using ramped pyrolysis: an example from the Hugo Island Trough. *Radiocarbon*. 55(1): 115-126.
- Rosenheim, B.E., Pendergraft, M.A., Flowers, G.C., Carney, R., Sericano, J., Amer, R.M., Chanton, J., Dincer, Z. and Wade, T. 2013c Employing extant stable carbon isotope data in Gulf of Mexico sedimentary organic matter for oil spill studies. *In review*.
- Ryerson T.B. et al. 2011. Atmospheric emissions from the Deepwater Horizon spill constrain air-water partitioning, hydrocarbon fate, and leak rate. *Geophysical Research Letters*. 38: 1-6

- Sanders H.L., Grassle J.F., Hampson G.R., Morse L.S., Garner-Price S. and Jones C.C. 1980. Anatomy of an oil spill: long-term effects from the grounding of the barge Florida off West Falmouth, Massachusetts. *Journal of Marine Research*. 38(2): 265-380.
- SCAT, S.C.a.A.T. 2013. Environmental Response Management Application, edited by NOAA.
- Short, J.W. et al. 2007. Slightly Weathered Exxon Valdez Oil Persists in Gulf of Alaska Beach Sediments after 16 Years. *Environmental Science & Technology*. 41: 1245-1250.
- Silliman B.R., van de Koppel J., McCoy M.W., Diller J., Kasozi G.N., Earl K., Adams P.N. and Zimmerman A.R. 2012. Degradation and resilience in Louisiana salt marshes after the BP-Deepwater Horizon oil spill. *Proceedings of the National Academy of Science USA*. 109(28): 11234-11-239.
- Smith B.N. and Epstein S. 1971. Two categories of $^{13}\text{C}/^{12}\text{C}$ ratios for higher plants. *Plant Physiology*. 47: 380-384.
- Sofer Z. 1984. Stable Carbon Isotope Compositions of Crude Oils: Application to Source Depositional Environments and Petroleum Alteration. *AAPG Bulletin*. 68(1): 31-49.
- Stuiver M. and Pollach H.A. 1977. Reporting of ^{14}C data, *Radiocarbon* 19(3), 355-363.
- Wang H., Hackley K.C., Panno S.V., Coleman D.D., Liu J.C.L. and Brown J. 2003. Pyrolysis combustion ^{14}C dating of soil organic matter. *Quaternary Research*. 60(3): 348-355.
- Wang Z., Fingas M. and Page D. 1999. Oil Spill Identification. *Journal of Chromatography A*. 843: 369-411
- Ward D.M., Atlas R.M., Boehm P.D., Calder J.A. 1980. Microbial Biodegradation and Chemical Evolution of Oil from the Amoco Spill. *Ambio*. 9(6): 277-283.
- White H.K., Liu X., Lima A.L.C., Eglington T.I. and Reddy C. 2005. Abundance, Composition, and Vertical Transport of PAHs in Marsh Sediments. *Environmental Science & Technology*. 39: 8273-8280.
- Wolfe D.A. et al. 1994. The Fate of the Oil Spilled from the Exxon Valdez. *Environmental Science & Technology*. 28(13): 561-568.

Zengel, S. and Michel J. 2013. Deepwater Horizon Oil Spill: Salt Marsh Oiling Conditions, Treatment Testing and Treatment History in Northern Barataria Bay, Louisiana (Interim Report October 2011). U.S. Dept. of Commerce, NOAA Technical Memorandum NOS OR&R 42. Seattle, WA: Emergency Response Division, NOAA. 74 pp.

Biography

Matthew A. Pendergraft attended Southwestern Community College for two years until transferring to the University of California San Diego in 2003. There he earned a Bachelor of Arts in Spanish Literature and a Bachelor of Science in Environmental Systems – Environmental Chemistry in 2007. After working in the Port of San Diego's Department of Environmental Services, he moved to Buenos Aires, Argentina in 2008. There he participated in atmospheric chemistry projects measuring fluorides in the air as a result of an aluminum production plant and multiple atmospheric contaminants originating from an oil refinery. In 2011 he moved to New Orleans to study at Tulane University's Department of Earth and Environmental Sciences under the leadership of Brad E. Rosenheim. For his Master of Science research, he investigated thermochemical changes in oil from coastal environments in Southeastern Louisiana impacted by the 2010 BP Deepwater Horizon oil spill. He also assisted in offshore research helping collect samples from the water column and sea floor looking for isotopic indications of oil and oceanic processes in the Gulf of Mexico.